UNIVERSIDAD DE INVESTIGACIÓN DE TECNOLOGÍA EXPERIMENTAL YACHAY

Escuela de Ciencias Biológicas e Ingeniería

TITULO: Design of an Exoskeleton Prototype for Lower Limb Rehabilitation

Trabajo de integración curricular presentado como requisito para la obtención del título de Ingeniera Biomédica

Autor:

Avila Briones, Laura Nicole

Tutor:

Mgs. Villalba Meneses, Gandhi Fernando

Co-tutor:

Ph.D. Andrés Tirado

Urcuqui, abril 2024

AUTORÍA

Yo, **LAURA NICOLE AVILA BRIONES**, con cédula de identidad 1315344653, declaro que las ideas, juicios, valoraciones, interpretaciones, consultas bibliográficas, definiciones y conceptualizaciones expuestas en el presente trabajo; así cómo, los procedimientos y herramientas utilizadas en la investigación, son de absoluta responsabilidad de el/la autora (a) del trabajo de integración curricular. Así mismo, me acojo a los reglamentos internos de la Universidad de Investigación de Tecnología Experimental Yachay.

Urcuquí, abril 2024.

Firmado electrónicamente por:
LAURA NICOLE AVILA BRIONES

Laura Nicole Avila Briones

CI: 1315344653

AUTORIZACIÓN DE PUBLICACIÓN

Yo, **LAURA NICOLE AVILA BRIONES,** con cédula de identidad 1315344653, cedo a la Universidad de Investigación de Tecnología Experimental Yachay, los derechos de publicación de la presente obra, sin que deba haber un reconocimiento económico por este concepto. Declaro además que el texto del presente trabajo de titulación no podrá ser cedido a ninguna empresa editorial para su publicación u otros fines, sin contar previamente con la autorización escrita de la Universidad.

Asimismo, autorizo a la Universidad que realice la digitalización y publicación de este trabajo de integración curricular en el repositorio virtual, de conformidad a lo dispuesto en el Art. 144 de la Ley Orgánica de Educación Superior

Urcuquí, abril 2024.

Firmado electrónicamente por:
LAURA NICOLE AVILA BRIONES

Laura Nicole Avila Briones

CI: 1315344653

Agradecimiento

Quiero expresar mi más sincero agradecimiento a todos los que han sido parte de esta trayectoria universitaria. Primero, a mis padres y hermanos por su apoyo inquebrantable y su creencia en mis aspiraciones académicas, siendo mi firme ancla. También quiero agradecer a mis mascotas Oscar y Floky por su compañía.

A Ariana, gracias por ser esa amistad constante y por siempre estar ahí cada vez que regresaba a casa.

Un agradecimiento especial a mi novio, Mario, por su apoyo inquebrantable y su creencia en mis habilidades. A mis amigos que hice en mi vida universitaria, especialmente a Ronny e Isaac, su amistad tiene un lugar especial en mi corazón.

Mi más sincero agradecimiento a mi tutor de tesis, Fernando Villalba, por su orientación y retroalimentación constructiva.

Estoy profundamente agradecida por las contribuciones colectivas de estas personas, las cuales han desempeñado un papel integral en mi trayectoria académica.

Laura Nicole Avila Briones

Resumen

CONADIS indica que el 45,66% de las personas registradas con discapacidad en el Ecuador presentan deficiencias físicas. Gran parte está en edad laboral y tiene una calidad de vida degenerada. De estos, una cantidad considerable de discapacidades físicas, como las de las extremidades inferiores, se deben a daños en el cerebro o la médula espinal. Dada su frecuencia y los intentos de aliviarlos, varias soluciones de tratamiento intentan devolver la movilidad y el bienestar al afectado, desencadenando el desarrollo de exoesqueletos de la cojera inferior. El presente proyecto persigue la creación de un prototipo similar. Softwares CAE-CAD adecuados ayudarán, como SolidWorks, al diseño estructural, y un análisis de elementos finitos garantizará su integridad. Además, utilizando Simscape Multibody de Simulink, el sistema de control se simulará mediante una acción de bucle abierto.

Las evaluaciones preliminares, que incluyen la comparación de los movimientos en ambos modelos, es decir, los de Opensim y Simulink, respaldan una alta similitud y, por lo tanto, el diseño es válido. Además, el FEA con una tensión de Von Mises de 3,697e+00 N/m^2, un desplazamiento resultante de 2,778e-01 mm y la deformación equivalente de 2,686e-05 proporcionan la información necesaria. El análisis del factor de seguridad revela la seguridad de la estructura, obteniéndose así el factor 2.229e+01 y 1.903e+07. La integración exitosa de métodos avanzados en forma de herramientas y softwares avanzados contribuirá en gran medida a garantizar que se aborde el requisito más crucial de la rehabilitación avanzada de las extremidades inferiores. Este prototipo logrará ser funcional y, en última instancia, mejorará el nivel de vida de las personas.

Palabras clave: Tecnología de exoesqueletos, Movilidad humana, Simulink, Exoesqueleto de miembros inferiores, Análisis de Elementos Finitos, SolidWorks

Abstract

CONADIS indicates that 45.66% of people registered with disabilities in Ecuador have physical impairments. A great part is within the labor force's age and have degenerated quality of life. From these, a considerable amount of physical impairments such as those on the lower limbs is caused by damage to the brain or spinal cord. Given their frequency and the attempts to alleviate them, several treatment solutions try to return mobility and well-being to the affected, triggering the development of exoskeletons for the lower limp. The present project pursues the creation of a similar prototype. Suitable CAE-CAD software will help, like SolidWorks, to structural design, and a finite element analysis will guarantee its integrity. In addition, using Simulink's Simscape Multibody, the control system will be simulated through open-loop action.

The preliminary assessments, which include comparing the movements in both the models, that is the Opensim and Simulink models, support high similarity, and hence the above design is valid. Also, the FEA with Von Mises stress of 3.697e+00 N/m^2, resultant displacement of 2.778e-01 mm, and the equivalent strain of 2.686e-05, provide the necessary insights. The safety factor analysis reveals the safety of the structure, and the 2.229e+01 factor and 1.903e+07 is thus obtained. The successful integration of advanced methods in the form of software tools and methodologies will highly contribute to ensuring that the most crucial requirement of advanced lower limb rehabilitation. This prototype will achieve the functional requirement, ultimately improving the standard of life for.

Keywords: Exoskeleton technology, Human mobility, Simulink, Lower limb exoskeleton, Finite Element Analysis, SolidWorks

Content

List of Figures

List of Tables

List of Abbreviations

3D: Three Dimensional

BLEEX: Berkeley Lower Extremity Exoskeleton

CAD: Computer-Aided Design

CAM: Computer-Aided Manufacturing

CAE: Computer-Aided Engineering

CONADIS: Consejo Nacional para la Igualdad de Discapacidades

DC: Direct current

DoF: Degree of Freedom

EEG: electromyography

EMG: electroencephalography

ESTRN: Equivalent strain

FEA: Finite Element Analysis

HAL: Hybrid Assisted Limb

PDMs: Product Data Management

QFD: Quality Function Deployment

SEA: Series Elastic Actuation

URES: Resultant Displacements

VON: Von Misses Stress

WHO: World Health Organization

XML: eXtensible Markup Language

Chapter 1: Introduction

This chapter will address the prevalence of disability and the importance of using lower limb exoskeletons as a potential solution to improve the quality of life for individuals with mobility impairments. The use of exoskeletons can provide numerous benefits, including increased mobility and independence, reduced fatigue and strain on the body, and improved overall health and well-being. Therefore, understanding the problem and the potential solutions available through the use of exoskeletons is crucial in addressing the needs of individuals with mobility impairments. Additionally, both the general and specific objectives behind the current project will be presented.

1.1.Thesis Overview

The field of exoskeleton technology has seen remarkable advancements in recent years, offering the potential to revolutionize human mobility and assistance. This thesis embarks on a comprehensive exploration of exoskeletons, from understanding their fundamental principles to applying advanced methodologies for design and analysis.

Chapter 1 lays the foundation, providing an in-depth description of the problem and justifying the need to address it. The objectives of this study, both general and specific, are outlined, setting the stage for a systematic investigation into exoskeleton technology.

In Chapter 2, the complexities of exoskeletons are unraveled. The walking process, or gait cycle, is dissected to grasp the intricacies of human locomotion. An exploration of joints and degrees of freedom within exoskeletons sheds light on the mechanical intricacies of these wearable devices. The chapter also categorizes various types of lower limb exoskeletons and defines the essential requirements for their design.

Chapter 3 delves into the methodology employed in this study. It elucidates the process of data selection based on human anthropometry, introduces biomechanical analysis using OpenSim, and outlines the criteria for model selection in line with predefined requirements. Additionally, this chapter covers structural design and the application of Finite Element Analysis (FEA) within SolidWorks, providing a comprehensive view of the research methodology.

Chapter 4 bridges theory and practice by presenting the results of Simulink simulations and engaging in comprehensive discussions. These discussions explore the implications of the findings, bringing us closer to unlocking the true potential of exoskeleton technology.

Through this thesis, the aim is to contribute to the ongoing evolution of exoskeleton technology, pushing the boundaries of what is possible in human mobility assistance and paving the way for a more inclusive and accessible future.

1.2.Description of the problem

According to the World Health Organization (WHO), disability is an issue that affects people of all ages economically and socially. About 15% of the world's population has experienced having a disability and statistics show that this percentage has increased over time (*Disability*, n.d.). In Ecuador, the figure for the prevalence of disability has increased in the last decade from 0.28% in 2001 to 2,67% in 2021 (Figure 1), where 54.16% belong to the age group from 25 years to 64 years (Consejo Nacional para la Igualdad de Discapacidades, 2021). Moreover, according to statistics, there is a higher percentage of people with physical disabilities, being 45.66% of the Ecuadorian population reported with disabilities (Consejo Nacional para la Igualdad de Discapacidades, 2021). Today there are multiple causes for physical and motor disability, including

spinal injuries, strokes, and degenerative conditions of the spinal cord as the most common causes(Giannini et al., 2010; Tsao et al., 2022).

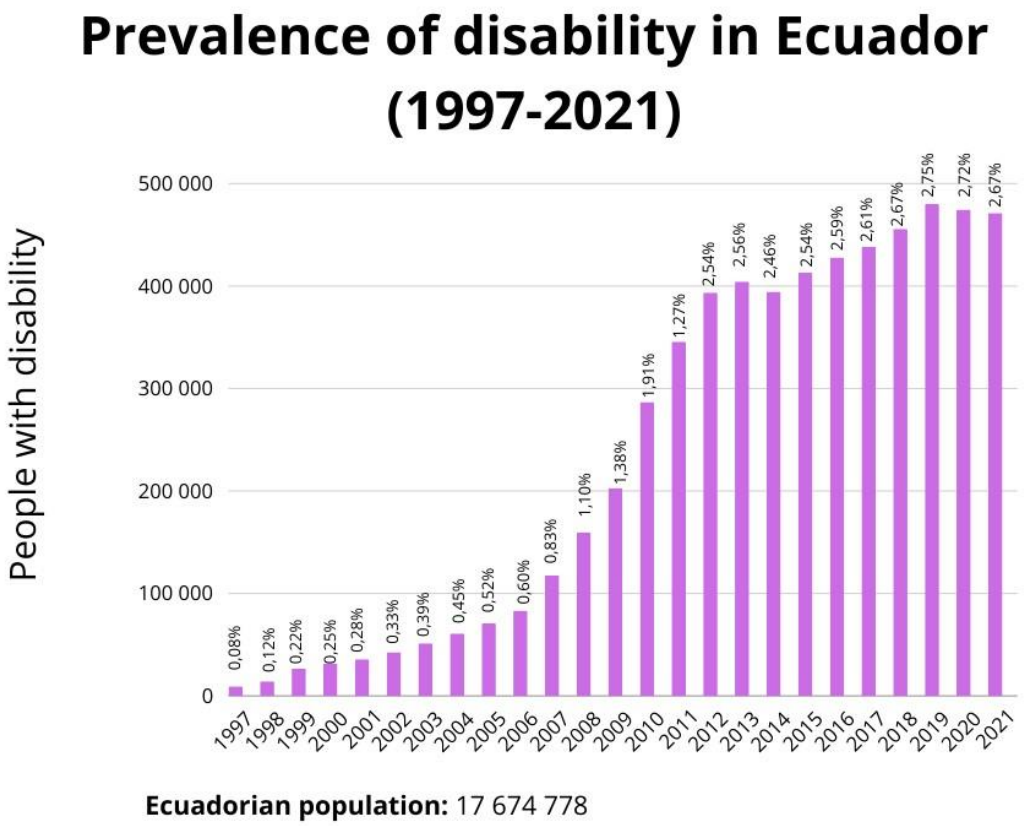

Figure 1: *Prevalence of disability in Ecuador every year*

Note: Prevalence of disability in Ecuador from 1997 to 2021. By Consejo Nacional para la Igualdad de Discapacidades, (CONADIS). (2021). Estadísticas de Discapacidad Consejo Nacional para la Igualdad de Discapacidades. *Ministerio de Salud Pública.*

Today, to a large extent, these cases are treated through rehabilitation processes; manually, physiotherapists require an arduous physical effort to carry out the treatment. This also leads to staff burnout (Bejer et al., 2019; Pniak et al., 2021; Śliwiński et al., 2014). Moreover, there are many barriers that do not allow full access to physical therapy. For example, that there is not enough money, the necessary equipment does not exist, or physical barriers as location (Aparecida Padilha Clemente et al., n.d.; Mlenzana et al., 2013). This affects the daily lives of those affected.

The complexity of the execution of the different treatments, the increase in the number of patients to be treated, the intense physical activities and the overexertion carried out by the physiotherapist, and the barriers to do not allow the treatment opens the possibility of errors and mistakes, which consequently could produce side effects in the muscles and patient's joints.

1.3 Justification of the problem

Currently, technological advances in robotics have led to the design and use of exoskeletons for medical applications this being a powerful tool for rehabilitation(Bortole et al., 2015; Iwamoto et al., 2019; Rehmat et al., 2018; Shi et al., 2019; Vaughan-Graham et al., 2020; Xue et al., 2022). Therefore, exoskeletons provide assistance that enhances the physical qualities of patients with neurological diseases such as spinal injuries, strokes and degenerative conditions of the spinal cord, allowing an increase in their strength, resistance and reduce fatigue thus improving their functionality of the upper and lower limbs.

In human gait, lower limbs play an important role, because those generate more torque than the other parts while walking (Pamungkas et al., 2019).

The best-known lower limb exoskeletons for rehabilitation and improving the lifestyle of patients are the exoskeletons of: starting by Berkeley Lower Extremity Exoskeleton (BLEEX) (A. B. Zoss et al., 2006), ReWalk (Awad et al., 2020; Esquenazi et al., 2012; Foerster, 2015), Ekso Bionics (Bach Baunsgaard et al., 2017; Read et al., 2020; Stearns-Yoder & Brenner, 2018). Lokomat(Alashram et al., 2021; Baronchelli et al., 2021; Nam et al., 2017), and Hybrid Assistive Limb (HAL) (Grüneberg, 2021; Taki et al., 2022; Yoshioka et al., 2021). And the success of these devices comes from both design and automation systems, giving the patient comfort, ergonomics, and improved mobility of these extremities. However, the access to them could be expensive and

delayed. For that reason, the present work seeks to design an active exoskeleton for lower limb rehabilitation in adults. For this it will be used software for its 3D design and mechatronic analysis.

1.4 Objectives

1.4.1 General objective

Design the mechanical structure of an adjustable lower limb active exoskeleton for adults and implement an automation system for it.

1.4.2 Specific objectives

- To design a 3D model in SOLIDWORKS of lower limb exoskeleton for adults using the concurrent design method.
- Evaluate control strategies using the OpenSim, and MATLAB to demonstrate the effectiveness of the proposed control method.
- Obtain a functional and safe prototype of the exoskeleton that fits the anthropometry of adults.

Chapter 2: Understanding exoskeletons

In this chapter, we will dig into various fundamental concepts necessary for understanding the functioning of lower limb exoskeletons. These concepts will include the gait cycle, joint mechanics and degrees of freedom in the legs, types of lower limb exoskeletons, guidelines for concurrent engineering and related works. By exploring these topics, we can gain a profounder understanding of the complex mechanisms and principles underlying exoskeleton design and operation, which can ultimately lead to more effective and efficient engineering solutions.

2.1. Walking process or gait cycle

First, to understand the kinematics of exoskeletons, it is important to study the human gait cycle. This can be separated into two primary phases, stance phase and swing phase. The Stance phase takes the 60 to 62% of the entire gait cycle, and is the phase in which the leg is in the floor. On the other hand, the swing phase takes the 38% to 40% of the gait cycle (Schmeltzpfenning & Brauner, 2013). Also, the gait cycle can be divided into eight phases. Which are: initial contact, loading response, midstance, terminal stance, pre swing, initial swing or toe off, mid swing, and terminal or late swing (Nandy et al., 2021). These phases occur in that order and are interspersed on each leg.

The descriptions of the eight phases of the gait are the following based on (Kharb et al., 2011).

2.1.1. Initial contact: During this phase, the reference limb shows a flexed hip, an extended knee, and a dorsiflexed ankle in a neutral position. The heel makes contact with the floor, while the other limb is in the terminal stance. The loading response pattern of the limb is determined by the

joint postures at the moment when the foot just touches the floor, which is depicted by the shading in the diagram (Kharb et al., 2011).

2.1.2. Loading response: During the loading response phase, the body weight is shifted onto the limb that moves forward. The heel acts as a rocker and the knee is flexed to absorb the shock. The ankle's plantar flexion prevents excessive heel rocking by making contact with the floor with the forefoot. At this point, the other limb is in the pre-swing phase, and this marks the beginning of the double stance period. This phase starts when the foot touches the floor and lasts until the other foot is lifted for the swing(Kharb et al., 2011).

2.1.3. Midstance: During the first half of the single limb support phase, the limb moves forward over the stationary foot by dorsiflexing the ankle (using the ankle as a rocker) while the knee and hip extend. At this time, the opposite limb is in its mid swing phase. This phase starts when the other foot is lifted and lasts until the body weight is centered over the forefoot (Kharb et al., 2011).

2.1.4. Terminal stance: During the second half of single limb support, the limb advances over the forefoot rocker as the heel lifts. The knee extends further and then slightly flexes again. The limb moves to a more trailing position due to increased hip extension. The opposite limb is in its terminal swing phase. This phase marks the end of single limb support and starts with the heel rise, continuing until the opposite foot hits the ground. Throughout this phase, the body weight is shifting forward (Kharb et al., 2011).

2.1.5. Pre swing: Phase 5, known as Pre-Swing, is initiated by the start of terminal double support caused by the other limb making floor contact. The reference limb responds by increasing ankle plantar flexion, increasing knee flexion, and losing hip extension. The opposite limb is in

Loading Response. This phase is the second terminal double stance interval in the gait cycle and begins with the initial contact of the opposite limb and ends with ipsilateral toe-off. It is also known as the weight release and weight transfer phase. Although the abrupt transfer of body weight unloads the limb, the unloaded limb does not actively contribute to the event. Instead, it uses its freedom to prepare for the rapid demands of swing. All the motions and muscle actions that occur at this time are related to the latter task (Kharb et al., 2011).

2.1.6. Initial swing or toe off: The limb is propelled forward through a combination of hip flexion and increased knee flexion, lifting the foot off the ground. The ankle undergoes partial dorsiflexion during this phase, while the other limb is in its early mid stance. This phase lasts about one-third of the entire swing period and begins when the foot is lifted off the ground, ending when the swinging foot reaches the same position as the stance foot (Kharb et al., 2011).

2.1.7. Mid swing: The limb is brought forward in front of the body weight line through additional hip flexion. The knee is permitted to extend passively due to gravity while the ankle maintains a neutral dorsiflexion position. The other limb is in the late mid stance phase. This is the second phase of the swing period and starts when the swinging limb is opposite the stance limb. The phase finishes when the swinging limb is forward and the tibia is vertical, meaning the hip and knee flexion postures are equal (Kharb et al., 2011).

2.1.8. Terminal or late swing: In this phase, the limb is moved forward by flexing the knee while keeping the hip in its previously flexed position and the ankle in a neutral dorsiflexed position. Meanwhile, the other limb is in the terminal stance phase. This phase marks the end of the swing period and begins with a vertical tibia, ending with the foot making contact with the ground. Limb advancement is completed as the shank moves ahead of the thigh. See the accompanying figure for a visual representation (Kharb et al., 2011).

As example, in figure 2 can be observed the gait cycle with right and left legs. In 1, right leg is in the initial contact phase, and left leg is the pre swing phase. Then, in 2 right leg is in loading response phase and left leg is in initial swing phase. In 3, right leg is in the midstance and the left leg is in the mid swing phase. In 4, right leg is in terminal stance phase and left leg is in terminal or late swing. In 5, right leg is in the pre swing phase and left leg is in initial contact phase. Then, in 6 right leg is in initial swing and left leg is in loading response phase. Subsequently, in 7 right leg is in mid swing phase and left leg is in midstance phase. And finally, in 8 right left is in terminal swing phase while left leg is in terminal stance. Then, the cycle is repeated.

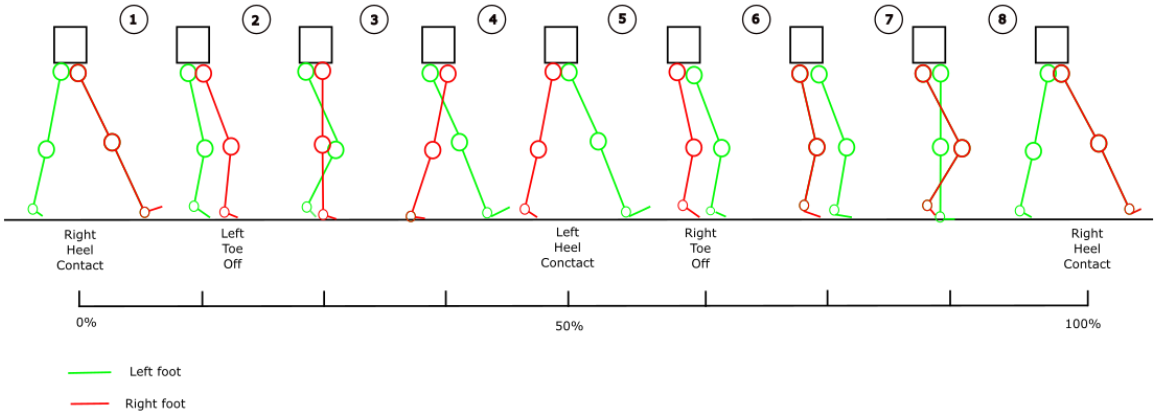

***Figure 2**: Human gait analysis. With right and left legs with eight phases.*

Note: Phase 1 corresponds to 2.1.1, phase 2 corresponds to 2.1.2, phase 3 corresponds to 2.1.3, phase 4 corresponds to 2.1.4, phase 5 corresponds to 2.1.5, phase 6 corresponds to 2.1.6, phase 7 corresponds to 2.1.7, and phase 8 corresponds to 2.1.8.

2.2 Joints and degree of freedom found in an exoskeleton

Nowadays, The Exoskeletons for human body has three principal group of joints in the lower limbs. These are the hip, knees and ankles, and each one has its movements or degrees of freedom. For example, the hip has three Degrees of Freedom (DoF), the knee has two DoF, and the

ankle has three DoF (Kalita et al., 2021). The summary of the movement and the degree of freedom will be indicated in the following table (Table 1).

Table 1

Summary of Degrees of Freedom (DoF) and movements of each lower limb joint

Joint	**DoF**	**Movements**
Hip	3	Abduction-adduction Flexion-Extension Internal-External rotation
Knee	2	Flexion- Extension Rotation
Ankle	3	Plantar flexion-dorsiflexion Abduction-adduction Eversion-Inversion

Note: DoF; Degree of freedom

The dominant movements of legs take place in the sagittal plane. So, researchers have focused and simplified the DoF into three or two. This includes flexion and extension of hips and knee joints, and plantar flexion and dorsiflexion for ankle joint. However, this simplification makes the device less useful for the final users. For that reason, it has been sought to include more mobility in the exoskeletons of the lower limbs. Those includes exoskeleton with 5 DoF, 6 DoF and 7 DoF.

2.3 Types of lower limb exoskeletons

Lower limb exoskeletons are devices that can be worn to aid individuals with mobility impairments while walking and standing (Moeller et al., 2023). Various types of lower limb exoskeletons are available, each with their own specific advantages and benefits. As in figure 3 is

shown, the types can be classified into powered, unpowered and hybrid and the classification according its joints.

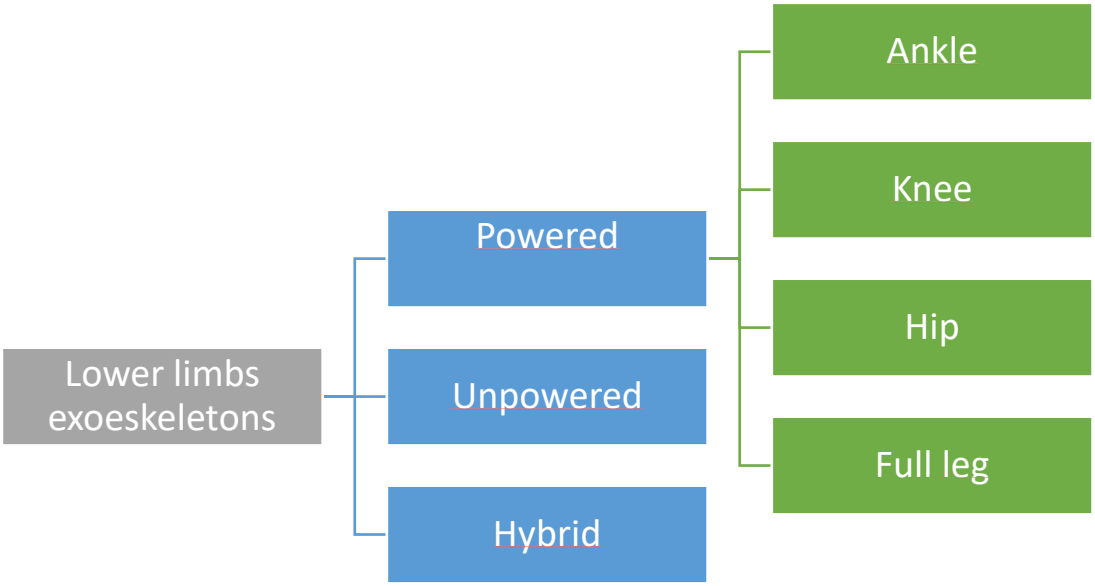

Figure 3: *Classification of lower limb exoskeletons.*

Here are definitions of the most commons types:

- **Powered Knee Exoskeletons:** These exoskeletons are created to provide additional support to the knee joint (Villa-Parra et al., 2015). They frequently feature a brace that is worn around the knee and thigh, along with a motorized component that provides extra power to the leg (Arazpour et al., 2015; Varghese et al., 2017). These can be used by individuals with knee weakness or instability, as well as those with lower limb paralysis (Chen et al., 2019).
- **Powered Ankle Exoskeletons:** These types of exoskeletons are created to provide additional support to the ankle joint (Kian et al., 2022). They commonlly consist of a brace that is worn around the ankle and foot, along with a motorized component

that provides extra power to the foot. These can be used by individuals with ankle weakness or instability, as well as those with lower limb paralysis(Chang et al., 2015).

- **Powered hip exoskeleton:** These are wearable devices that use different kinds of motors. Hydraulics, or other types of actuators to provide additional support and assistance during movements that involve the hips and lower limbs. They can be used in a variety of applications such as rehabilitation, physical therapy, industrial settings, and military applications.
- **Full-Leg Exoskeletons:** These exoskeletons provide additional support to the entire lower limb, from the hip to the ankle (T. Wang et al., 2022). They typically feature a set of motorized legs that are worn over the user's own legs. Full-leg exoskeletons can be used by individuals with mobility impairments, including those with spinal cord injuries, stroke, and muscular dystrophy (T. Wang et al., 2022).
- **Hybrid Exoskeletons:** These exoskeletons are a combination of powered and unpowered exoskeletons, providing the advantages of both (Aguilar-Sierra et al., 2014). They generally consist of a support that is worn around the leg, along with a combination of passive and active components (actuators) that provide support and assistance. Hybrid exoskeletons can be used by individuals with mild to moderate mobility impairments, as well as people who require assistance with balance and stability.

The choice of which type of lower limb exoskeleton to use will depend on the needs and abilities of the user, as each type has its own set of benefits and drawbacks. With ongoing research

and development, we can anticipate even more innovative types of lower limb exoskeletons in the future.

2.4. Requirements for a lower limb exoskeleton

In general, designing an exoskeleton requires consideration of several factors. Even in a lower limb exoskeleton. For the design is important to know the voice of the engineer and the user voice according to (Riba Romeva, 2002)

2.4.1. User voice

It is responsible for delivering the characteristics that the finished product must have, and those characteristics are the following:

- Easy to use
- It allows movements
- With a long lifespan
- Battery that last a long time
- Secure
- That fits to the user
- Not too heavy
- Cheap and easy to maintain
- Relivable

2.4.2. Voice of the engineer:

This is responsible for technically transforming the requirements of the user voice, and obtaining the following characteristics to determine the exoskeleton (Riba Romeva, 2002).

- **Comfort:** The exoskeleton must be comfortable, with padding in appropriate areas and may need adjustable straps to fit various body sizes (Minchala et al., 2017).
- **Mobility:** The exoskeleton must not impede the wearer's natural movement or range of motion (Dragusanu et al., 2022).
- **Durability:** The exoskeleton should be designed to withstand regular use and the wear and tear associated with movement. According to estimates, the lifespan of an Ekso exoskeleton device, which comes with rechargeable batteries, can be up to four years if regular maintenance is performed. These estimates take into account the usage of Ekso, which is typically six to eight times per day, with an average usage duration of one hour (*The Technology | Ekso Exoskeleton for Rehabilitation in People with Neurological Weakness or Paralysis | Advice | NICE*, n.d.).
- **Power source:** The exoskeleton needs a reliable power source, such as a battery or rechargeable energy source (Minchala et al., 2017).
- **Control system:** The exoskeleton requires a user-friendly control system that enables the wearer to operate it intuitively (Dragusanu et al., 2022).
- **Safety:** The exoskeleton must be designed with safety in mind, with features such as emergency stops and impact-resistant materials (Nugent & van der Vorm, 2015).
- **Weight:** The exoskeleton should be lightweight to minimize user fatigue and reduce the overall load on the wearer's legs (Dragusanu et al., 2022).
- **Customization:** The exoskeleton should be designed to allow for customization and adjustments to fit individual user needs and preferences.
- **Cost:** The exoskeleton should be affordable for potential users. Some developers consider some types of actuators to reduce costs such as electrical actuator (Minchala

et al., 2019; U & Rajendrakumar, 2021). It also minimizes the maintenance cost of the device and gives it an ease of maintenance.

- **Compliance:** The exoskeleton should be designed to meet regulatory and legal requirements for medical devices, including any necessary certifications and approvals (Nugent & van der Vorm, 2015).

These concepts will help us to develop the conceptual design of the exoskeleton and evaluate the existing alternatives for the prototype design. Conceptual design is a very important step for concurrent design.

2.5. Lower Limb Exoskeletons in Rehabilitation

This section explores the current state of development of exoskeletons specifically tailored for lower limb rehabilitation. It will explore various designs, technologies, and approaches alongside an analysis of their effectiveness and limitations.

As is known in the field of rehabilitation, exoskeletons help people with disabilities perform movements that would otherwise be challenging or impossible. For example, the Hank exoskeleton, with a CE mark in Europe as a medical device, stands out for having six motorized joints, an adaptive gait pattern, and the ability to be controlled either manually (by tablet) or by voice command (Megía-García et al., 2022). One important feature to mention is the motorized ankle, which is essential to avoid drop foot and equine foot stations, as well as being necessary for the impulse at the beginning of the swinging phase and key to maintaining balance.

Another example is the Angel Legs M20, developed by Angel Robotics, which operates as an exoskeleton walking assistance robot designed for gait rehabilitation, especially for patients with incomplete paraplegia undergoing walking therapy (Rahman & Shamsuddin, 2023). Remarkable

features include 7 DoF adjustable length, real-time training monitoring, and the fact that it does not require a body sensor like some other exoskeletons.

Andago V2.0, developed by Hocoma, is an exoskeleton that combines self-directed gait, body weight support, and mobility to facilitate intensive training of various functional mobility and balance tasks (Marks et al., 2019). This technology can be used by therapists to safely perform overground gait and balance training on patients with walking balance impairments. Some key features include active patient-following, upright and hands-free gait, and safe and efficient therapy. This option stands as a practical choice for rehabilitation centers.

The MindWalker exoskeleton is a ground-breaking achievement at the intersection of technology and medicine. This technology is controlled by brain signals and represents the first of its kind. It uses bioelectrical signals (like EEG and EMG) and non-bioelectrical signals (like accelerometers, load cells, and encoders) to perform the movement of the lower limbs (S. Wang et al., 2015). Its actuators are designed using the principle of Series Elastic Actuation (SEA) and provide support for hip adduction, hip flexion/extension, and knee flexion/extensions.

These devices are designed to be increasingly lighter, more ergonomic, and more efficient, with the aim of integrating effectively into users' daily activities and improving their quality of life.

2.6. Design Methods for Prototyping of Lower Limb Exoskeletons for Rehabilitation

In this section, it will be detailed and analyzed design methodologies employed in the design of prototypes of exoskeletons for lower limb rehabilitation, with a particular focus on concurrent engineering principles. Concurrent design is an engineering approach that integrates multiple perspectives throughout the design process and product or service development. This

approach simultaneously considers functional and manufacturing requirements, as well as other aspects such as quality, maintenance and environmental impacts.

The prototyping and design method, applied in an exoskeleton can be related to the concepts of concurrent engineering and rapid prototyping mentioned in the context of the website. Concurrent engineering is a way of conceiving the design and development engineering of products globally and interactively, where functional and manufacturing requirements are considered simultaneously (Riba Romeva, 2002). Here are some key points of concurrent design according to Riba Romeva.

First, both the product lifecycle requirements and the range of products manufactured by the company are integrated. Then, Computer- assisted tools such as CAD, CAE, and CAM are used for product design and development (Riba Romeva, 2002). Finally, the rapid prototyping techniques, as 3D printing methods, expedite the creation of prototypes. It facilitates the evaluation and validation of the design.

These techniques are particularly valuable in the development of the complex products like exoskeletons, where swift iteration and design validation are essential for ensuring the quality and functionality of the final product.

2.7. Previous Works on the Design of Exoskeleton Prototypes for Lower Limb Rehabilitation

This section will provide a comprehensive review and summary of past research, related projects, and pertinent literature concerning the design of prototypes of exoskeletons aimed at lower limb rehabilitation. By doing so, it will offer additional context for the project and facilitate its placement within the broader landscape of research and development in this specialized field.

In the following table (table 2), we can observe different examples of lower limb exoskeletons

Table 2

Examples of lower limb exoskeletons

Type (according to articulation)	Name	Type of actuator	DoF	Reference
Ankle-Knee	Wake-up	Active- DC motors	2	(Rossi et al., 2014)
Ankle	Harvard University	Active- Pneumatics	2	(Park et al., 2011)
Hip-knee	No specified	Passive- springs	2	(Zhou et al., 2020)
Hip-ankle	LOPES	Active- DC motors	3	(Veneman et al., 2007)
Hip-knee-ankle	ALLEX	Active- DC motors	4	(Minchala et al., 2019)
Hip-knee-ankle	Ekso bionics lower limb exoeskeleton	Active- DC motors	6	(Gardner et al., 2017)
Hip-knee-ankle	BLEEX	Active- hydraulic- and passive-spring	7	(A. Zoss et al., 2005)
Hip-knee-ankle	Centre for Advanced Robotics Research	Active- pneumatic and electric	10	(N. R. S. Costa & Caldwell, 2006)

Note: DoF: Degree of freedom. DC: Direct current.

The table shows a variety of lower limb exoskeletons for rehabilitation, organized according to the main joint and type of actuator used. Firstly, devices designed for the ankle and knee joint are included, such as the "Wake-up" with active actuator (DC motors)(Rossi et al., 2014), and the Harvard University exoskeleton with active pneumatic actuators(Park et al., 2011). Next, devices for the hip and knee, such as an unspecified one with passive springs, are presented. Additionally,

devices spanning the hip, knee, and ankle, like the "LOPES" with active DC motors(Veneman et al., 2007) and the "ALLEX" with the same active motors, are shown(Minchala et al., 2017). Other devices, such as the Ekso Bionics lower limb exoskeleton, demonstrate a higher number of Degrees of Freedom (DoF) and utilize active DC motors (Gardner et al., 2017). Finally, more complex exoskeletons, like the "BLEEX" with active hydraulic actuators and passive springs (A. Zoss et al., 2005), and the device from the Centre for Advanced Robotics Research, which uses active pneumatic and electric actuators and has a high number of DoF, are presented (N. Costa & Caldwell, 2006).

Chapter 3: Methodology

In figure 4 is detailed the methodology of the present work. It is detailed in six stages.

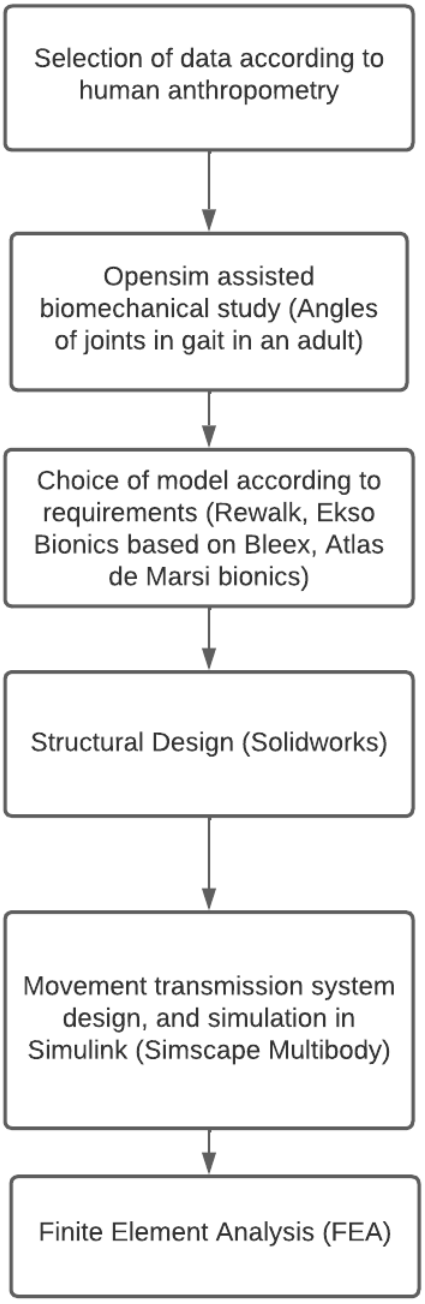

Figure 4: *Mental map of the methodology.*

3.1. Selection of data according to human anthropometry

Anthropometry is the scientific study of human body measurements and proportions. It involves the measurement of various aspects of the human body, such as height, weight, body mass index (BMI), waist circumference, and limb lengths (Tovée, 2012). Anthropometry can be used to determine a range of physical characteristics, including body composition, muscle strength, and flexibility. This information can be used in a variety of fields, including medicine, sports science, ergonomics, and industrial design. In this case, for a lower limb exoskeleton design (Alemany et al., 2022).

Anthropometry can vary for several reasons, including genetic factors, age, gender, ethnicity, geographical location, and lifestyle. Body size and shape are largely determined by genetics, and traits such as height, limb lengths, and body proportions are influenced by genes(Brolin, n.d.). Age-related changes, such as growth and development in children and changes in body composition and bone density in older adults, can also affect anthropometry. Additionally, sex can play a role in anthropometry, with males generally having different body sizes and proportions than females. Ethnicity and geographic location may also have an impact, as environmental factors and genetic backgrounds can vary between populations. Lifestyle factors like diet, physical activity, and occupation can also influence anthropometry, with individuals who lead an active lifestyle and have a healthy diet likely having different measurements than those with a sedentary lifestyle and poor eating habits.

For this reason, the study will use information from a population located near Ecuador, compiling anthropometric data from four Latin American countries. The design of the exoskeleton will use measurements from a sample of 2,100 individuals from both sexes in Colombia. (Avila Chaurand et al., 2015) (See APPENDIX A).

3.2. OpenSim assisted biomechanical study

OpenSim is an open-source software platform for creating and simulating musculoskeletal models of the human body. Model 2392 is one of the many musculoskeletal models available in the OpenSim repository. This model, specifically, is a full-body musculoskeletal model of an average male with 92 Degrees of Freedom (DoF).

The OpenSim model 2392 includes models of the bones, joints, ligaments, and muscles of the body. The bones are represented by rigid bodies, and the joints are modeled as idealized joints with one or more DoF (Seth & Anderson, 2017). The ligaments are represented as nonlinear springs, and the muscles are represented as Hill-type muscle models.

The model has been widely validated and can be used to simulate a wide range of movements and activities, such as walking, running, and jumping. It can also be used to study the effects of different interventions, such as surgical procedures or the use of assistive devices.

Overall, OpenSim model 2392 is a powerful tool for studying human movement and can be used in a variety of research and clinical applications. In the present project t is necessary the data of angles of hip rotation, hip adduction, hip flexion, knee flexion/extension, and ankle flexion/extension (See APPENDIX B).

3.3. Choice of model according to requirements

In this section, we will make a well-informed decision regarding the selection of an exoskeleton model based on our established requirements and evaluation criteria. It has been identified three distinct exoskeleton models, each with its own unique features and capabilities.

The aim is to carefully assess these models and determine which one aligns most closely with our predefined requirements and criteria. The evaluation process will help us make a judicious

choice that optimizes the design for its intended purpose and ensures it meets the desired specifications and performance metrics.

Through a systematic analysis of the models using the Corrected Ordinal Method of Weighted Criteria, we will derive insights that guide us toward selecting the most suitable exoskeleton model for our project. This choice will ultimately contribute to the successful realization of our goals and objectives in developing an effective and efficient exoskeleton system.

3.3.1. Selection of requirements

In section 2.4 it was described some features of exoskeleton. For this, it is necessary to apply concurrent design. It is necessary to use a Quality Function Deployment (QFD) matrix. The results in the figure 5 was made with the requirements given by Riba (Riba Romeva, 2002).

			Functional Requirements											
		Direction of Improvement	□	□	□	▲			▲	▲	▼	Competitive		
Relative Weight	Customer Importance	Customer Requirements	Comfort	Mobility	Durability	Power source	Safety	Customization	Weight	Cost	Compliance	Our Product	Competitor 1	Competitor 2
12%	6	Easy to use	●	○				○		▽		1	4	3
18%	9	It allows movements	○	●			●	○	▽		▽	1	3	3
12%	6	With a long lifepan	▽	▽	●	○	●	▽	▽	●	○	1	4	4
16%	8	Battery that last a long time	●	▽	○	●	▽		▽	○	○	1	2	2
4%	2	Secure	○	▽	▽		●	▽	▽	▽	○	1	3	4
10%	5	That fits to the user	●	▽	▽	▽	▽	●	▽	○	▽	1	5	5
6%	3	Not too heavy	●	▽	▽	▽	▽		●	○	○	1	3	3
16%	8	Cheap and easy to maintain	○	▽	○	○	▽	▽		●		1	2	2
8%	4	Relivable	○	○	▽	▽	●				●	1	4	3
		Importance Rating Sum (Importance x	535,29	280	227	247	418	208	112	357	210			
		Relative Weight	21%	11%	9%	10%	16%	8%	4%	14%	8%			
		Our Product	1	1	1	1	1	1	1	1	1			
		Competitor 1	4	3	4	2	3	5	3	2	4			
		Competitor 2	3	3	4	2	4	5	3	2	3			
		Technical Competitive Assessment												

Correlations	
Positive	+
Negative	-
No Correlation	

Relationships		Weight
Strong	●	9
Medium	○	3
Weak	▽	1

Direction of Improvemen	
Maximize	▲
Target	□
Minimize	▼

Figure 5: *QFD matrix*

In this study will be considered three main characteristics: Comfort, Safety and cost. This is because the decision of the prototype model is based in three preexistent exoskeletons from free patents.

3.3.2 Selection of the model

It will be considered three models of exoskeletons. Then, they will be evaluated by Corrected ordinal method of weighted criteria (Riba Romeva, 2002)

Model 1 belongs to patent ES2575255A1 from Marsi Bionics. The present invention refers to an exoskeleton for human movement assistance, adjustable to the user in dimensions, tensions, and joint ranges. This adjustment can be manual or automatic. Its placement on the user can be in the anterior-posterior direction in the sagittal plane, and can be placed from lying down or sitting

without the need for functional transfer. The exoskeleton features a modular design, compatible with human biomechanics, which reproduces natural and physiological movement in the user, with up to 6 degrees of mobility actuated and controlled by limb, guaranteeing user balance stability during locomotion.

On the other hand, model 2 belongs to the US8070700B2 document. It is a patent for a lower limb exoskeleton developed at the University of California, Berkeley. The exoskeleton is designed to assist individuals with lower limb impairments in walking and standing, and features a modular design that can be adjusted to fit users of different sizes and needs. The exoskeleton has three degrees of freedom at the hip and knee joints, allowing for movement in multiple directions, as well as one degree of freedom at the ankle joint. In total 7 degree of freedom. The device is powered by motors and controlled by a computer system that responds to the user's movements and helps to maintain balance and stability.

Model 3 belongs to US7153242B2 document. It is a patent for the "ReWalk" exoskeleton device, which is designed to assist individuals with lower limb paralysis or weakness to stand up and walk. This exoskeleton is a wearable robotic device that consists of a frame worn around the user's torso and legs, along with motorized joints that mimic the movement of human joints at the hips and knees. The device is controlled by a computer system that responds to the user's movements and balances their weight as they walk. The patent describes the mechanical and electronic components of the ReWalk exoskeleton, including the joint mechanisms, motors, and sensors that allow the device to operate. It also discusses the methods used to control the device and adjust it to fit the user's body size and gait pattern.

The ReWalk exoskeleton has been used in clinical settings to assist individuals with spinal cord injuries or other conditions that affect lower limb function. The device has been shown to

improve mobility, reduce the risk of secondary health complications, and enhance overall quality of life for individuals with lower limb paralysis or weakness.

3.3.2.1. Evaluation of solutions

The determination of a good design will depend on the analysis carried out on the proposed alternatives. These should not be focused on analyzing their appearance but on the design itself. For decision making, two important elements must be taken into account, which are the following:

•Alternatives: The alternatives must be at least two and whose characteristics must be different.

•Criteria: These should be taken on the basis of the evaluations that should be made to the alternatives.

We have both, the alternatives are the models explained above and the criterions are the results of the QDF matrix.

3.3.2.1.1. Corrected ordinal method of weighted criteria.

One of the ways to find a solution between different criteria is just to know the order of evaluation preference. The recommended method is the corrected ordinal method of weighted criteria, which does not need to perform the evaluation of parameters of each property and without the need to numerically estimate the weight of each criterion.

This method uses a table where it analyzes each criterion and at the same time it is related to the remaining most criteria and assigns the following values.

• 1 is determined whether the criterion (or solution) of the rows is higher (or better; >) than that of the columns (Riba Romeva, 2002).

• 0.5 is determined if the criterion (or solution) of the rows is equivalent (=) to that of the columns (Riba Romeva, 2002).

• 0 is determined if the criterion (or solution) of the rows is lower (or worse; <) than that of the columns (Riba Romeva, 2002).

Now it will be evaluated the criterions and give them a weighting value.

Table 3

Weighted criteria matrix

Criterion	**Comfort**	**Safety**	**Cost**	**Σ+1**	**weighting value**
Comfort		0,5	0,5	2	0,33
Safey	0,5		1	2,5	0,42
Cost	0,5	0		1,5	0,25
			Total	6	1

Table 4

Evaluation of the specific weight of the comfort criterion

Criterion	**Model 1**	**Model 2**	**Model 3**	**Σ+1**	**weighting value**
Model 1		0,5	0,5	2	0,31
Model 2	0,5		1	2,5	0,38
Model 3	0,5	0,5		2	0,31
			Total	6,5	1

Table 5

Assessment of the specific weight of the safety criterion

Criterion	**Model 1**	**Model 2**	**Model 3**	**Σ+1**	**weighting value**
Model 1		0,5	1	2,5	0,38
Model 2	0,5		1	2,5	0,38
Model 3	0	0,5		1,5	0,23
			Total	6,5	1

Table 6

Evaluation of the specific weight of the cost criterion

Criterion	**Model 1**	**Model 2**	**Model 3**	**Σ+1**	**weighting value**
Model 1		0,5	0,5	2	0,33
Model 2	0,5		0,5	2	0,33
Model 3	0,5	0,5		2	0,33
			Total	6	1

According to table 7, Model 2 is the best placed among the solutions.

Table 7

Conclusion table

	Comfort	**Safety**	**Cost**	**Σ**	**Priority**
Model 1	0,1025641	0,16025641	0,08333333	0,34615385	2
Model 2	0,12820513	0,16025641	0,08333333	0,37179487	1
Model 3	0,1025641	0,09615385	0,08333333	0,28205128	3

3.4. Structural Design

SolidWorks is a 3D CAD software program used for creating detailed 3D models of structures, products, and parts. It enables engineers and designers to simulate the structure's behavior under different conditions and loads, saving time and cost (*SOLIDWORKS | 3D CAD Design Software & PDM Systems,* n.d.). The design process begins with a basic shape or outline created through 2D sketches that are extruded to produce a 3D model, or through SolidWorks' 3D sketching tools. Features such as holes, chamfers, and fillets can be added to enhance functionality and aesthetics, created with tools such as extruding, revolving, sweeping, and lofting.

For this project, it was created several pieces in this software (See APPENDIX C). In total there were 15 piece to generate the desired movement. The following pictures will illustrate the part of the exoskeleton.

In Figure 6, it is shown the elements of the exoskeleton for hip joint in a posterior view. The hip part is divided into two pieces, one for each leg, plus one in the upper part of the pelvis. In Figure 7, it is shown a lateral view of the exoskeleton with the hip, shank, thigh and foot. And, in Figure 8, the frontal view of the exoskeleton assembly.

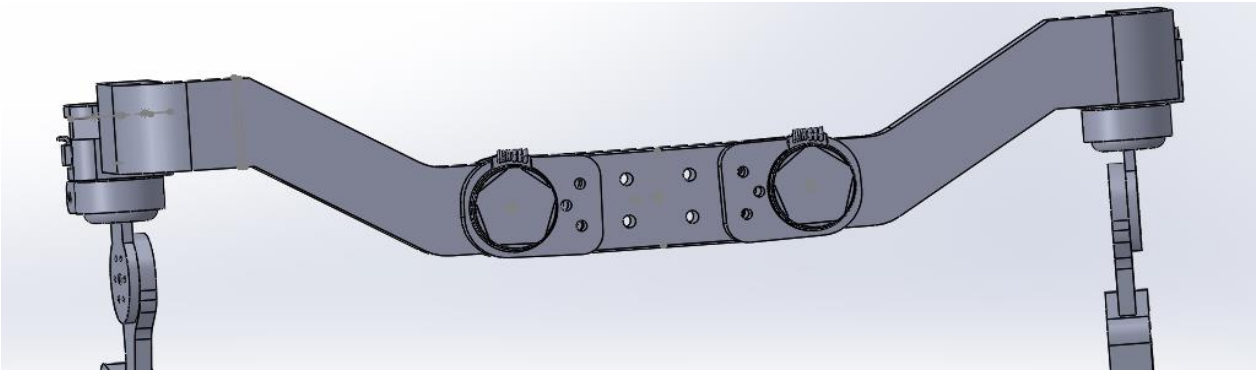

Figure 6*: Hip joint of the model from posterior view*

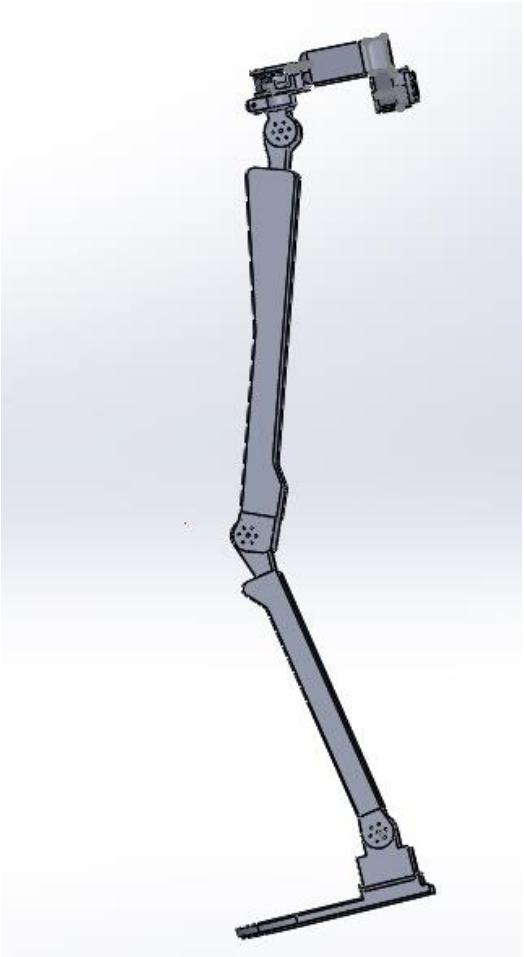

Figure 7*: Exoskeleton in lateral view.*

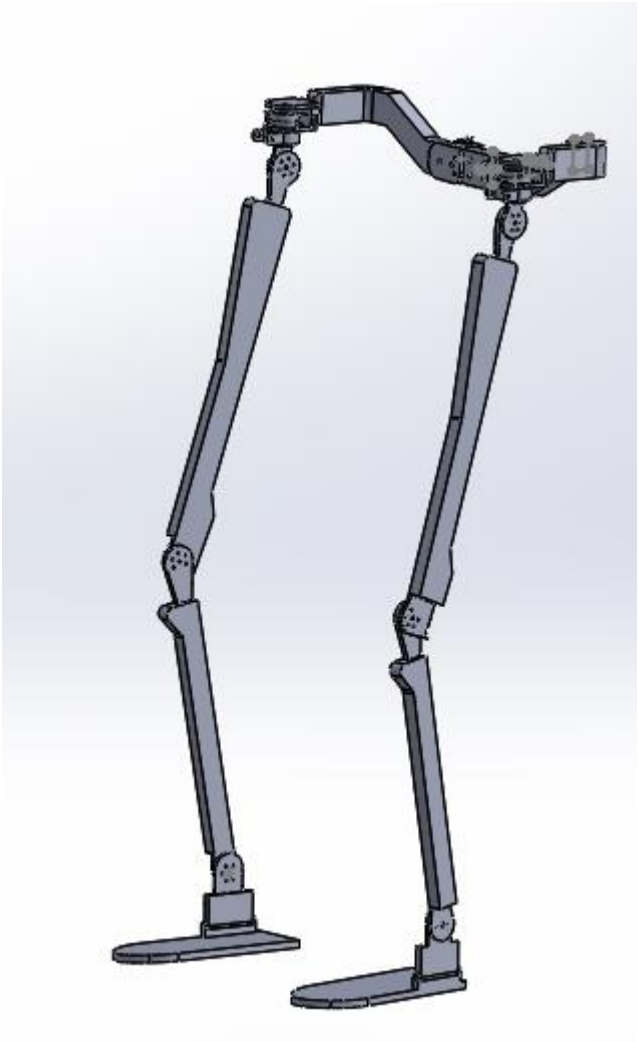

Figure 8*: Final assembly of exoskeleton*

Before exporting a model from SolidWorks to the Simscape Multibody XML format (.xml), it is needed to ensure that the model is properly prepared for simulation and meets the requirements for exporting. Here are the necessary steps:

- **Verify the Model:** Check the 3D model for correctness, completeness, and any potential issues that might affect the simulation. Ensure that all components are properly mated, and joints are correctly defined. This includes the correct definition of the Coordinate system of each piece.

- **Create Joints and Connections:** Use SolidWorks' assembly features to create joints or mates that define the relative motion between components. Simscape Multibody will interpret these mates as joints during the export process.
- **Establish Physical Properties:** Assign appropriate mass properties (mass, center of mass, inertia) to each component to ensure accurate dynamics during simulation.
- **Export the Model:** With Simscape Multibody Link installed, you can use the "Save As" or "Export" feature in SolidWorks to export the model to the Simscape Multibody XML format (.xml). This will create an XML file containing the model's information, including bodies, joints, constraints, and physical properties.

3.5. Simulink simulation

Once the model is created, it can be simulated in Simulink to analyze the performance of the system under different conditions and loads. Simscape Multibody allows for the creation of complex and detailed models that can accurately represent the behavior of the system, including factors such as friction and elasticity.

The simulation can be used to optimize the design of the system, identify potential issues, and improve its overall performance. The results of the simulation can also be used to generate reports and visualize the system's behavior, making it easier to communicate the design and performance to others.

Inverse dynamics analysis is indispensable when designing lower limb exoskeletons. It allows engineers and researchers to determine the forces, torques, and control inputs required to generate specific leg motions and support the wearer's movements effectively. By understanding the biomechanics and dynamics involved, designers can optimize the exoskeleton's control

algorithms, ensuring smoother and more natural gait patterns, reduced user effort, and enhanced stability.

Designing and analyzing a lower limb exoskeleton is a multifaceted process that involves mechanical design, kinematics, dynamics, and control. In this section, we outline a methodology for performing inverse dynamics analysis using Simscape Multibody for a lower limb exoskeleton that has been previously designed in SolidWorks.

3.5.1. Exportation from Solidworks

To export a CAD model from SolidWorks to Simulink or Simscape Multibody, open your SolidWorks model, and export it with Simscape multibody plugin. This saves the model in a compatible file format (.xml) that can be open in Simulink. Defining coordinate systems and position relationships to ensure accurate alignment and interaction with other components is important in this part. Then, in Simscape Multibody, import the CAD file in a easy way. Finally, it is ready to connect the imported model to your simulation setup. In figure 9, it can be observed the model exported to Simulink.

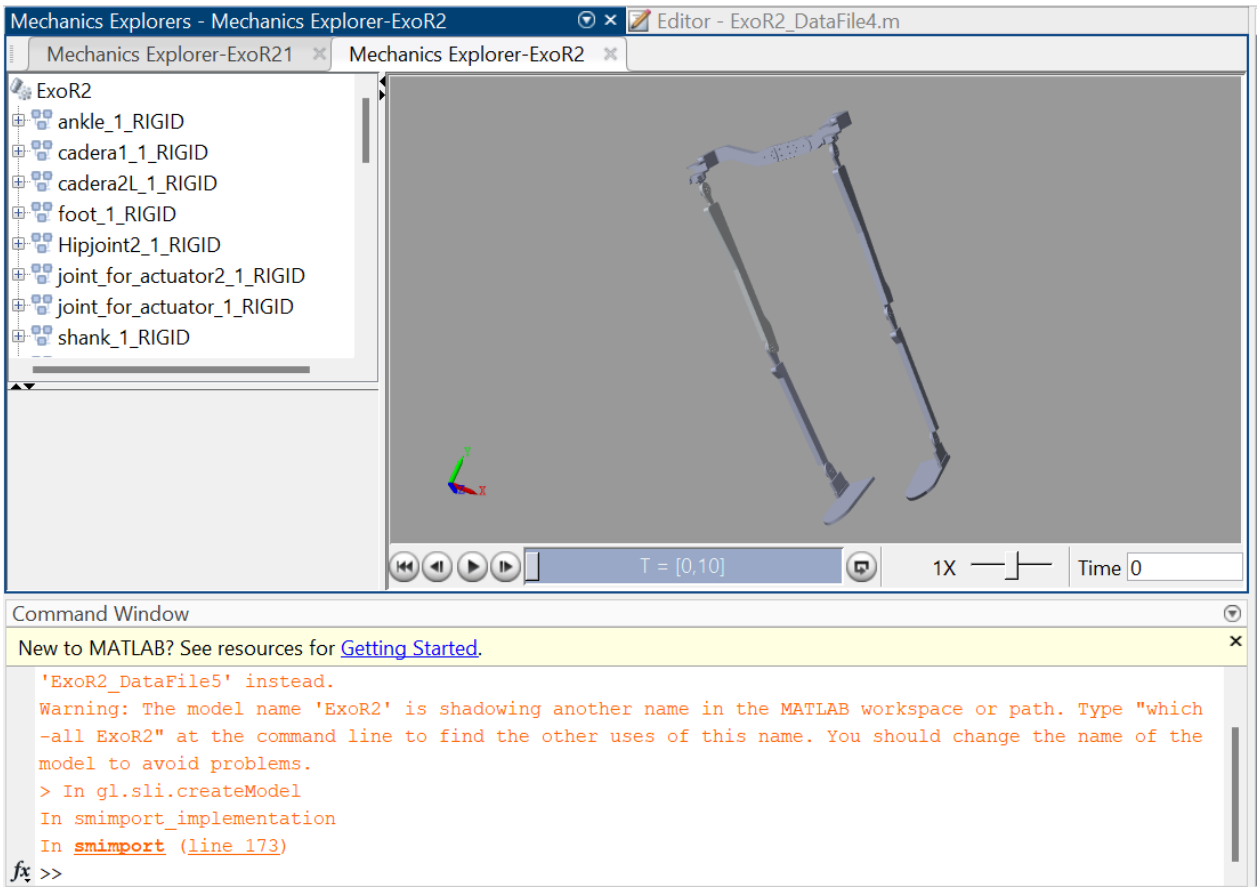

Figure 9: *Model imported in Simulink using Simscape multibody*

3.5.2. Model Building in Simscape Multibody

In Simscape Multibody, build the dynamic model by importing the exported CAD model and specifying physical properties. Key tasks include:

Rigid Body Definitions: It is defined the rigid bodies based on the exoskeleton components, specifying their mass, moments of inertia, and dimensions.

Joints: Add joints to represent the connections between exoskeleton components. Specify joint types (e.g., revolute, prismatic) and axis orientations to accurately mimic the exoskeleton's mechanical behavior.

Sensors: Incorporate sensors to capture data during simulation. Connect these sensors to appropriate points on the model or data collection.

3.5.3 Motion Specification

Define the desired leg motions and gait patterns that the exoskeleton should facilitate. This could involve specifying joint angles, velocities, or accelerations to mimic walking, running, or other activities. This is why, data from Simulink is used to create a trajectory for the different joints of the model. Then this data were treated in MATLAB to get a desired motion (See APPENDIX D).

3.5.4 Control System Integration

Implement the control system within Simscape Multibody to design and integrate the control algorithms. These algorithms should consider the desired leg motions, sensor feedback, and control objectives. In the context of Simscape Multibody, an open-loop control system might be used to set a desired trajectory for a mechanical system (such as a robot or exoskeleton) and calculate the torques required to follow that trajectory without taking into account real-time sensor feedback (See APPENDIX D).

3.5.5 Inverse Dynamics Simulation

Perform an inverse dynamics simulation to calculate the joint forces and torques required to achieve the specified leg motions. Simscape Multibody's inverse dynamics solver applies the principles of dynamics to compute these quantities accurately.

3.6. Finite Element Analysis (FEA) in SOLIDWORKS

Finite Element Analysis (FEA) in SOLIDWORKS is a simulation technique used to analyze the structural behavior of components and assemblies under various loading conditions. FEA is

widely used in engineering and design to predict how a product or component will react to real-world forces, vibrations, thermal effects, and other physical phenomena.

Here's a description of the Finite Element Analysis process in SOLIDWORKS:

- **Solver Setup:** Configure the solver settings, such as the type of analysis (static, dynamic, thermal, etc.), convergence criteria, and solution options.
- **Material Properties:** Assigning appropriate material properties to the model is essential for accurate analysis. SOLIDWORKS allows you to select material properties from a material library or define custom material properties. In this case it is used Aluminon 1060 with the following properties (Table 8).

Table 8

Aluminon 1060 properties.

Value	Property	Unit
Elastic modulus	69000	N/mm^2
Poisson coefficient	0.33	N/D
Cutting modulus	27000	N/mm^2
Mass density	2700	kg/m^3
Traction limit	689.356	N/mm^2
Compression limit		N/mm^2
Yield strength	275.742	N/mm^2
Coefficient of thermal expansion	2.4e-05	/K
Thermal conductivity	200	W/(m.K)
Specific heat	900	J/(kg.K)
Material damping quotient		N/D

- **Loads and Boundary Conditions:** Define the loads (forces, pressures, etc.) and boundary conditions (constraints) that represent the operating conditions of the component or

assembly. These include fixed supports, forces, moments, and thermal conditions. It will be defined in tables 9, 10 and 11.

Table 9

Loads details.

Load Name	IMAGE	Load details	
Force-1	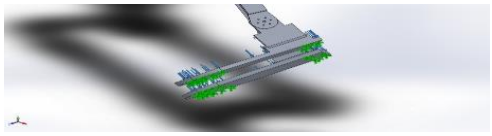	**Entities:**	**2 face(s)**
		Type:	**Apply Normal Force**
		Value:	**9000 N**
Force-2	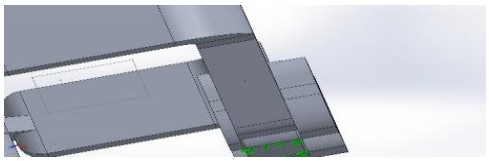	**Entities:**	**1 faces(s)**
		Type:	**Apply Normal Force**
		Value:	**40 N**
Gravity-1	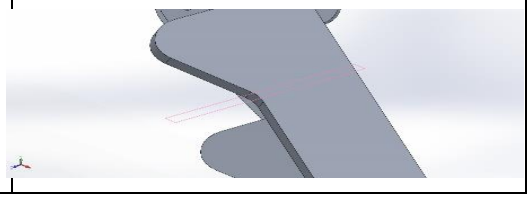	**Reference:**	**Floor**
		Values:	**0,0 -9,81**
		Units	**m/s^2**

Table 10

Constrains Details of fixed 1

Constraint Name	**Constraint Image**	**Constraint Details**	
Fixed-1	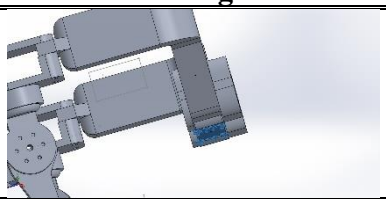	**Entities:**	3 face(s)
		Type:	Fixed geometry

Resultant Forces (Fixed-1)				
Components	***X***	***Y***	***Z***	***Resultant***
Reaction Force (N)	*24.0405*	*-22.0447*	*8.51918*	*33.7119*
Reaction Moment (N.m)	*0*	*0*	*0*	*0*

Table 11

Constrains Details of fixed 2

Constraint Name	**Constraint Image**	**Constraint Details**	**Constraint Name**
Fixed-2	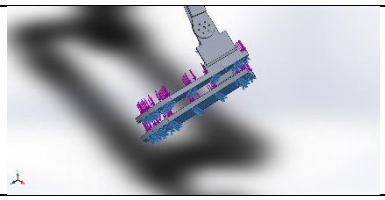	**Entities:**	2 face(s)
		Type:	Fixed geometry

Resultant Forces (Fixed-2)				
Components	**X**	**Y**	**Z**	**Resultant**
Reaction Force (N)	-13.99210	11.31960	-800.311	18.01540
Reaction Moment (N.m)	0	0	0	0

- **Mesh Generation:** FEA works by discretizing the 3D model into a mesh of small geometric elements, such as triangles or tetrahedrons. This process is called meshing. SOLIDWORKS automatically generates the mesh based on the geometry and specified mesh settings. The density and quality of the mesh can impact the accuracy and computational cost of the analysis. It was used the basically functions of meshing of the software, because it will lead to a easy solving. Mesh details are specified in Table 12 and in Figure 10 it is shown the mesh and the loads in the entire.

Table 12

Mesh details

Mesh information	
Type of mesh	Solid mesh
Meshing tool used	Curvature-based mesh
Jacobians points for high-quality mesh	29 points

Maximum element size	28.3114 mm
Minimum element size	5.66228 mm
Mesh quality	High-order quadratic elements
Remesh failed parts independently	Disable

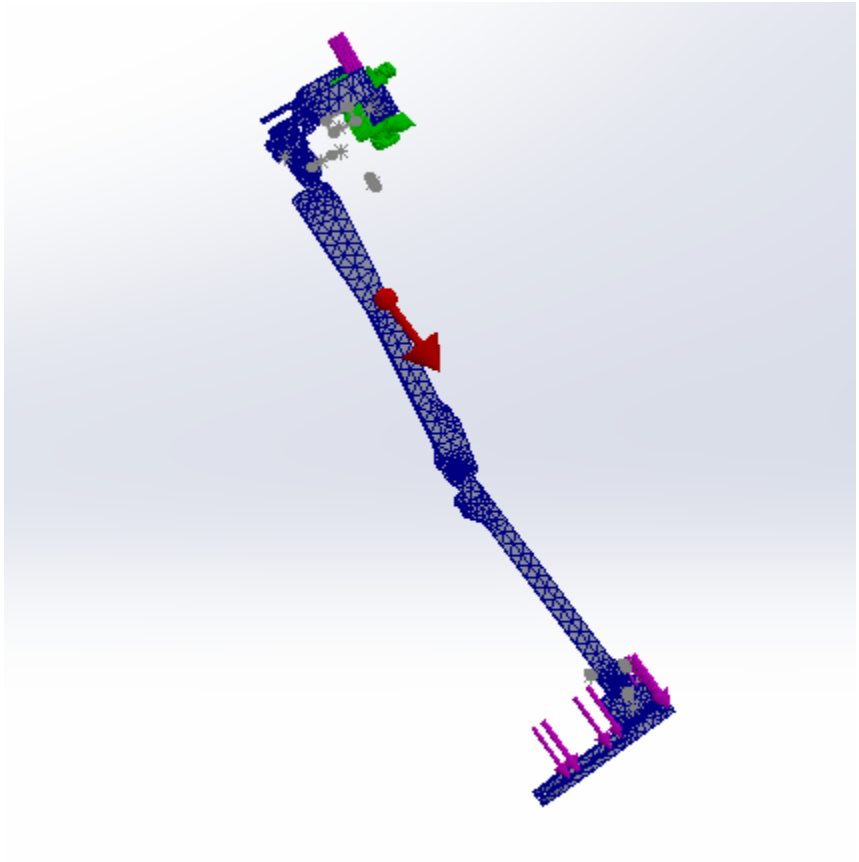

Figure 10: *FEA meshing with loads and boundary conditions of the 3D model in Solidworks*

- **Solving the Model:** Initiate the FEA process, where SOLIDWORKS' FEA solver performs matrix calculations to simulate the behavior of the model under the applied loads and constraints.

Chapter 4: Results and Discussions

Having meticulously followed a structured methodology for exporting a CAD model from SolidWorks to Simulink with Sims cape Multibody, as well as conducting Finite Element Analysis (FEA) to assess structural integrity, we are now poised to explore the rich array of outcomes and insights that have emerged from this comprehensive approach. This section presents the tangible results of our endeavors, offering a holistic view of how the CAD model performs within the simulation environment and how it withstands structural demands under varying conditions. By examining these results, we can gain valuable insights into the behavior, dynamics, and interactions of the mechanical system, enabling us to make informed decisions, optimize designs, validate functionality, and ensure the structural robustness of the lower limb exoskeleton.

In this case the model simulates the walking process for its rehabilitation.

4.1. Simulink Simulation

The simulation of an exoskeleton using Simscape Multibody represents a pivotal step in the development and evaluation of assistive technologies designed to enhance human mobility and support. This comprehensive simulation enables us to gain valuable insights into the performance, behavior, and effectiveness of the exoskeleton under various conditions. In this section, we will present the results obtained from this simulation, shedding light on key aspects of the exoskeleton's functionality.

4.1.1. Exoskeleton Functionality Evaluation:

The primary objective of this simulation was to assess the functionality of the exoskeleton. By employing Simscape Multibody, we conducted a detailed analysis of the exoskeleton's behavior,

focusing on its ability to assist users in performing the walking process. In figure 11, can be observed the simulation running.

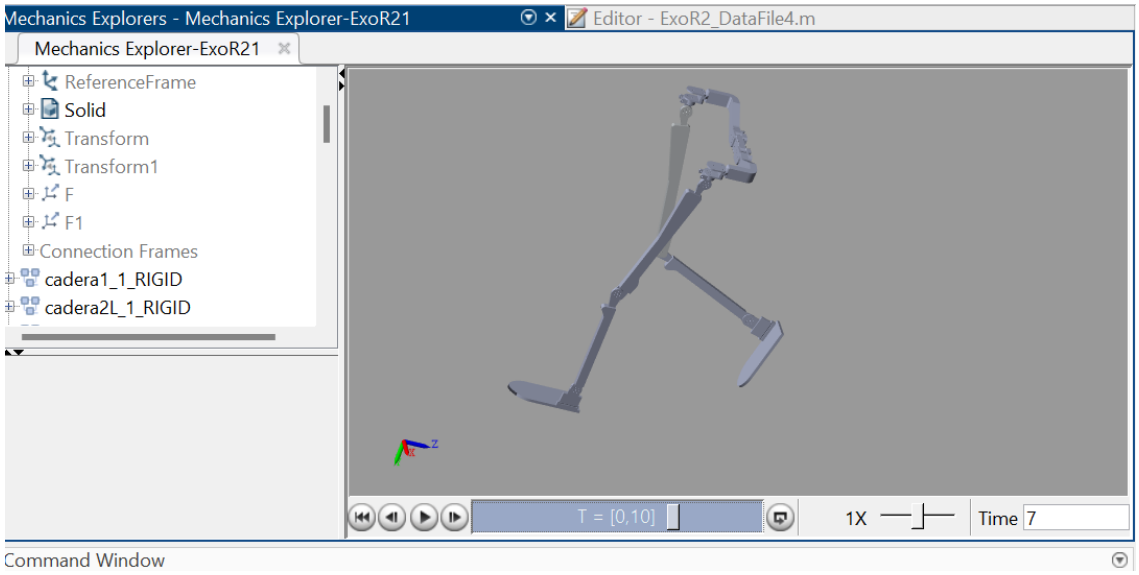

Figure 11: *Simulation window of the exoskeleton.*

4.1.2. Sensor Feedback of the open loop control system

The exoskeleton's effectiveness is greatly influenced by its sensor feedback. Through this simulation, we evaluated the responsiveness of these algorithms in real-time, ensuring that the exoskeleton can adapt to the user's intentions. It was defined a torque and position sensor in each joint.

In figure 12 and 13 can be observed that the position signal is similar, so the simulation meets the objective.

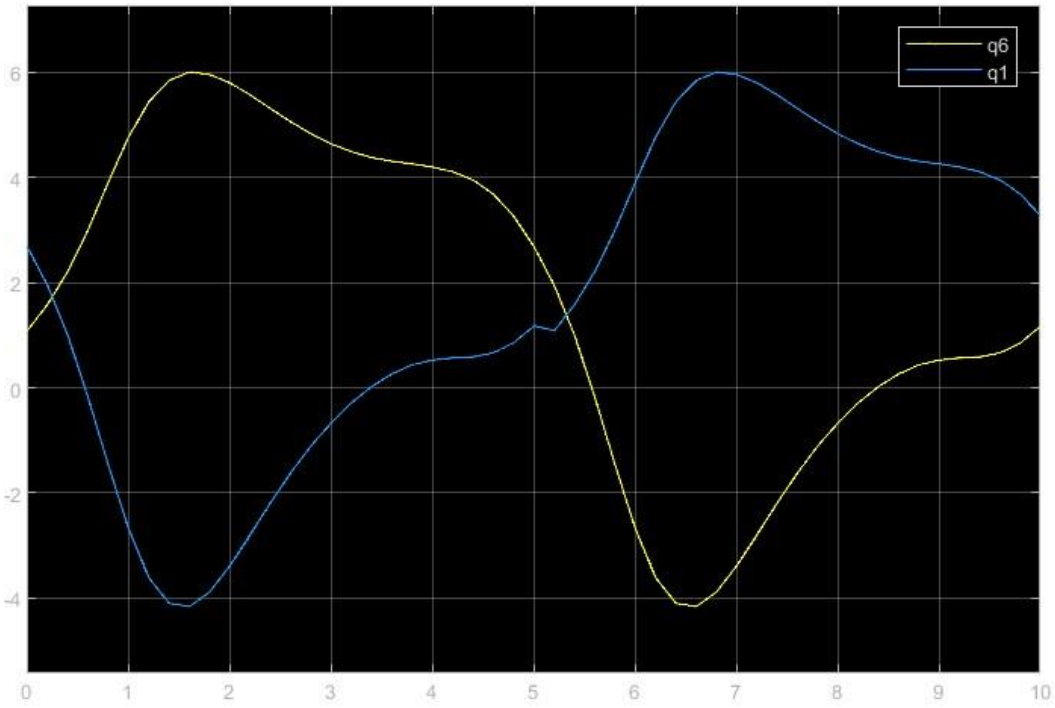

Figure 12: *Position signal output in degrees of Hip adduction of both legs.*

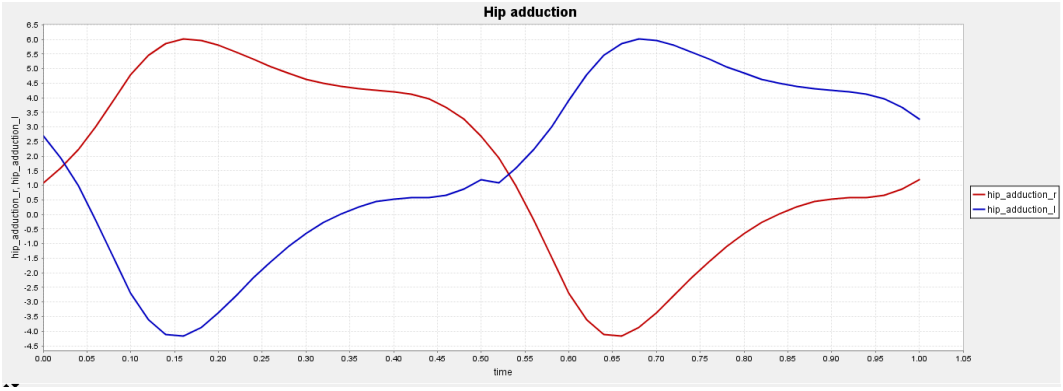

Figure 13: *Hip adduction signal from OpenSim*

In figure 14 and 15 can be observed that the position signal is similar for hip rotation, so the simulation meets the objective.

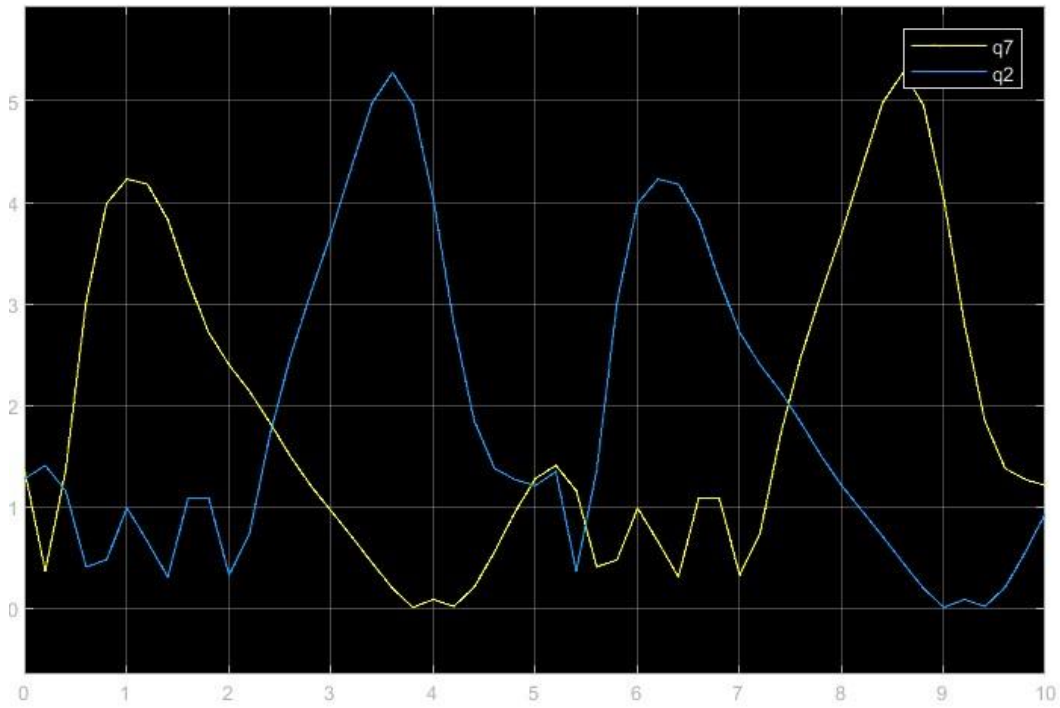

Figure 14: *Position signal output in degrees of Hip rotation of both legs.*

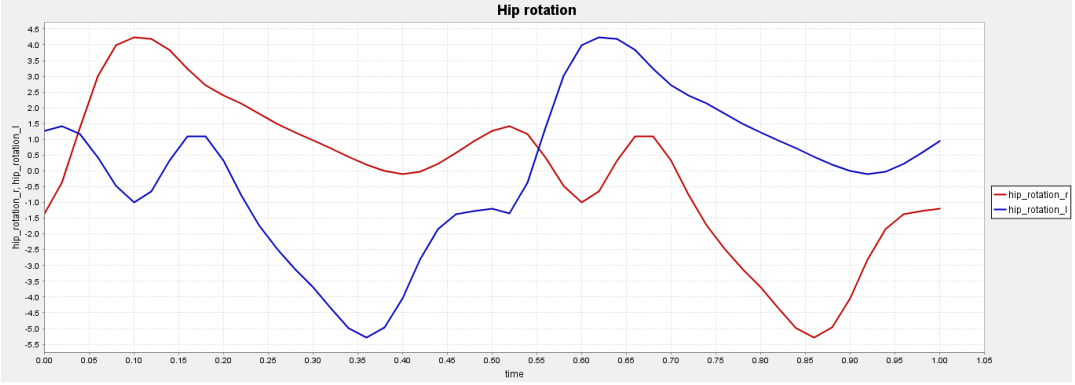

Figure 15: *Hip rotation signal from OpenSim*

In figure 16 and 17 can be observed that the position signal is similar, so the simulation meets the objective.

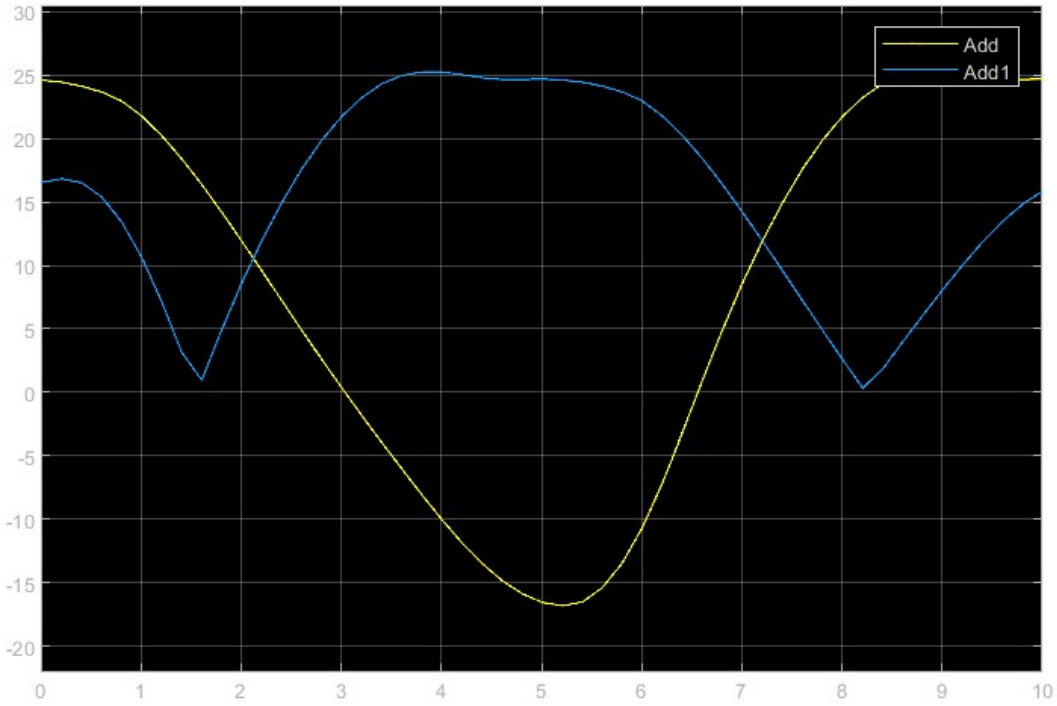

Figure 16: *Position signal output in degrees of Hip flexion of both legs.*

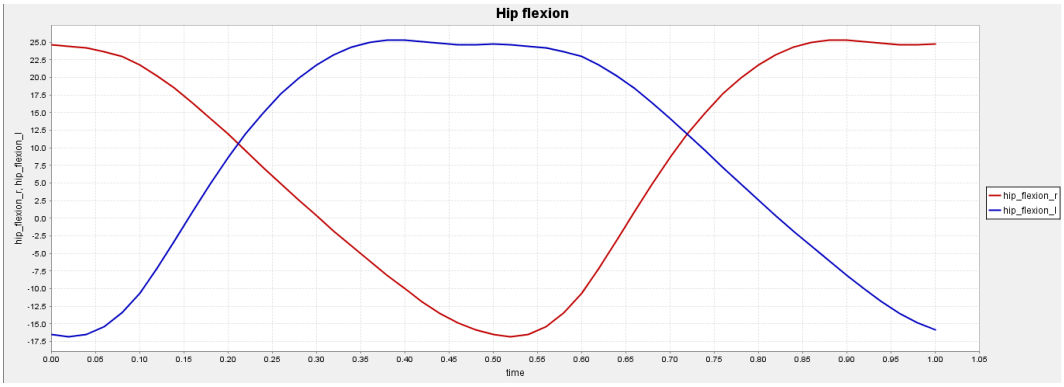

Figure 17: *Hip flexion signal from OpenSim*

In figure 18 and 19 can be observed that the position signal are similar, so the simulation meets the objective.

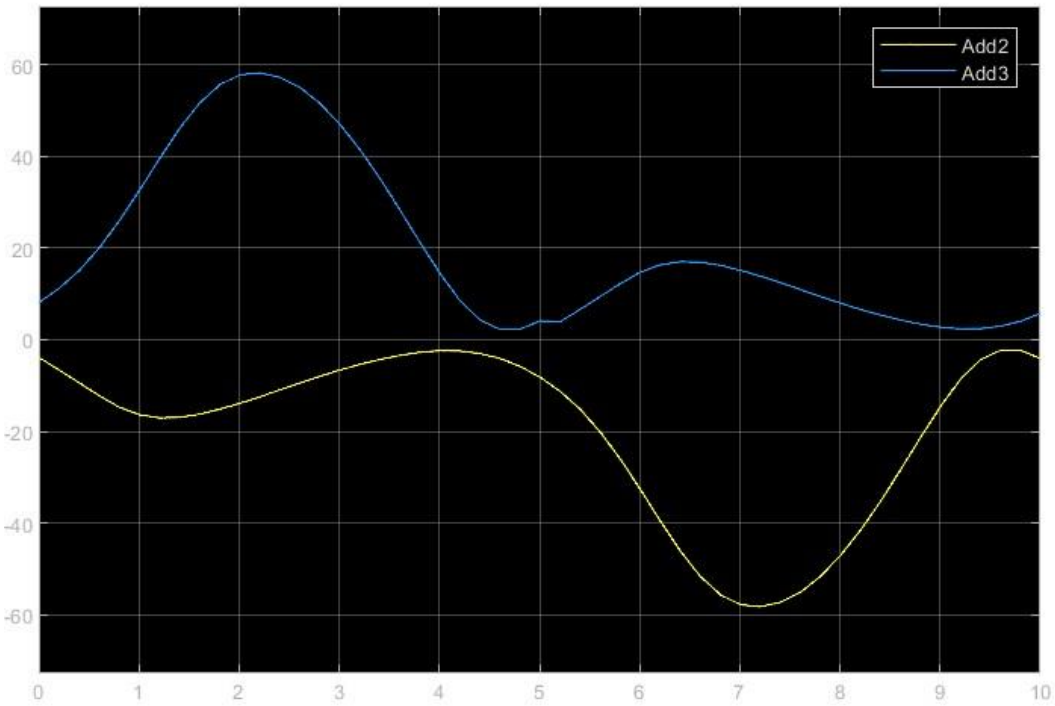

Figure 18: *Position signal output in degrees of knee flexion of both legs.*

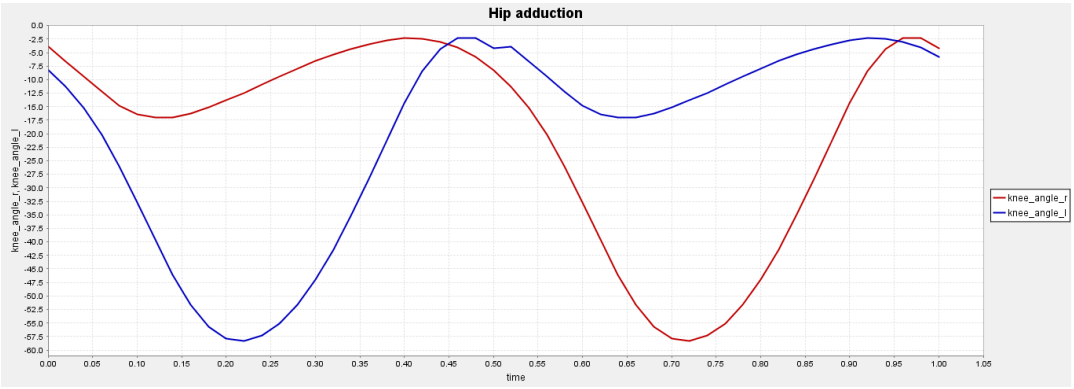

Figure 19: *Knee flexion signal from OpenSim*

In figure 20 and 21 can be observed that the position signal is similar, so the simulation meets the objective.

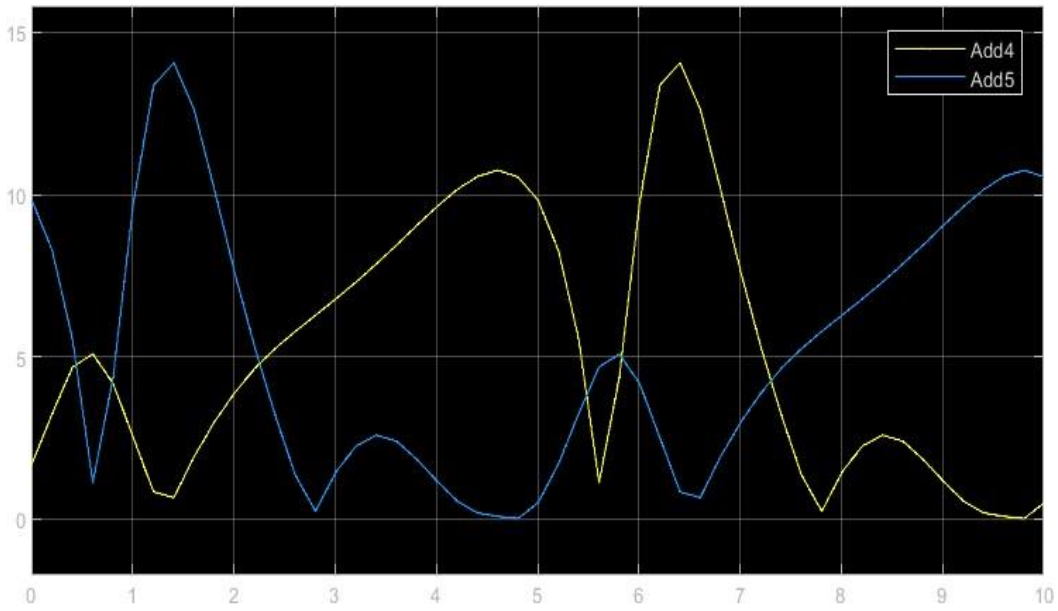

Figure 20: *Position signal output in degrees of Ankle angle of both legs.*

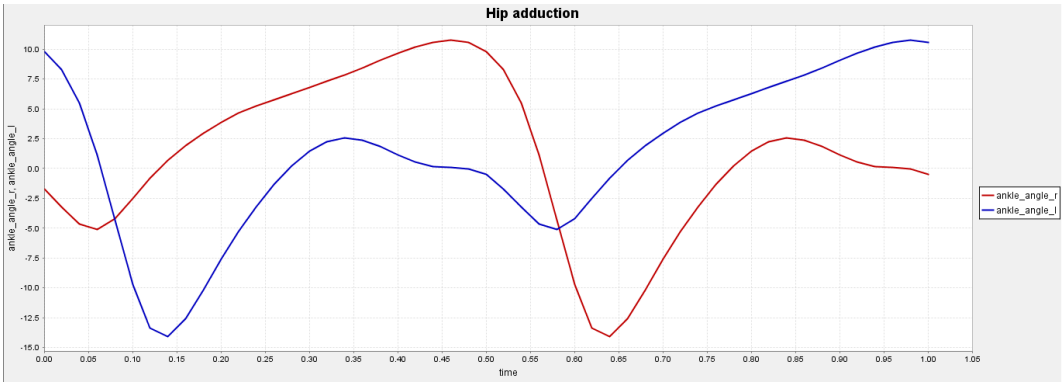

Figure 21: *Ankle angle signal from OpenSim.*

Next, we incorporated torque signals into our analysis, resulting in the determination of the required torque to achieve a specific motion angle. These desired torque values are graphically depicted over a 10-second timeframe in Figures 22, 23, 24, 25, and 26. Those values can be used for a future design of the exoskeleton.

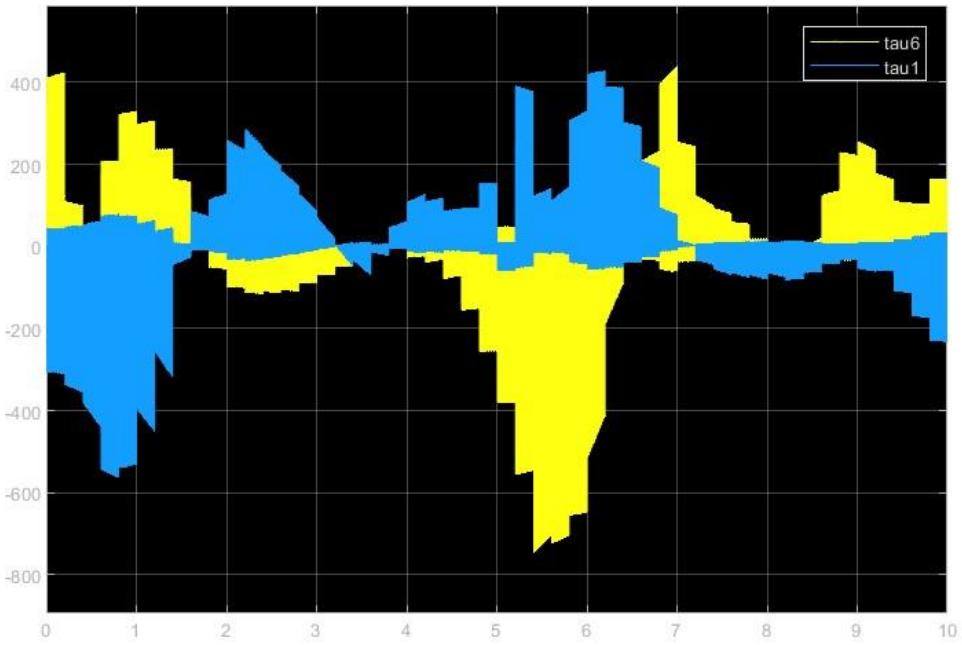

Figure 22: *Torque signal output in nm of Hip adduction of both legs.*

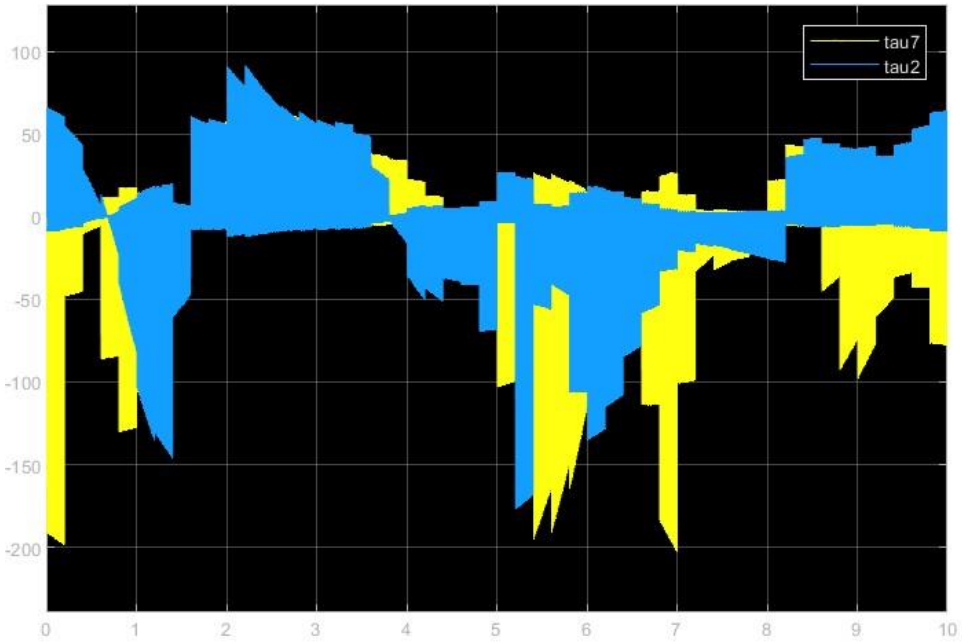

Figure 23: *Torque signal output in nm of Hip flexion of both legs.*

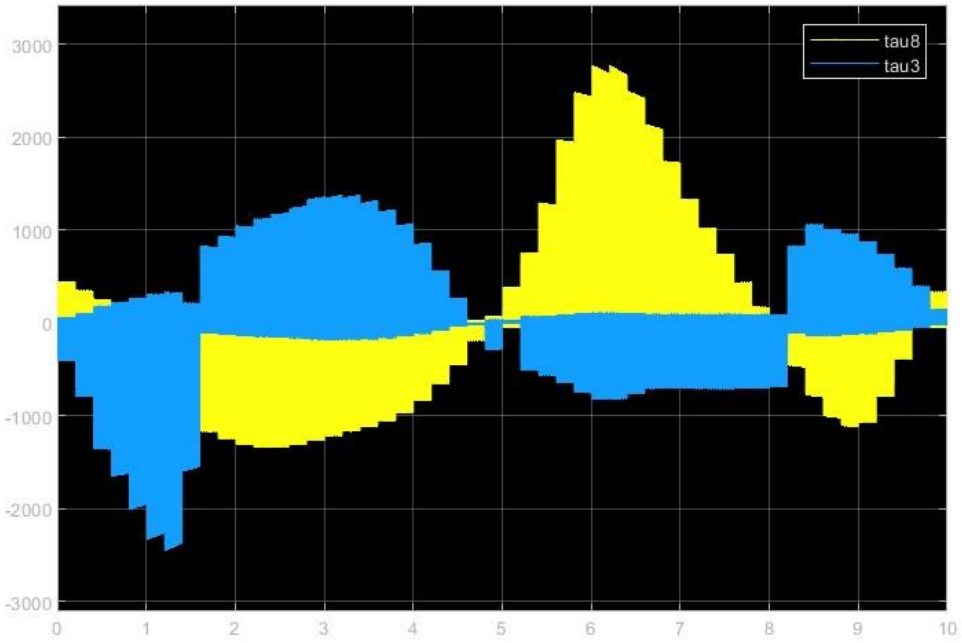

Figure 24: *Torque signal output in nm of Hip rotation of both legs.*

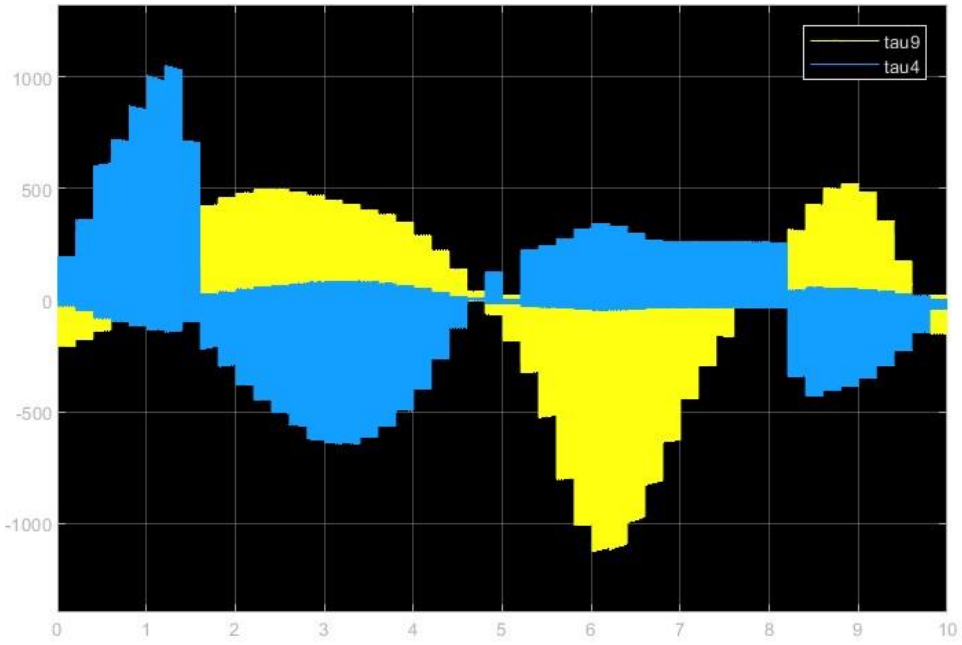

Figure 25: *Torque signal output in nm of knee flexion of both legs.*

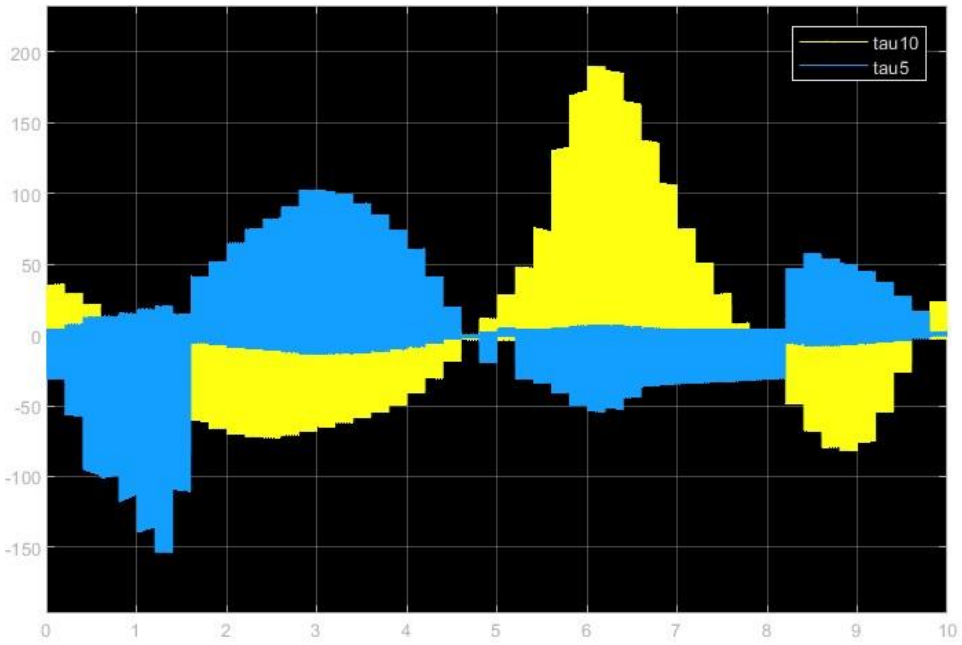

Figure 26: *Torque signal output in nm of ankle angles of both legs*

4.2. FEA results

Finite Element Analysis (FEA) is a powerful numerical technique used to solve complex engineering and scientific problems by dividing them into smaller, more manageable elements(Ruffoni & van Lenthe, 2011). In the context of structural mechanics, FEA is employed to predict how components and structures behave under various loads, providing invaluable insights into stress distribution, deformation, and other critical parameters. In this report, we will delve into the key findings and interpretations of the FEA simulation. This includes a comprehensive analysis of Von Misses stress, displacement, deformation, and safety factor. Additionally, we will discuss how these results align with design specifications and safety requirements.

4.2.1. Quality of the mesh

For this meshing, there are a total of 82,668 nodes in the analysis. Also, it have been generated 44,841 elements in total for the simulation. The highest aspect ratio among the elements

is 383.63. This suggests that some elements are highly elongated or distorted compared to others. The percentage of elements whose aspect ratio is < 3 shows that 77% of the elements have an aspect ratio less than 3. This indicates that the majority of elements are relatively well-proportioned in terms of their shape. The percentage of elements whose aspect ratio is > 10 indicates that only 0.33% of elements have an aspect ratio greater than 10, that means that a very small percentage of elements are highly distorted or elongated. There are no distorted elements in your simulation, as the percentage is 0. This is a positive indicator, suggesting that the elements are not overly distorted or skewed. And it took 6 seconds to generate the mesh for your analysis.

In summary, this data provides insights into the quality and characteristics of the mesh used in the simulation. While there are some elements with high aspect ratios, the majority appear to be well-proportioned, and there are no significantly distorted elements. The summary is in Table 13.

Table 13

Mesh details

Total number of nodes	82668
Total number of elements	44841
Maximum aspect ratio	383.63
% of elements whose aspect ratio is < 3	77
% of elements whose aspect ratio is > 10	0.33
Percentage of distorted elements	0
Time to complete the mesh (hh:mm:ss):	00:00:06

4.2.2. Results Analysis

This report presents a comprehensive analysis of critical parameters obtained from an FEA simulation, shedding light on the performance and integrity of the analyzed structure.

The report focuses on four key aspects:

Von Mises Stress (VON): Stress distribution is a fundamental factor in understanding how materials respond to external forces. The Von Mises stress provides a holistic perspective, encompassing both normal and shear stresses, allowing us to pinpoint regions of potential failure or excessive deformation (Crawford, 1998). The minimum value in the simulation is 3.697e+00 N/m^2 at Node 73797, while maximum value is 2.555e+06 N/m^2 at Node 26792 (Figure 27).

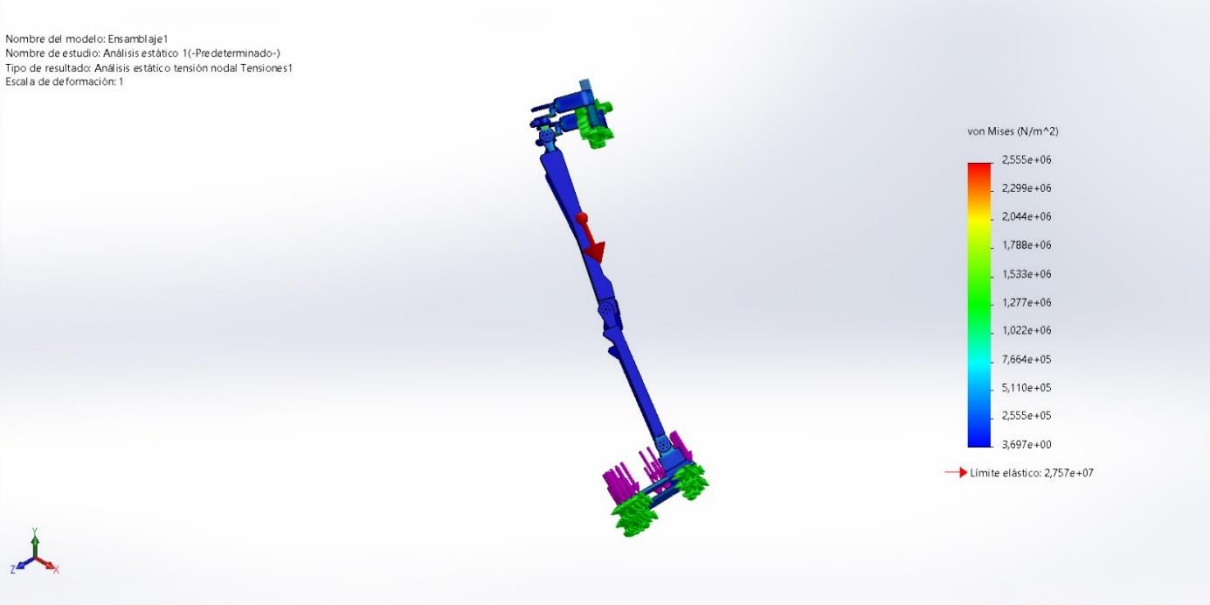

Figure 27: *Von misses stress.*

Resultant Displacements (URES): Displacement analysis is essential for evaluating structural stability and deformation characteristics. The resultant displacements reveal how the structure responds to applied loads, providing insights into its structural integrity(Wu et al., 2021). The minimum value is 0.000e+00 mm at Node 19673 and the maximum: 2.778e-01 mm at Node 32862. Those values are found in Figure 28.

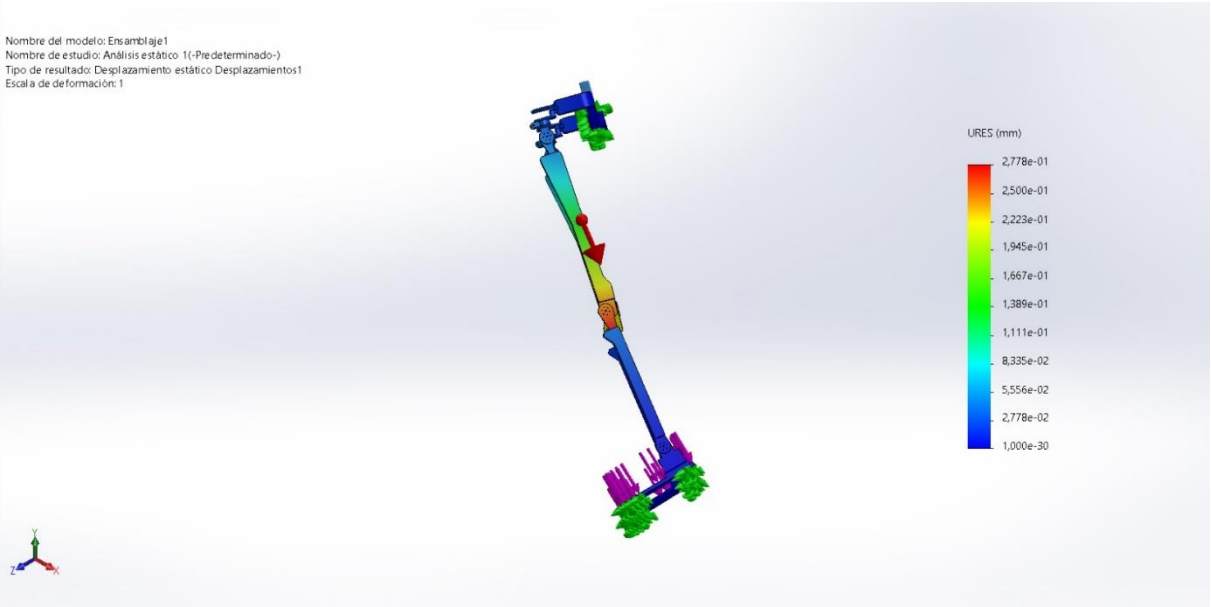

Figure 28: *Resultant Displacements (URES)*

Equivalent Strain (ESTRN): Strain measures the deformation of materials, and the equivalent strain is a vital parameter for assessing how much a material has deformed under load. This is crucial for predicting structural performance and longevity(Wu et al., 2021). The minimum value is1.097e-10 at element 16408 and the maximum value is 2.686e-05 at element 14409. Those values are found in Figure 29.

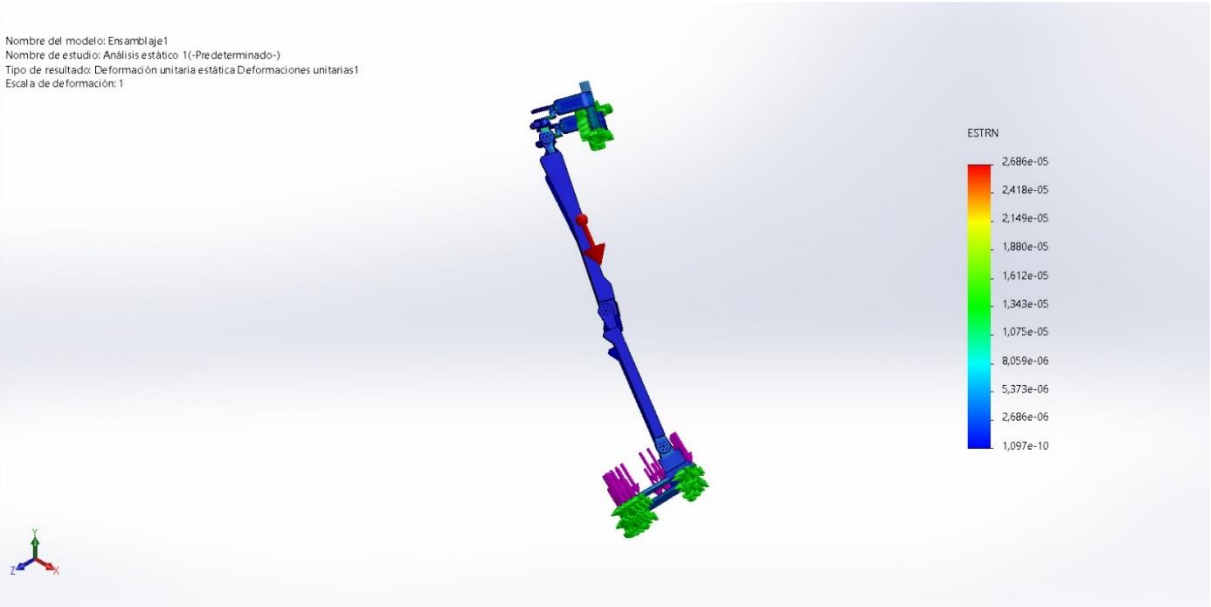

Figure 29: *Equivalent Strain (ESTRN)*

Maximum Normal Stress: The maximum normal stress denotes the highest tensile or compressive stress experienced within the structure. Identifying this peak stress is crucial for evaluating structural safety and durability. This is for safety factor. The minimum value is 2.229e+01 at Node 26792, while the maximum value is 1.903e+07 at Node 31002.(Burdekin, 2007). With this, a safety factor greater than 1 indicates that the structure can withstand the applied loads without failure. A safety factor less than 1 may indicate potential structural failure. Then, the structure can withstand the applied loads and meets the safety conditions. Those values are found in Figure 30.

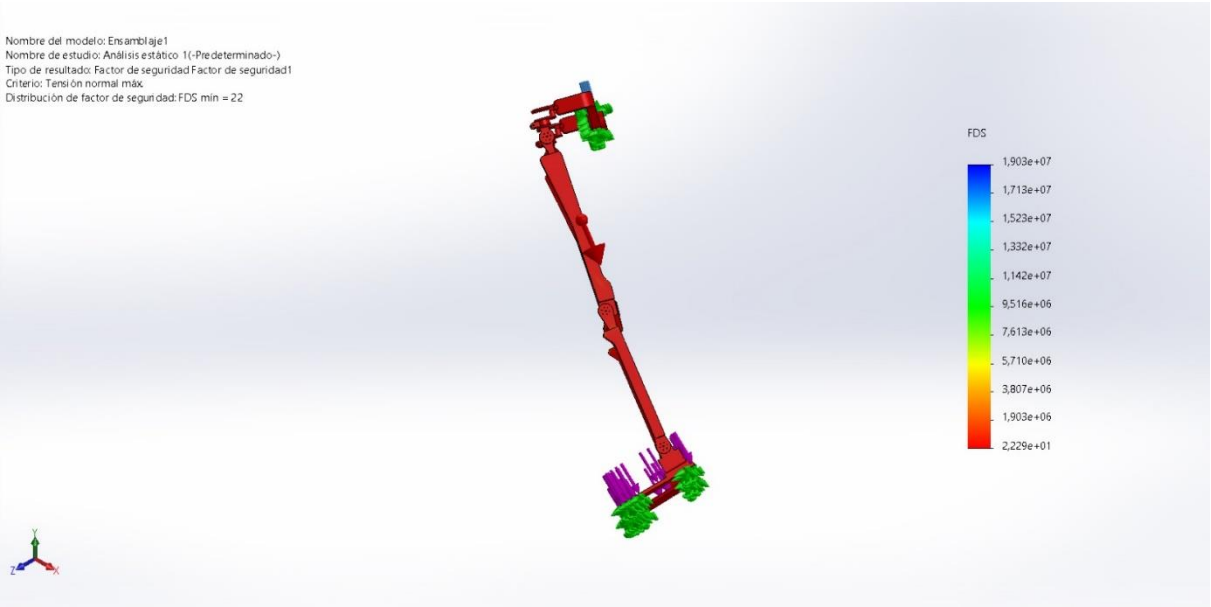

Figure 30: *Maximum Normal Stress (Safety Factor)*

The summary of the results is in Table 14.

Table 14

Summary of FEA results

Name	**Type**	**Mín.**	**Max.**
Stress1	VON: Von Mises Stress	3.697e+00N/m^2 Node: 73797	2.555e+06N/m^2 Node: 26792
Disolacement1	URES: Resultant Displacements	0.000e+00mm Node: 19673	2.778e-01mm Node: 32862
Equivalent Strain1	ESTRN: Equivalent Strain	1.097e-10 Element: 16408	2,686e-05 Element: 14409
Safety factor1	Maximum Normal Stress	2.229e+01 Node: 26792	1.903e+07 Node: 31002

4.3. Limitations of the present work

This work is subject of several limitations, which warrant consideration. First of all, the study may have relied on simplified assumptions concerning biomechanical processes or user behaviors, potentially simplifying real-world scenarios. For example, forces that simulate human muscles were not considered in the Simulink simulation. As a result, the outcomes of this study

might not fully capture the complexities in human movement and its interaction with the exoskeleton device. Also, the simulations not consider environmental factors that could affect exoskeleton performance, such as terrain variations or unexpected obstacles.

Regarding anthropometric data of individuals, the study utilized average from other datasets, which many not fully align the target. This was for the limited availability of anthropometric data for Ecuadorians or individuals from Latin America.

Also is necessary to apply a rapid prototype of the design and actuators with the data of torques obtained. The current model with materials stronger than those used in FDM printing, and economic limitations are present. This approach could leave an interesting insight into the model in real scenarios.

In summary, this study has identified valuable vision into exoskeleton technology. However, it is important to address the limitations that exist. Understanding these limitations is crucial for enhancing the robustness of findings in the current field of exoskeletons technology.

4.4. Comparative Analysis of related works

It is identified some studies with similar approaches. In one study (Lugo et al., 2014), , a design of an exoskeleton with 3 DoF was proposed using co-simulation with OpenSim, SolidWorks and Simulink to obtain a lightweight, personalized, and cost-effective model. Biomechanical factors and variables of human movement and gait were employed to determine the exoskeleton's characteristics. The verification of the mechanical base, served to control it, this is simulated in Simmechanics (now called Simscape multidody), here a control proposal is displayed with a trajectory tracker PID device (which is a closed-loop approach that gives retro alimentation to the system), but as mentioned, control can still optimize for better results. The objective was to assist

the patient in generating basic flexion and extension movements. The results of simulation of the movements in SolidWorks shown to be similar to the present thesis. However, is just for three DoF. A FEA was not performed, yet they gave a real prototype.

Other approach is found in other study (Li et al., 2022). The article focuses on the dynamic analysis of an exoskeleton designed for gait rehabilitation. A detailed dynamic model of the exoskeleton is developed, simplified as a five-bar model, considering two walking modes: single-leg support and double-leg support. The method employes was Lagrange to dynamically analyze walking patterns and determine joint torques. Furthermore, the accuracy of the theoretical analysis is verified through dynamic simulations using ADAMS software. The obtained results provide a solid theoretical basis for motor selection and control system design of the rehabilitation robot, which is essential for future progress in exoskeleton technologies for rehabilitation.

In the following table is found a comparation of these approaches.

Table 15

Comparative table of relate works

Author or reference	DoF	Type of control	FEA analysis	Physical prototype	Simulation performance
Avila Briones	5	Open-loop	Yes	No	Good performance
(Lugo et al., 2014)	3	PID control (Close loop)	Yex	No	Good performance
(Li et al., 2022)	7	No described	No	No	Good performance

(Rossi et al., 2014)	2	PID control	No	Yes	Good performance
(Zhou et al., 2020)	2	Passive	No	Yes	Good performance

On the contrary, this research is focused in the uses of concurrent design for the design of the prototype. For instance, future approaches should be focused in the evaluation of the real performance of the device, and the simulations with more realistic scenarios.

Chapter 5: Conclusions

This comprehensive study focuses on designing and evaluating an adjustable lower limb active exoskeleton for adults, coupled with an automation system. It was adopted various advanced tools and methodologies, including SOLIDWORKS for 3D modeling and FEA for structural integrity assessment, OpenSim, and MATLAB for control strategies,here, the key insights from the research and discussions are summarized:

It was successfully created a 3D model of the lower limb exoskeleton for adults using SOLIDWORKS, implementing concurrent design methods. This model forms the basis for subsequent simulations and analyses. Also, the FEA results shown to demonstrate safety of the device with loads for a person of 70 kg. Von Mises stress, resultant displacements, equivalent strain, and safety factors were meticulously analyzed. Notably, findings indicated that the structure possesses a safety factor greater than 1, signifying its capability to withstand applied loads. The quality of the mesh employed in the simulation was assessed. The results revealed that although some elements exhibited high aspect ratios, most of the elements featured well-proportioned shapes. Importantly, none of the elements exhibited significant distortion. However, it is necessary to implement other scenarios in future investigations.

Through simulations conducted in OpenSim, and Simulink, the control strategy was rigorously examined. These simulations effectively demonstrated the viability of the proposed control methods, particularly in simulating the walking process for rehabilitation purposes. By harnessing Simscape Multibody within Simulink, a pivotal simulation of the exoskeleton's performance was conducted. This simulation provided valuable insights into the exoskeleton's functionality, particularly in assisting users during the walking process.

The effectiveness of the open-loop control system was assessed through sensor feedback analysis. Position signals for various joint movements were scrutinized, observing a close alignment between the simulation and the defined objectives, affirming the system's responsiveness.

In summary, this study represents a significant advancement in the development of lower limb active exoskeletons for adult users. Through the incorporation of innovative design, control strategies, and rigorous analysis, the research has showcased the potential of exoskeletons to enhance mobility rehabilitation in gait cycle. The insights presented here contribute significantly to the continuing progress of assistive technologies and hold a promising outlook for the future of exoskeleton development. However, future improvements are needed.

Bibliography

Aguilar-Sierra, H., Lopez, R., Yu, W., Salazar, S., & Lozano, R. (2014). A lower limb exoskeleton with hybrid actuation. *Proceedings of the IEEE RAS and EMBS International Conference on Biomedical Robotics and Biomechatronics*, 695–700. https://doi.org/10.1109/BIOROB.2014.6913859

Alashram, A. R., Annino, G., & Padua, E. (2021). Robot-assisted gait training in individuals with spinal cord injury: A systematic review for the clinical effectiveness of Lokomat. *Journal of Clinical Neuroscience*, *91*, 260–269. https://doi.org/10.1016/J.JOCN.2021.07.019

Alemany, S., Remon, A., Ballester, A., Vicente Durá, J., Nácher, B., Parrilla, E., & Carlos González, J. (2022). Data management and processing of 3D body scans. *Digital Manufacturing Technology for Sustainable Anthropometric Apparel*, 97–116. https://doi.org/10.1016/B978-0-12-823969-8.00007-1

Aparecida Padilha Clemente, K. I., Vieira da Silva, S. I., Inoue Vieira, G. I., Carla de Bortoli, M. I., Setsuko Toma, T. I., Delgado Ramos III, V., & Aparecida Padilha Clemente, K. (n.d.). *Barriers to the access of people with disabilities to health services: a scoping review*. https://doi.org/10.11606/s1518-8787.2022056003893

Arazpour, M., Hutchins, S. W., & Bani, M. A. (2015). The efficacy of powered orthoses on walking in persons with paraplegia. *Prosthetics and Orthotics International*, *39*(2), 90–99. https://doi.org/10.1177/0309364613520031

Avila Chaurand, R., Prado Leon, L. R., & Gonzalez Muñoz, E. L. (2015). Dimensiones antropométricas de población latinoamericana. In *ResearchGate* (Issue May 2015).

Awad, L. N., Esquenazi, A., Francisco, G. E., Nolan, K. J., & Jayaraman, A. (2020). The ReWalk ReStore™ soft robotic exosuit: A multi-site clinical trial of the safety, reliability, and feasibility of exosuit-augmented post-stroke gait rehabilitation. *Journal of NeuroEngineering and Rehabilitation*, *17*(1), 1–11. https://doi.org/10.1186/S12984-020-00702-5/FIGURES/4

Bach Baunsgaard, C., Vig Nissen, U., Katrin Brust, A., Frotzler, A., Ribeill, C., Kalke, Y. B., León, N., Gómez, B., Samuelsson, K., Antepohl, W., Holmström, U., Marklund, N., Glott, T., Opheim, A., Benito, J., Murillo, N., Nachtegaal, J., Faber, W., & Biering-Sørensen, F. (2017). Gait training after spinal cord injury: safety, feasibility and gait function following 8 weeks of training with the exoskeletons from Ekso Bionics. *Spinal Cord 2017 56:2*, *56*(2), 106–116. https://doi.org/10.1038/s41393-017-0013-7

Baronchelli, F., Zucchella, C., Serrao, M., Intiso, D., & Bartolo, M. (2021). The Effect of Robotic Assisted Gait Training With Lokomat® on Balance Control After Stroke: Systematic Review and Meta-Analysis. *Frontiers in Neurology*, *12*, 1073. https://doi.org/10.3389/FNEUR.2021.661815/BIBTEX

Bejer, A., Domka-Jopek, E., Probachta, M., Lenart-Domka, E., & Wojnar, J. (2019). Burnout syndrome in physiotherapists working in the Podkarpackie province in Poland. *Work*, *64*(4), 809–815. https://doi.org/10.3233/WOR-193042

Bortole, M., Venkatakrishnan, A., Zhu, F., Moreno, J. C., Francisco, G. E., Pons, J. L., & Contreras-Vidal, J. L. (2015). The H2 robotic exoskeleton for gait rehabilitation after stroke: Early findings from a clinical study Wearable robotics in clinical testing. *Journal of NeuroEngineering and Rehabilitation*, *12*(1), 1–14. https://doi.org/10.1186/s12984-015-0048-y

Brolin, E. (n.d.). *Anthropometric diversity and consideration of human capabilities-Methods for virtual product and production development*.

Burdekin, F. M. (2007). General principles of the use of safety factors in design and assessment. *Engineering Failure Analysis*, *14*(3), 420–433. https://doi.org/10.1016/j.engfailanal.2005.08.007

Chang, S. R., Kobetic, R., Audu, M. L., Quinn, R. D., & Triolo, R. J. (2015). Powered Lower-Limb Exoskeletons to Restore Gait for Individuals with Paraplegia – a Review. *Case Orthopaedic Journal*, *12*(1), 75.

Chen, B., Zi, B., Wang, Z., Qin, L., & Liao, W. H. (2019). Knee exoskeletons for gait rehabilitation and human performance augmentation: A state-of-the-art. *Mechanism and Machine Theory*, *134*, 499–511. https://doi.org/10.1016/J.MECHMACHTHEORY.2019.01.016

Consejo Nacional para la Igualdad de Discapacidades, (CONADIS). (2021). *Estadísticas de Discapacidad – Consejo Nacional para la Igualdad de Discapacidades*. Ministerio de Salud Publica. https://www.consejodiscapacidades.gob.ec/estadisticas-de-discapacidad/

Costa, N., & Caldwell, D. G. (2006). Control of a biomimetic "soft-actuated" 10DoF lower body exoskeleton. *Proceedings of the First IEEE/RAS-EMBS International Conference on Biomedical Robotics and Biomechatronics, 2006, BioRob 2006*, *2006*, 495–501. https://doi.org/10.1109/BIOROB.2006.1639137

Costa, N. R. S., & Caldwell, D. G. (2006). Control of a biomimetic "soft-actuated" lower body 10dof exoskeleton. *IFAC Proceedings Volumes (IFAC-PapersOnline)*, *8*(PART 1). https://doi.org/10.3182/20060906-3-it-2910.00131

Crawford, R. J. (1998). Processing of Plastics. *Plastics Engineering*, 245–342. https://doi.org/10.1016/B978-075063764-0/50006-6

Disability. (n.d.). Retrieved September 19, 2022, from https://www.who.int/health-topics/disability#tab=tab_2

Dragusanu, M., Troisi, D., Villani, A., Prattichizzo, D., & Malvezzi, M. (2022). Design and Prototyping of an Underactuated Hand Exoskeleton With Fingers Coupled by a Gear-Based

Differential. *Frontiers in Robotics and AI*, *9*, 69. https://doi.org/10.3389/FROBT.2022.862340/BIBTEX

Esquenazi, A., Talaty, M., Packel, A., & Saulino, M. (2012). The Rewalk powered exoskeleton to restore ambulatory function to individuals with thoracic-level motor-complete spinal cord injury. *American Journal of Physical Medicine and Rehabilitation*, *91*(11), 911–921. https://doi.org/10.1097/PHM.0B013E318269D9A3

Foerster, V. (2015). *Cadth Issues in Emerging Health Technologies 2 Cadth Issues in Emerging Health Technologies*.

Gardner, A. D., Potgieter, J., & Noble, F. K. (2017). A review of commercially available exoskeletons' capabilities. *2017 24th International Conference on Mechatronics and Machine Vision in Practice, M2VIP 2017*, *2017-Decem*, 1–5. https://doi.org/10.1109/M2VIP.2017.8211470

Giannini, M. J., Bergmark, B., Kreshover, S., Elias, E., Plummer, C., & O'Keefe, E. (2010). Understanding suicide and disability through three major disabling conditions: Intellectual disability, spinal cord injury, and multiple sclerosis. *Disability and Health Journal*, *3*(2), 74–78. https://doi.org/10.1016/J.DHJO.2009.09.001

Grüneberg, P. (2021). Empowering Patients in Interactive Unity with Machines: Engineering the HAL (Hybrid Assistive Limb) Robotic Rehabilitation System. *Humans and Devices in Medical Contexts*, 255–280. https://doi.org/10.1007/978-981-33-6280-2_10

Iwamoto, Y., Imura, T., Suzukawa, T., Fukuyama, H., Ishii, T., Taki, S., Imada, N., Shibukawa, M., Inagawa, T., Araki, H., & Araki, O. (2019). Combination of Exoskeletal Upper Limb Robot and Occupational Therapy Improve Activities of Daily Living Function in Acute Stroke Patients. *Journal of Stroke and Cerebrovascular Diseases*, *28*(7), 2018–2025. https://doi.org/10.1016/J.JSTROKECEREBROVASDIS.2019.03.006

Kalita, B., Narayan, J., & Dwivedy, S. K. (2021). Development of Active Lower Limb Robotic-Based Orthosis and Exoskeleton Devices: A Systematic Review. *International Journal of Social Robotics*, *13*(4), 775–793. https://doi.org/10.1007/S12369-020-00662-9

Kharb, A., Saini, V., Jain, Y., & Dhiman, S. (2011). A review of gait cycle and its parameters. *IJCEM Int J Comput Eng Manag*, *13*(July), 78–83.

Kian, A., Widanapathirana, G., Joseph, A. M., Lai, D. T. H., & Begg, R. (2022). Application of Wearable Sensors in Actuation and Control of Powered Ankle Exoskeletons: A Comprehensive Review. *Sensors*, *22*(6), 2244. https://doi.org/10.3390/S22062244/S1

Li, G., Su, Q., Xi, W., Song, Z., Bao, R., & Du, Z. (2022). Dynamic analysis and design of a multipurpose lower limb exoskeleton for rehabilitation. *International Journal of Advanced Robotic Systems*, *19*(6), 172988062211351. https://doi.org/10.1177/17298806221135140

Lugo, E., Ponce, P., Molina, A., & Castro, S. (2014). *Co-simulación del Diseño Biomecánico para un Exoesqueleto Robótico del Miembro Inferior*.

Marks, D., Schweinfurther, R., Dewor, A., Huster, T., P Paredes, L., Zutter, D., & C Möller, J. (2019). The Andago for overground gait training in patients with gait disorders after stroke - results from a usability study. *Physiotherapy Research and Reports*, *2*(2). https://doi.org/10.15761/PRR.1000128

Megía-García, A., del-Ama, A. J., Lozano-Berrio, V., Sinovas-Alonso, I., Comino-Suárez, N., & Gil-Agudo, A. (2022). *Safety, Feasibility and Acceptance with HANK Ambulatory Robotic Exoskeleton in Incomplete Spinal Cord Injury Patients* (pp. 935–939). https://doi.org/10.1007/978-3-030-70316-5_149

Minchala, L. I., Astudillo-Salinas, F., Vazquez-Rodas, K. P. and A., Minchala, L. I., Astudillo-Salinas, F., & Vazquez-Rodas, K. P. and A. (2017). Mechatronic Design of a Lower Limb Exoskeleton. *Design, Control and Applications of Mechatronic Systems in Engineering*. https://doi.org/10.5772/67460

Minchala, L. I., Velasco, A. J., Blandin, J. M., Astudillo-Salinas, F., & Vazquez-Rodas, A. (2019). *Low Cost Lower Limb Exoskeleton for Assisting Gait Rehabilitation: Design and Evaluation*. https://doi.org/10.1145/3365265.3365276

Mlenzana, N. B., Frantz, J. M., Rhoda, A. J., & Eide, A. H. (2013). Barriers to and facilitators of rehabilitation services for people with physical disabilities: A systematic review. *African Journal of Disability*, *2*(1). https://doi.org/10.4102/AJOD.V2I1.22

Moeller, T., Moehler, F., Krell-Roesch, J., Dežman, M., Marquardt, C., Asfour, T., Stein, T., & Woll, A. (2023). Use of Lower Limb Exoskeletons as an Assessment Tool for Human Motor Performance: A Systematic Review. *Sensors 2023, Vol. 23, Page 3032*, *23*(6), 3032. https://doi.org/10.3390/S23063032

Nam, K. Y., Kim, H. J., Kwon, B. S., Park, J. W., Lee, H. J., & Yoo, A. (2017). Robot-assisted gait training (Lokomat) improves walking function and activity in people with spinal cord injury: a systematic review. *Journal of NeuroEngineering and Rehabilitation*, *14*(1), 1–13. https://doi.org/10.1186/S12984-017-0232-3/FIGURES/7

Nandy, A., Chakraborty, S., Chakraborty, J., & Venture, G. (2021). Introduction. *Modern Methods for Affordable Clinical Gait Analysis*, 1–15. https://doi.org/10.1016/B978-0-323-85245-6.00012-6

Nugent, R., & van der Vorm, J. (2015). ScienceDirect Standards for the safety of exoskeletons used by industrial workers performing manual handling activities: A contribution from the Robo-Mate project to their future development-review under responsibility of AHFE Conference. *Procedia Manufacturing*, *3*, 1418–1425. https://doi.org/10.1016/j.promfg.2015.07.306

Pamungkas, D. S., Caesarendra, W., Susanto, S., Soebakti, H., & Analia, R. (2019). Overview: Types of lower limb exoskeletons. In *Electronics (Switzerland)* (Vol. 8, Issue 11). https://doi.org/10.3390/electronics8111283

Park, Y. L., Chen, B. R., Young, D., Stirling, L., Wood, R. J., Goldfield, E., & Nagpal, R. (2011). Bio-inspired active soft orthotic device for ankle foot pathologies. *IEEE International Conference on Intelligent Robots and Systems*, 4488–4495. https://doi.org/10.1109/IROS.2011.6048620

Pniak, B., Leszczak, J., Adamczyk, M., Rusek, W., Matosz, P., & Guzik, A. (2021). Occupational burnout among active physiotherapists working in clinical hospitals during the COVID-19 pandemic in south-eastern Poland. *Work*, *68*(2), 285–295. https://doi.org/10.3233/WOR-203375

Rahman, R. A. A., & Shamsuddin, S. (2023). A mini-review of robotic applications for lower-limb rehabilitation in Malaysia. *Malaysian Journal of Movement, Health & Exercise*, *12*(2), 41–47. https://doi.org/10.4103/mohe.mohe_19_23

Read, E., Woolsey, C., McGibbon, C. A., & O'Connell, C. (2020). Physiotherapists' Experiences Using the Ekso Bionic Exoskeleton with Patients in a Neurological Rehabilitation Hospital: A Qualitative Study. *Rehabilitation Research and Practice*, *2020*, 1–8. https://doi.org/10.1155/2020/2939573

Rehmat, N., Zuo, J., Meng, W., Liu, Q., Xie, S. Q., & Liang, H. (2018). Upper limb rehabilitation using robotic exoskeleton systems: a systematic review. *International Journal of Intelligent Robotics and Applications 2018 2:3*, *2*(3), 283–295. https://doi.org/10.1007/S41315-018-0064-8

Riba Romeva, C. (2002). *Diseño concurrente*.

Rossi, S., Patanè, F., Del Sette, F., & Cappa, P. (2014). WAKE-up: A wearable ankle knee exoskeleton. *Proceedings of the IEEE RAS and EMBS International Conference on Biomedical Robotics and Biomechatronics*, *August*, 504–507. https://doi.org/10.1109/biorob.2014.6913827

Ruffoni, D., & van Lenthe, G. H. (2011). Finite Element Analysis in Bone Research: A Computational Method Relating Structure to Mechanical Function. In *Comprehensive Biomaterials* (pp. 91–111). Elsevier. https://doi.org/10.1016/B978-0-08-055294-1.00093-3

Schmeltzpfenning, T., & Brauner, T. (2013). Foot biomechanics and gait. *Handbook of Footwear Design and Manufacture*, 27–48. https://doi.org/10.1533/9780857098795.1.27

Seth, A., & Anderson, F. (2017). *Gait 2392 and 2354 Models*.

Shi, D., Zhang, W., Zhang, W., & Ding, X. (2019). A Review on Lower Limb Rehabilitation Exoskeleton Robots. In *Chinese Journal of Mechanical Engineering (English Edition)* (Vol. 32, Issue 1). https://doi.org/10.1186/s10033-019-0389-8

Śliwiński, Z., Starczyńska, M., Kotela, I., Kowalski, T., Kryś-Noszczyk, K., Lietz-Kijak, D., Kijak, E., & Makara-Studzińska, M. (2014). Burnout among physiotherapists and length of service. *International Journal of Occupational Medicine and Environmental Health 2014 27:2*, *27*(2), 224–235. https://doi.org/10.2478/S13382-014-0248-X

SOLIDWORKS | 3D CAD Design Software & PDM Systems. (n.d.). Retrieved September 17, 2023, from https://www.solidworks.com/

Stearns-Yoder, K. A., & Brenner, L. A. (2018). Novel Psychological Outcomes With Ekso Bionics Technology. *Archives of Physical Medicine and Rehabilitation*, *99*(10), e70–e71. https://doi.org/10.1016/j.apmr.2018.07.249

Taki, S., Iwamoto, Y., Imura, T., Mitsutake, T., & Tanaka, R. (2022). Effects of gait training with the Hybrid Assistive Limb on gait ability in stroke patients: A systematic review of randomized controlled trials. *Journal of Clinical Neuroscience*, *101*, 186–192. https://doi.org/10.1016/J.JOCN.2022.04.001

The technology | Ekso exoskeleton for rehabilitation in people with neurological weakness or paralysis | Advice | NICE. (n.d.).

Tovée, M. J. (2012). Anthropometry. *Encyclopedia of Body Image and Human Appearance*, *1*, 23–29. https://doi.org/10.1016/B978-0-12-384925-0.00004-3

Tsao, C. W., Aday, A. W., Almarzooq, Z. I., Alonso, A., Beaton, A. Z., Bittencourt, M. S., Boehme, A. K., Buxton, A. E., Carson, A. P., Commodore-Mensah, Y., Elkind, M. S. V., Evenson, K. R., Eze-Nliam, C., Ferguson, J. F., Generoso, G., Ho, J. E., Kalani, R., Khan, S. S., Kissela, B. M., … Martin, S. S. (2022). Heart Disease and Stroke Statistics—2022 Update: A Report From the American Heart Association. *Circulation*, *145*(8), E153–E639. https://doi.org/10.1161/CIR.0000000000001052

U, U., & Rajendrakumar, P. K. (2021). Design of a Low-Cost Lower Limb Rehabilitation Exoskeleton System. *IOP Conference Series: Materials Science and Engineering*, *1132*(1), 012008. https://doi.org/10.1088/1757-899X/1132/1/012008

Varghese, J., Akhil, V. M., Rajendrakumar, P. K., & Sivanandan, K. S. (2017). A rotary pneumatic actuator for the actuation of the exoskeleton knee joint. *Theoretical and Applied Mechanics Letters*, *7*(4), 222–230. https://doi.org/10.1016/J.TAML.2017.08.002

Vaughan-Graham, J., Brooks, D., Rose, L., Nejat, G., Pons, J., & Patterson, K. (2020). Exoskeleton use in post-stroke gait rehabilitation: A qualitative study of the perspectives of persons post-stroke and physiotherapists. *Journal of NeuroEngineering and Rehabilitation*, *17*(1), 1–15. https://doi.org/10.1186/s12984-020-00750-x

Veneman, J. F., Kruidhof, R., Hekman, E. E. G., Ekkelenkamp, R., Van Asseldonk, E. H. F., & Van Der Kooij, H. (2007). Design and evaluation of the LOPES exoskeleton robot for interactive gait rehabilitation. *IEEE Transactions on Neural Systems and Rehabilitation Engineering : A Publication of the IEEE Engineering in Medicine and Biology Society*, *15*(3), 379–386. https://doi.org/10.1109/TNSRE.2007.903919

Villa-Parra, A. C., Delisle-Rodríguez, D., López-Delis, A., Bastos-Filho, T., Sagaró, R., & Frizera-Neto, A. (2015). Towards a Robotic Knee Exoskeleton Control Based on Human Motion Intention through EEG and sEMGsignals. *Procedia Manufacturing*, *3*, 1379–1386. https://doi.org/10.1016/J.PROMFG.2015.07.296

Wang, S., Wang, L., Meijneke, C., van Asseldonk, E., Hoellinger, T., Cheron, G., Ivanenko, Y., La Scaleia, V., Sylos-Labini, F., Molinari, M., Tamburella, F., Pisotta, I., Thorsteinsson, F., Ilzkovitz, M., Gancet, J., Nevatia, Y., Hauffe, R., Zanow, F., & van der Kooij, H. (2015). Design and Control of the MINDWALKER Exoskeleton. *IEEE Transactions on Neural Systems and Rehabilitation Engineering*, *23*(2), 277–286. https://doi.org/10.1109/TNSRE.2014.2365697

Wang, T., Zhang, B., Liu, C., Liu, T., Han, Y., Wang, S., Ferreira, J. P., Dong, W., & Zhang, X. (2022). A Review on the Rehabilitation Exoskeletons for the Lower Limbs of the Elderly and the Disabled. *Electronics 2022, Vol. 11, Page 388*, *11*(3), 388. https://doi.org/10.3390/ELECTRONICS11030388

Wu, X., Cheng, R., Liu, G., & Chan, T. H. T. (2021). Indirectly measuring the displacements of tension structures under dominant design loads by exerting simple testing loads. *Engineering Structures*, *248*, 113257. https://doi.org/10.1016/J.ENGSTRUCT.2021.113257

Xue, X., Yang, X., Tu, H., Liu, W., Kong, D., Fan, Z., Deng, Z., & Li, N. (2022). The improvement of the lower limb exoskeletons on the gait of patients with spinal cord injury: A protocol for systematic review and meta-analysis. *Medicine (United States)*, *101*(4), E28709. https://doi.org/10.1097/MD.0000000000028709

Yoshioka, T., Kubota, S., Sugaya, H., Arai, N., Hyodo, K., Kanamori, A., & Yamazaki, M. (2021). Feasibility and efficacy of knee extension training using a single-joint hybrid assistive limb, versus conventional rehabilitation during the early postoperative period after total knee arthroplasty. *Journal of Rural Medicine*, *16*(1), 22–28. https://doi.org/10.2185/JRM.2020-024

Zhou, L., Chen, W., Chen, W., Bai, S., Zhang, J., & Wang, J. (2020). Design of a passive lower limb exoskeleton for walking assistance with gravity compensation. *Mechanism and Machine Theory*, *150*, 103840. https://doi.org/10.1016/j.mechmachtheory.2020.103840

Zoss, A. B., Kazerooni, H., & Chu, A. (2006). Biomechanical design of the Berkeley Lower Extremity Exoskeleton (BLEEX). *IEEE/ASME Transactions on Mechatronics*, *11*(2), 128–138. https://doi.org/10.1109/TMECH.2006.871087

Zoss, A., Kazerooni, H., & Chu, A. (2005). On the mechanical design of the Berkeley Lower Extremity Exoskeleton (BLEEX). *2005 IEEE/RSJ International Conference on Intelligent Robots and Systems, IROS*, 3465–3472. https://doi.org/10.1109/IROS.2005.1545453

APPENDIX A - Anthropometry values

COLOMBIA

En posición de pie
Población laboral
Ambos sexos
20 a 59 años

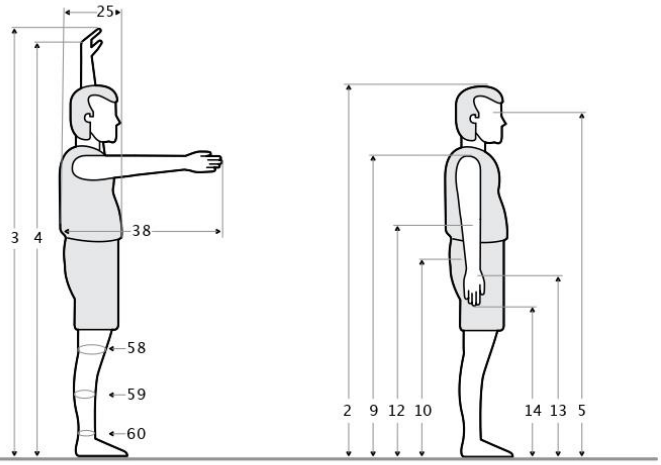

Dimensiones		fem. 20 - 59 años (n= 785)					masc. 20 - 59 años (n= 1315)				
				Percentiles					Percentiles		
		$\bar{x}$	D.E.	5	50	95	$\bar{x}$	D.E.	5	50	95
1	Masa corporal (Kg)	59.8	9.43	46.7	59.1	76.9	69.8	10.40	53.7	69.1	87.8
2	Estatura (cm)	155.8	5.87	146.7	155.6	166.1	168.8	6.50	158.0	168.6	179.2
3	Alcance vertical máximo	195.2	8.14	182.4	194.8	209.4	213.2	8.89	198.3	213.1	227.8
4	Alcance vertical con asimiento	181.5	7.79	169.5	181.1	195.1	198.3	8.28	184.2	198.3	211.9
5	Altura de los ojos	145.3	5.71	136.5	145.1	155.2	158.0	6.38	147.4	157.9	168.2
9	Altura acromial	127.2	5.19	119.1	127.1	136.1	137.9	5.78	128.2	137.9	147.3
10	Altura cresta ilíaca medial	92.5	4.54	85.6	92.3	100.4	100.6	4.87	92.5	100.7	108.5
12	Altura radial	98.1	4.16	91.4	97.8	105.2	106.4	4.64	98.7	106.5	114.3
13	Altura estiloidea	75.2	3.41	69.7	75.0	80.8	81.3	3.96	75.0	81.4	87.9
14	Altura dactilea dedo medio	59.3	2.94	54.6	59.3	64.0	63.5	3.47	57.8	63.6	69.2
25	Anchura del tórax	18.6	1.91	15.6	18.5	21.9	20.4	1.90	17.4	20.3	23.8
38	Alcance anterior brazo	65.8	3.18	61.0	65.6	71.5	71.4	3.30	66.3	71.4	76.9
58	Perímetro rodilla media	35.5	2.70	31.5	35.3	40.3	36.5	2.38	32.9	36.4	40.6
59	Perímetro pierna media	34.2	2.64	30.4	34.2	39.1	35.9	2.59	31.7	35.9	40.1
60	Perímetro supramaleolar	20.6	1.39	18.5	20.6	23.1	21.8	1.36	19.7	21.9	24.2

En posición sentado
Población laboral
Ambos sexos
20 a 59 años

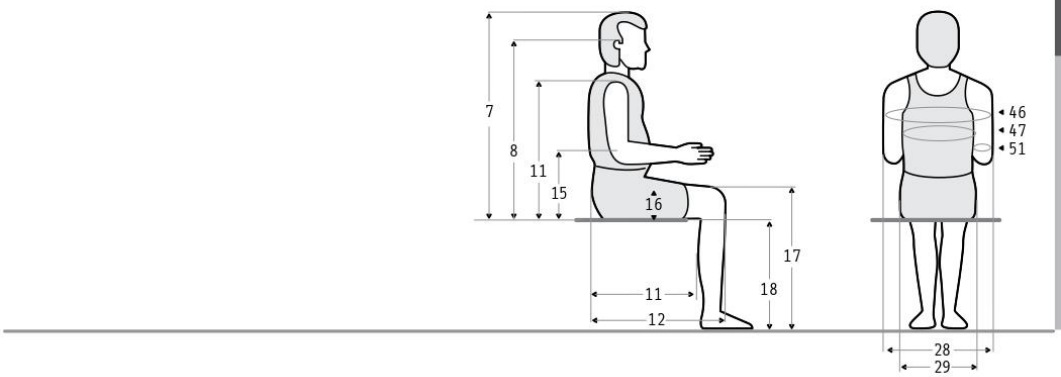

Dimensiones		fem. 20 - 59 años (n= 785)					masc. 20 - 59 años (n= 1315)				
				Percentiles					Percentiles		
		$\bar{x}$	D.E.	5	50	95	$\bar{x}$	D.E.	5	50	95
6	Altura sentado normal	81.7	3.05	76.8	81.7	86.7	86.0	3.50	80.2	85.9	91.8
7	Altura sentado erguido	83.0	2.80	78.5	83.0	87.7	88.6	3.21	83.5	88.6	94.0
8	Altura de los ojos	72.9	2.80	68.4	72.9	77.4	78.4	3.24	73.2	78.4	83.6
11	Altura acromial	55.0	2.37	51.2	55.2	58.7	58.8	2.74	54.2	58.8	63.2
15	Altura radial	22.9	2.22	19.0	23.1	26.4	23.7	2.46	19.4	23.8	27.7
16	Altura del muslo	14.1	1.30	12.1	14.1	16.5	14.9	1.24	12.9	15.0	17.1
17	Altura de la rodilla	48.4	2.35	44.7	48.5	52.4	52.5	2.56	48.2	52.5	56.6
18	Altura de la fosa poplítea	38.3	2.09	35.1	38.3	41.9	42.3	2.29	38.7	42.4	46.1
28	Anchura codo a codo	41.0	4.64	33.9	40.6	49.4	44.6	4.44	37.7	44.7	52.3
29	Anchura de las caderas	37.3	3.13	32.6	37.3	42.5	34.9	2.58	30.9	34.9	39.2
41	Largura nalga - fosa poplítea	46.1	2.62	42.0	46.1	50.4	46.8	2.44	42.7	46.8	50.8
42	Largura nalga - rodilla	55.0	2.60	51.0	55.0	59.5	56.9	2.57	52.7	57.0	61.3
46	Perímetro bideltoideo	104.1	6.94	93.4	103.5	116.0	113.4	6.83	102.5	113.4	124.6
47	Perímetro mesoesternal	88.7	6.33	78.9	88.3	100.0	96.4	6.46	86.2	96.3	107.0
51	Perímetro brazo flexionado	28.0	2.97	23.5	27.7	33.7	31.1	2.58	27.0	31.1	35.5

APPENDIX B -Angle joints

time	time	hip_adduction_l
0	0	2,68
1	0,02	1,94
2	0,04	0,99
3	0,06	-0,19
4	0,08	-1,48
5	0,1	-2,69
6	0,12	-3,62
7	0,14	-4,1
8	0,16	-4,16
9	0,18	-3,88
10	0,2	-3,38
11	0,22	-2,79
12	0,24	-2,18
13	0,26	-1,61
14	0,28	-1,1
15	0,3	-0,66
16	0,32	-0,28
17	0,34	0,03
18	0,36	0,27
19	0,38	0,44
20	0,4	0,53
21	0,42	0,57
22	0,44	0,59
23	0,46	0,67
24	0,48	0,86
25	0,5	1,18

time	time	hip_adduction_l
26	0,52	1,09
27	0,54	1,59
28	0,56	2,22
29	0,58	3,01
30	0,6	3,92
31	0,62	4,78
32	0,64	5,45
33	0,66	5,85
34	0,68	6,01
35	0,7	5,96
36	0,72	5,8
37	0,74	5,57
38	0,76	5,31
39	0,78	5,06
40	0,8	4,83
41	0,82	4,64
42	0,84	4,49
43	0,86	4,38
44	0,88	4,31
45	0,9	4,26
46	0,92	4,2
47	0,94	4,11
48	0,96	3,95
49	0,98	3,68
50	1	3,26

time	time	hip_adduction_r		time	time	hip_adduction_r
0	0	1,09		26	0,52	1,94
1	0,02	1,59		27	0,54	0,99
2	0,04	2,22		28	0,56	-0,19
3	0,06	3,01		29	0,58	-1,48
4	0,08	3,92		30	0,6	-2,69
5	0,1	4,78		31	0,62	-3,62
6	0,12	5,45		32	0,64	-4,1
7	0,14	5,85		33	0,66	-4,16
8	0,16	6,01		34	0,68	-3,88
9	0,18	5,96		35	0,7	-3,38
10	0,2	5,8		36	0,72	-2,79
11	0,22	5,57		37	0,74	-2,18
12	0,24	5,31		38	0,76	-1,61
13	0,26	5,06		39	0,78	-1,1
14	0,28	4,83		40	0,8	-0,66
15	0,3	4,64		41	0,82	-0,28
16	0,32	4,49		42	0,84	0,03
17	0,34	4,38		43	0,86	0,27
18	0,36	4,31		44	0,88	0,44
19	0,38	4,26		45	0,9	0,53
20	0,4	4,2		46	0,92	0,57
21	0,42	4,11		47	0,94	0,59
22	0,44	3,95		48	0,96	0,67
23	0,46	3,68		49	0,98	0,86
24	0,48	3,26		50	1	1,18
25	0,5	2,68				

time	time	ankle_angle_l
0	0	9,81
1	0,02	8,26
2	0,04	5,52
3	0,06	1,11
4	0,08	4,36
5	0,1	9,73
6	0,12	13,37
7	0,14	14,07
8	0,16	12,62
9	0,18	10,16
10	0,2	7,6
11	0,22	5,28
12	0,24	3,2
13	0,26	1,34
14	0,28	0,23
15	0,3	1,44
16	0,32	2,24
17	0,34	2,58
18	0,36	2,39
19	0,38	1,83
20	0,4	1,16
21	0,42	0,54
22	0,44	0,18
23	0,46	0,07
24	0,48	0,01
25	0,5	0,5

time	time	ankle_angle_l
26	0,52	1,7
27	0,54	3,25
28	0,56	4,68
29	0,58	5,08
30	0,6	4,17
31	0,62	2,5
32	0,64	0,83
33	0,66	0,65
34	0,68	1,92
35	0,7	2,98
36	0,72	3,88
37	0,74	4,64
38	0,76	5,25
39	0,78	5,78
40	0,8	6,28
41	0,82	6,78
42	0,84	7,3
43	0,86	7,86
44	0,88	8,44
45	0,9	9,05
46	0,92	9,63
47	0,94	10,16
48	0,96	10,56
49	0,98	10,75
50	1	10,54

time	time	ankle_angle_r
0	0	1,7
1	0,02	3,25
2	0,04	4,68
3	0,06	5,08
4	0,08	4,17
5	0,1	2,5
6	0,12	0,83
7	0,14	0,65
8	0,16	1,92
9	0,18	2,98
10	0,2	3,88
11	0,22	4,64
12	0,24	5,25
13	0,26	5,78
14	0,28	6,28
15	0,3	6,78
16	0,32	7,3
17	0,34	7,86
18	0,36	8,44
19	0,38	9,05
20	0,4	9,63
21	0,42	10,16
22	0,44	10,56
23	0,46	10,75
24	0,48	10,54
25	0,5	9,81

time	time	ankle_angle_r
26	0,52	8,26
27	0,54	5,52
28	0,56	1,11
29	0,58	4,36
30	0,6	9,73
31	0,62	13,37
32	0,64	14,07
33	0,66	12,62
34	0,68	10,16
35	0,7	7,6
36	0,72	5,28
37	0,74	3,2
38	0,76	1,34
39	0,78	0,23
40	0,8	1,44
41	0,82	2,24
42	0,84	2,58
43	0,86	2,39
44	0,88	1,83
45	0,9	1,16
46	0,92	0,54
47	0,94	0,18
48	0,96	0,07
49	0,98	0,01
50	1	0,5

time	time	hip_flexion_l
0	0	16,56
1	0,02	16,82
2	0,04	16,53
3	0,06	15,4
4	0,08	13,44
5	0,1	10,65
6	0,12	7,15
7	0,14	3,16
8	0,16	0,95
9	0,18	4,93
10	0,2	8,63
11	0,22	11,96
12	0,24	14,96
13	0,26	17,62
14	0,28	19,89
15	0,3	21,76
16	0,32	23,24
17	0,34	24,33
18	0,36	24,98
19	0,38	25,26
20	0,4	25,25
21	0,42	25,04
22	0,44	24,8
23	0,46	24,66
24	0,48	24,66
25	0,5	24,7

time	time	hip_flexion_l
26	0,52	24,61
27	0,54	24,45
28	0,56	24,13
29	0,58	23,68
30	0,6	22,96
31	0,62	21,78
32	0,64	20,24
33	0,66	18,41
34	0,68	16,38
35	0,7	14,19
36	0,72	11,91
37	0,74	9,58
38	0,76	7,22
39	0,78	4,87
40	0,8	2,57
41	0,82	0,33
42	0,84	1,85
43	0,86	3,98
44	0,88	6,06
45	0,9	8,1
46	0,92	10,06
47	0,94	11,88
48	0,96	13,5
49	0,98	14,85
50	1	15,88

time	time	hip_flexion_r
0	0	24,61
1	0,02	24,45
2	0,04	24,13
3	0,06	23,68
4	0,08	22,96
5	0,1	21,78
6	0,12	20,24
7	0,14	18,41
8	0,16	16,38
9	0,18	14,19
10	0,2	11,91
11	0,22	9,58
12	0,24	7,22
13	0,26	4,87
14	0,28	2,57
15	0,3	0,33
16	0,32	-1,85
17	0,34	-3,98
18	0,36	-6,06
19	0,38	-8,1
20	0,4	-10,06
21	0,42	-11,88
22	0,44	-13,5
23	0,46	-14,85
24	0,48	-15,88
25	0,5	-16,56

time	time	hip_flexion_r
26	0,52	-16,82
27	0,54	-16,53
28	0,56	-15,4
29	0,58	-13,44
30	0,6	-10,65
31	0,62	-7,15
32	0,64	-3,16
33	0,66	0,95
34	0,68	4,93
35	0,7	8,63
36	0,72	11,96
37	0,74	14,96
38	0,76	17,62
39	0,78	19,89
40	0,8	21,76
41	0,82	23,24
42	0,84	24,33
43	0,86	24,98
44	0,88	25,26
45	0,9	25,25
46	0,92	25,04
47	0,94	24,8
48	0,96	24,66
49	0,98	24,66
50	1	24,7

time	time	knee_angle_l
0	0	8,2
1	0,02	11,29
2	0,04	15,19
3	0,06	20,17
4	0,08	26,06
5	0,1	32,67
6	0,12	39,6
7	0,14	46,16
8	0,16	51,68
9	0,18	55,66
10	0,2	57,83
11	0,22	58,25
12	0,24	57,28
13	0,26	55,06
14	0,28	51,58
15	0,3	46,99
16	0,32	41,48
17	0,34	35,19
18	0,36	28,31
19	0,38	21,23
20	0,4	14,44
21	0,42	8,48
22	0,44	4,3
23	0,46	2,27
24	0,48	2,35
25	0,5	4,14

time	time	knee_angle_l
26	0,52	3,94
27	0,54	6,66
28	0,56	9,45
29	0,58	12,26
30	0,6	14,76
31	0,62	16,37
32	0,64	17,04
33	0,66	16,93
34	0,68	16,24
35	0,7	15,15
36	0,72	13,87
37	0,74	12,46
38	0,76	10,95
39	0,78	9,42
40	0,8	7,96
41	0,82	6,59
42	0,84	5,37
43	0,86	4,29
44	0,88	3,4
45	0,9	2,72
46	0,92	2,37
47	0,94	2,44
48	0,96	3
49	0,98	4,08
50	1	5,83

time	time	knee_angle_r
0	0	3,94
1	0,02	6,66
2	0,04	9,45
3	0,06	12,26
4	0,08	14,76
5	0,1	16,37
6	0,12	17,04
7	0,14	16,93
8	0,16	16,24
9	0,18	15,15
10	0,2	13,87
11	0,22	12,46
12	0,24	10,95
13	0,26	9,42
14	0,28	7,96
15	0,3	6,59
16	0,32	5,37
17	0,34	4,29
18	0,36	3,4
19	0,38	2,72
20	0,4	2,37
21	0,42	2,44
22	0,44	3
23	0,46	4,08
24	0,48	5,83
25	0,5	8,2

time	time	knee_angle_r
26	0,52	11,29
27	0,54	15,19
28	0,56	20,17
29	0,58	26,06
30	0,6	32,67
31	0,62	39,6
32	0,64	46,16
33	0,66	51,68
34	0,68	55,66
35	0,7	57,83
36	0,72	58,25
37	0,74	57,28
38	0,76	55,06
39	0,78	51,58
40	0,8	46,99
41	0,82	41,48
42	0,84	35,19
43	0,86	28,31
44	0,88	21,23
45	0,9	14,44
46	0,92	8,48
47	0,94	4,3
48	0,96	2,27
49	0,98	2,35
50	1	4,14

time	time	hip_rotation_l
0	0	1,28
1	0,02	1,41
2	0,04	1,16
3	0,06	0,41
4	0,08	0,48
5	0,1	0,99
6	0,12	0,66
7	0,14	0,31
8	0,16	1,09
9	0,18	1,09
10	0,2	0,33
11	0,22	0,74
12	0,24	1,71
13	0,26	2,48
14	0,28	3,11
15	0,3	3,7
16	0,32	4,35
17	0,34	4,98
18	0,36	5,28
19	0,38	4,96
20	0,4	4,03
21	0,42	2,81
22	0,44	1,85
23	0,46	1,38
24	0,48	1,27
25	0,5	1,21

time	time	hip_rotation_l
26	0,52	1,35
27	0,54	0,37
28	0,56	1,36
29	0,58	3,02
30	0,6	3,99
31	0,62	4,23
32	0,64	4,18
33	0,66	3,83
34	0,68	3,23
35	0,7	2,72
36	0,72	2,4
37	0,74	2,14
38	0,76	1,83
39	0,78	1,5
40	0,8	1,21
41	0,82	0,96
42	0,84	0,71
43	0,86	0,45
44	0,88	0,2
45	0,9	0,01
46	0,92	0,09
47	0,94	0,02
48	0,96	0,21
49	0,98	0,56
50	1	0,95

time	time	hip_rotation_r
0	0	1,35
1	0,02	0,37
2	0,04	1,36
3	0,06	3,02
4	0,08	3,99
5	0,1	4,23
6	0,12	4,18
7	0,14	3,83
8	0,16	3,23
9	0,18	2,72
10	0,2	2,4
11	0,22	2,14
12	0,24	1,83
13	0,26	1,5
14	0,28	1,21
15	0,3	0,96
16	0,32	0,71
17	0,34	0,45
18	0,36	0,2
19	0,38	0,01
20	0,4	0,09
21	0,42	0,02
22	0,44	0,21
23	0,46	0,56
24	0,48	0,95
25	0,5	1,28

time	time	hip_rotation_r
26	0,52	1,41
27	0,54	1,16
28	0,56	0,41
29	0,58	0,48
30	0,6	0,99
31	0,62	0,66
32	0,64	0,31
33	0,66	1,09
34	0,68	1,09
35	0,7	0,33
36	0,72	0,74
37	0,74	1,71
38	0,76	2,48
39	0,78	3,11
40	0,8	3,7
41	0,82	4,35
42	0,84	4,98
43	0,86	5,28
44	0,88	4,96
45	0,9	4,03
46	0,92	2,81
47	0,94	1,85
48	0,96	1,38
49	0,98	1,27
50	1	1,21

APPENDIX C – CAD model pieces

Exoskeleton assembly

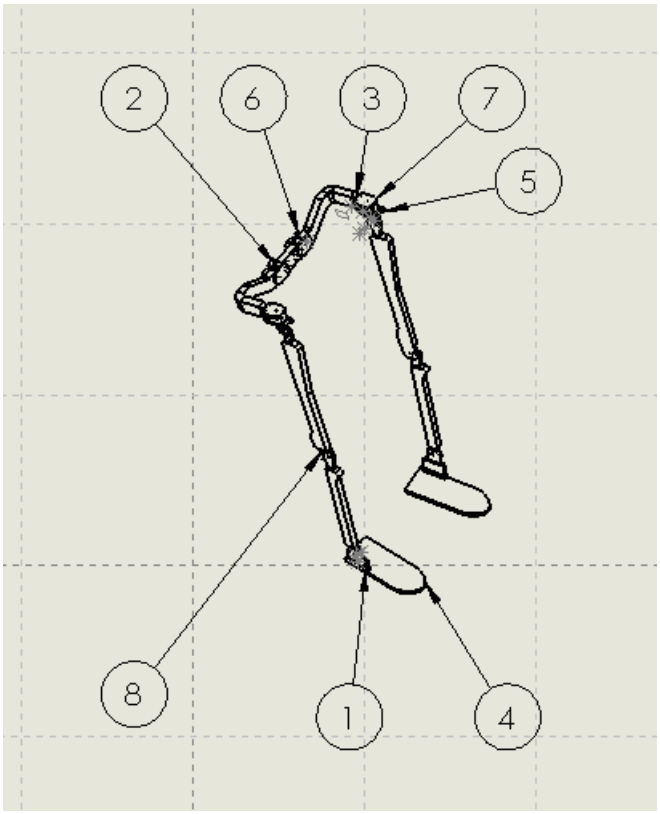

1 Ankle joint
2 Hip support
3 Hip rigid
4 Foot rigid
5 Thigh
6 Joint for hip adduction/abduction
7 Joint for hip rotation and flexion/extension
8 Shank

Hip support.

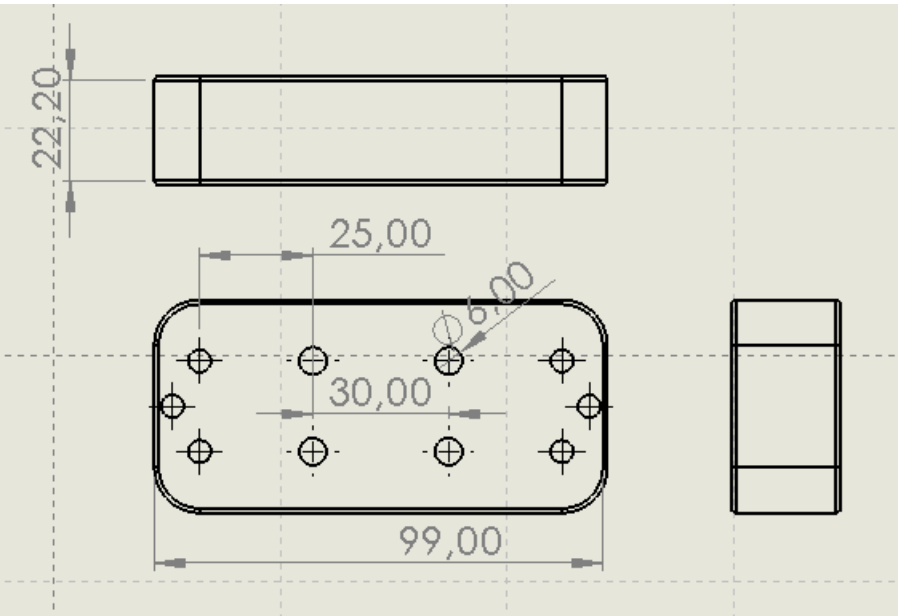

Measurements in mm

Hip rigid

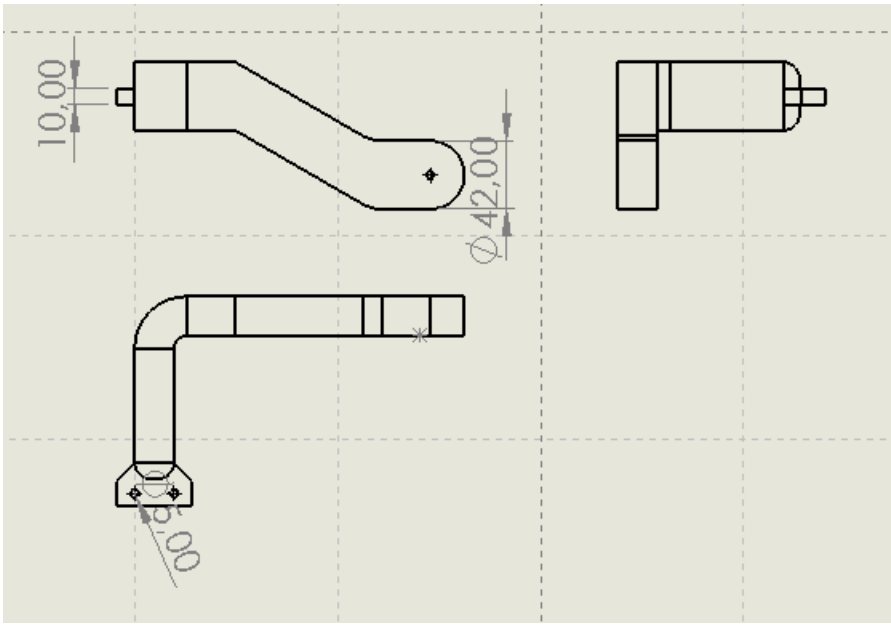

Measurements in mm

Joint for hip adduction/abduction

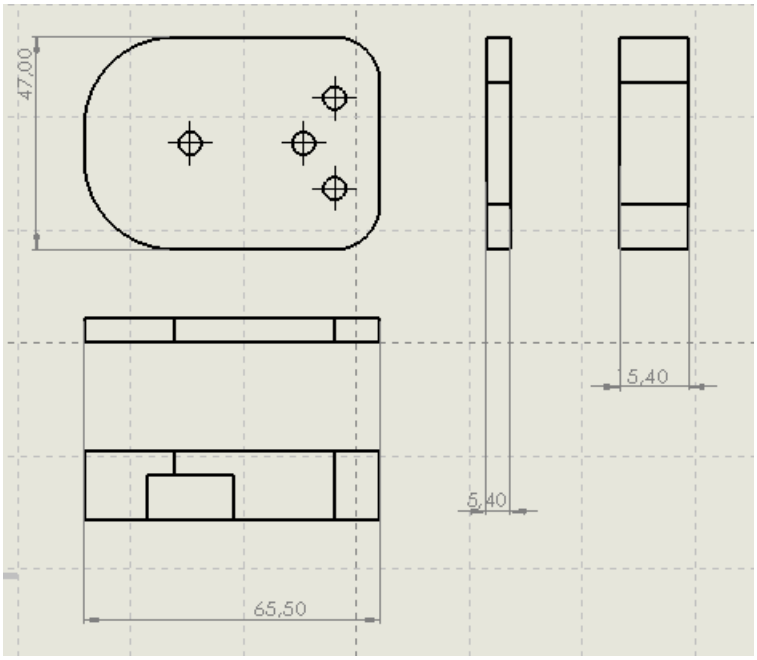

Measurements in mm

Joint for hip rotation and flexion/extension

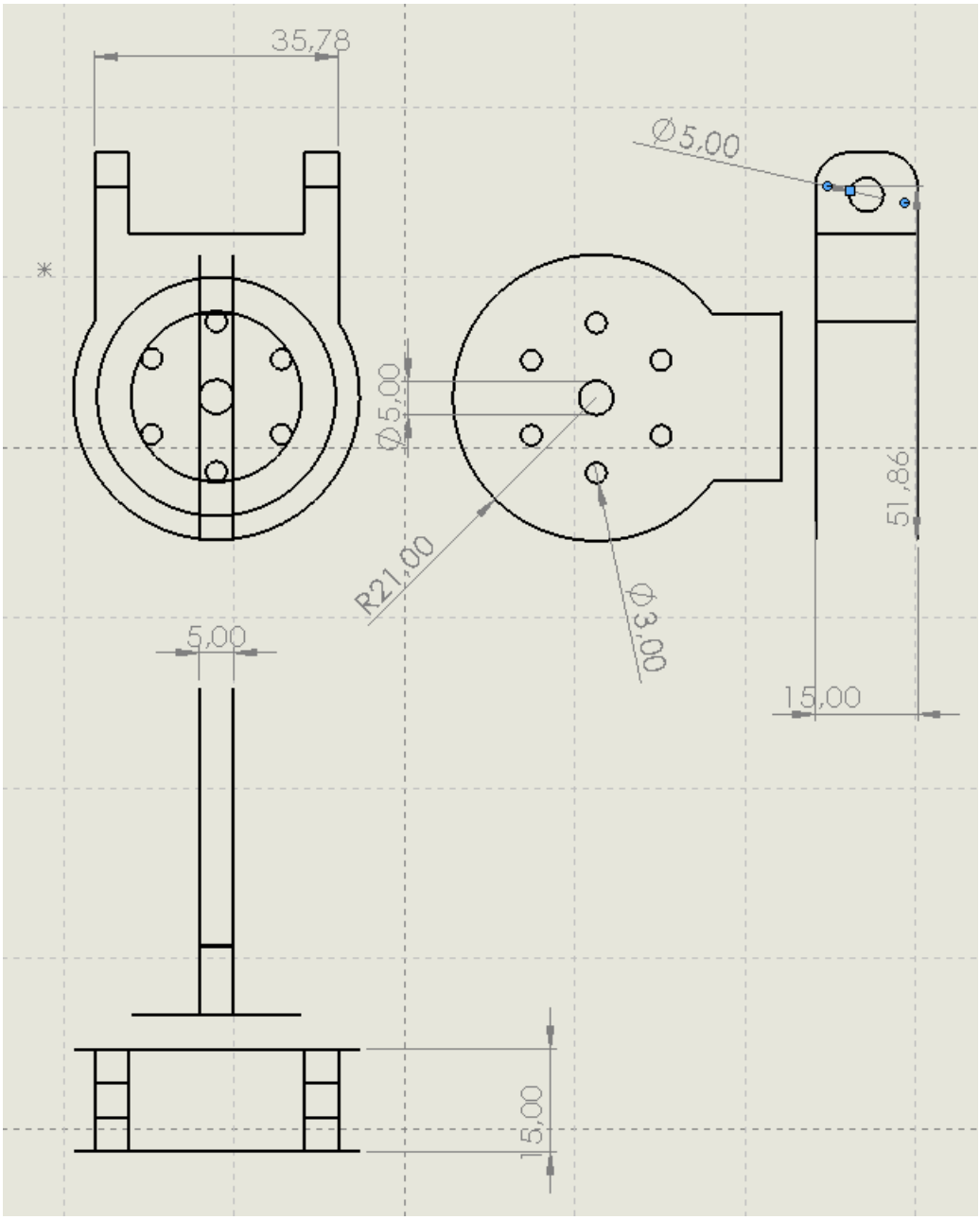

Measurements in mm

Thigh

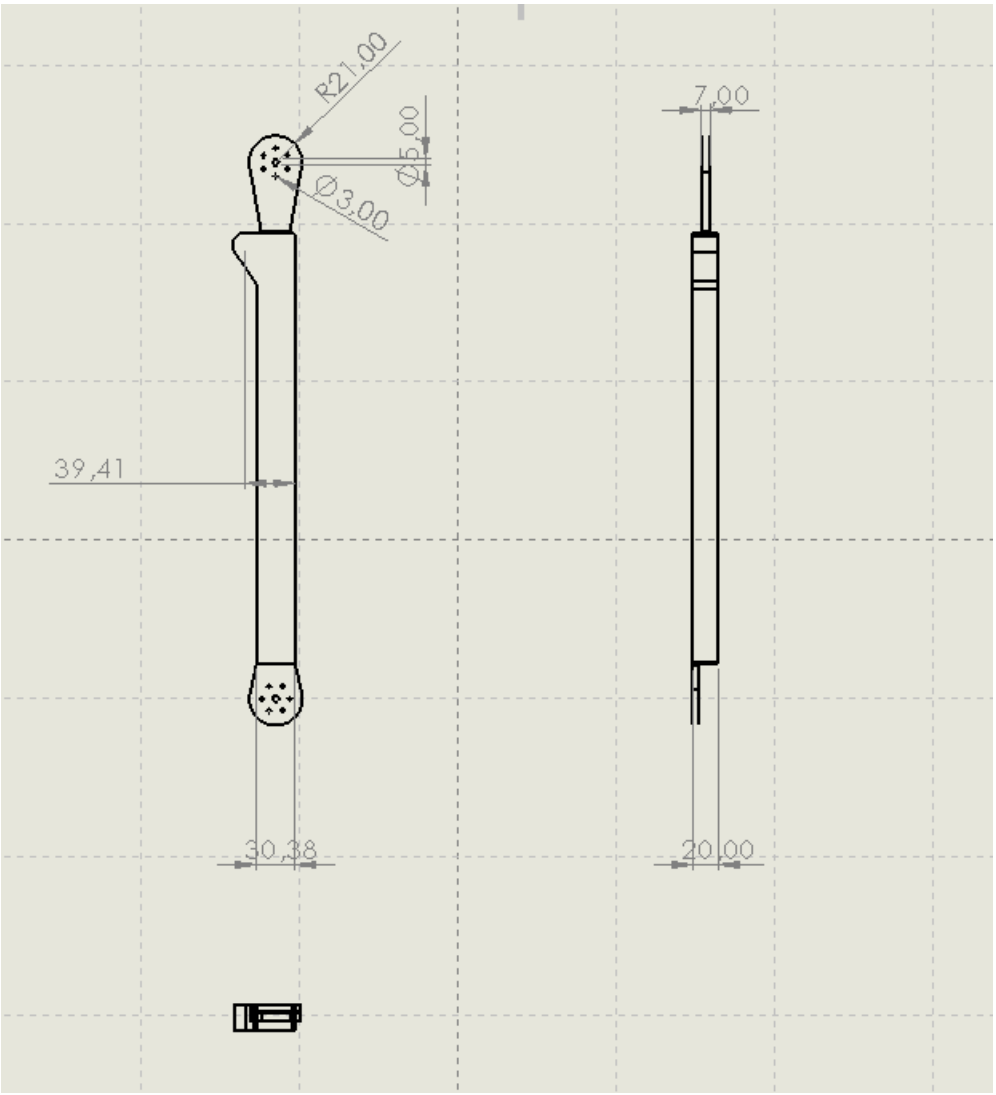

Measurements in mm

Shank

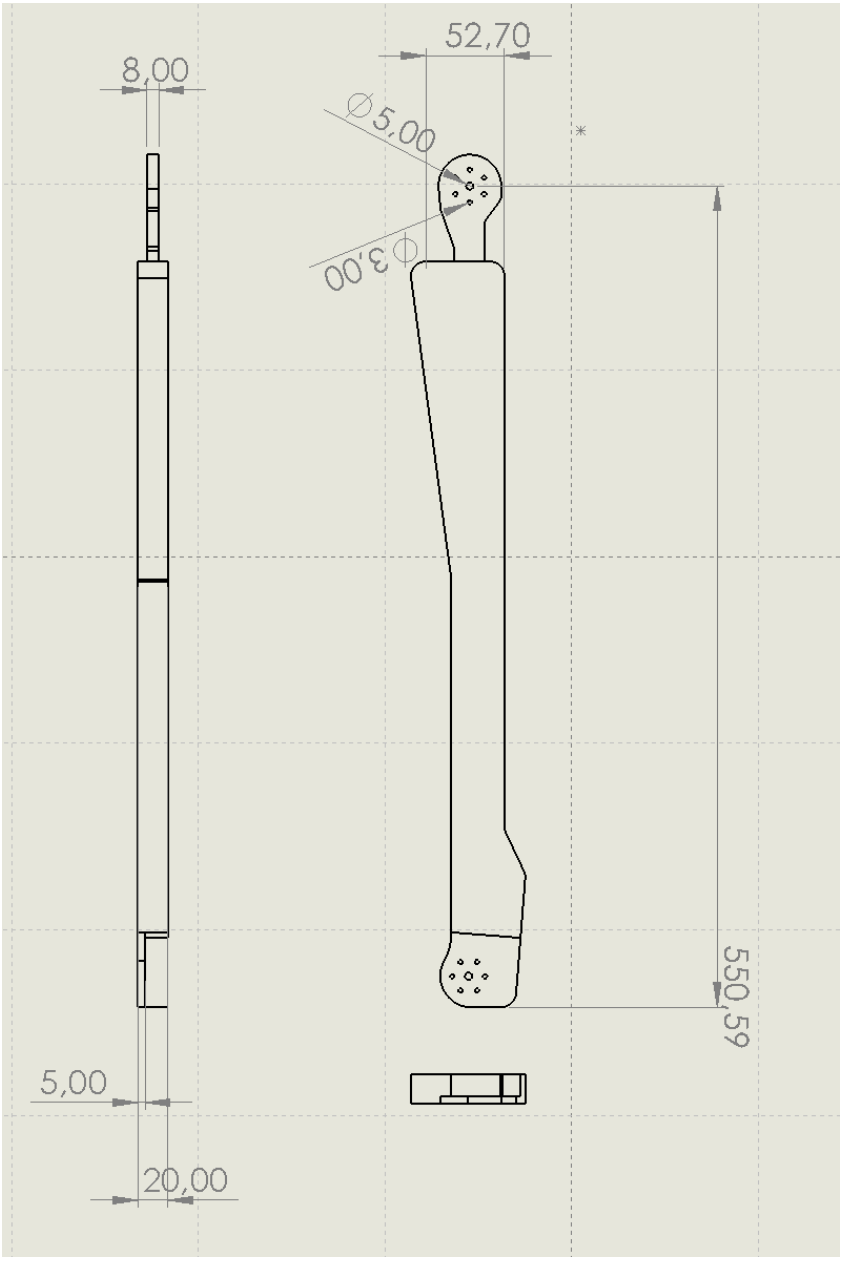

Measurements in mm

Ankle joint

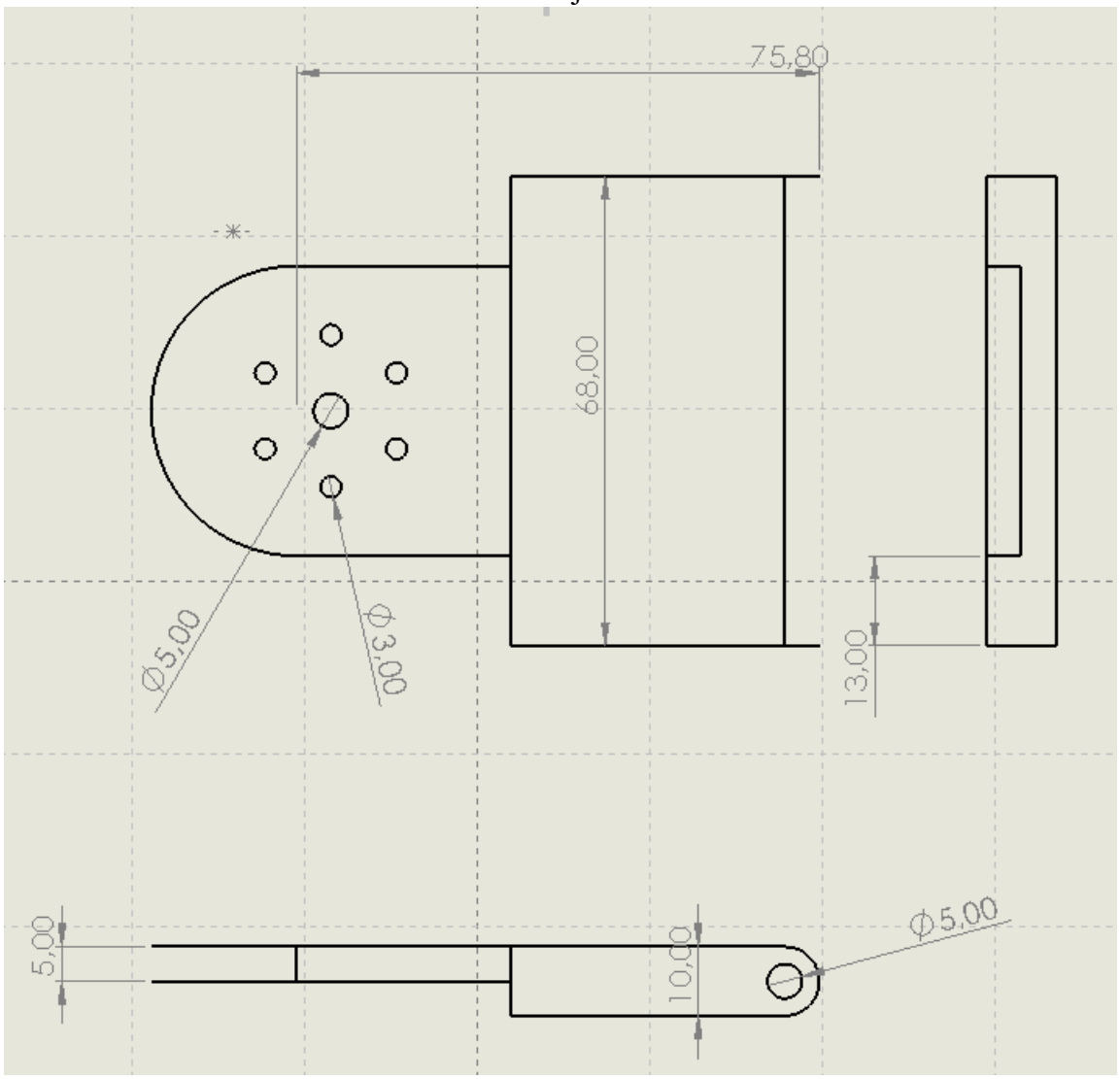

Measurements in mm

Foot rigid

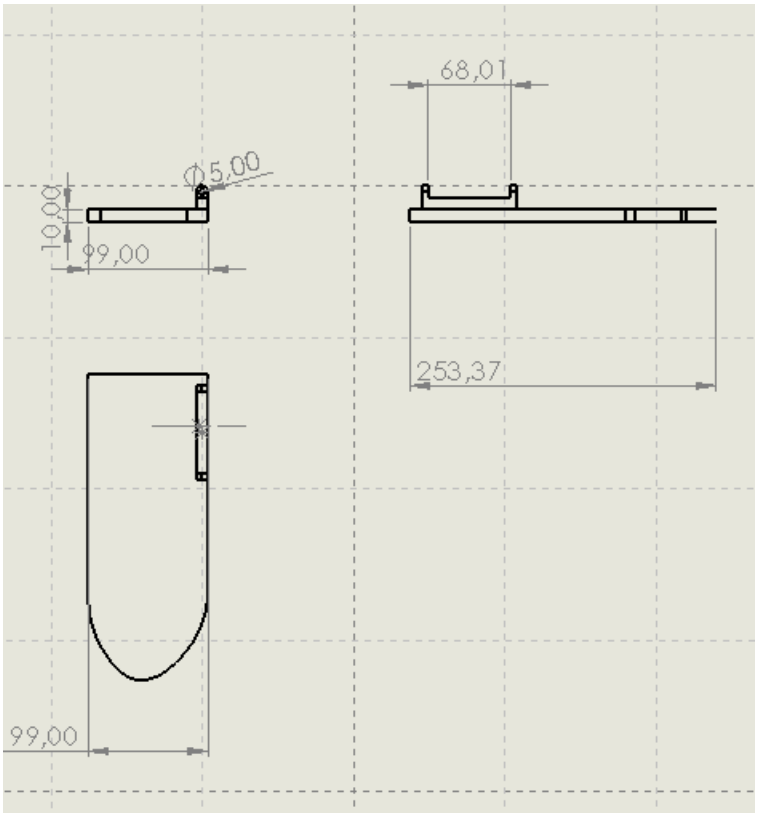

Measurements in mm

APPENDIX D – Open loop system control and MATLAB code

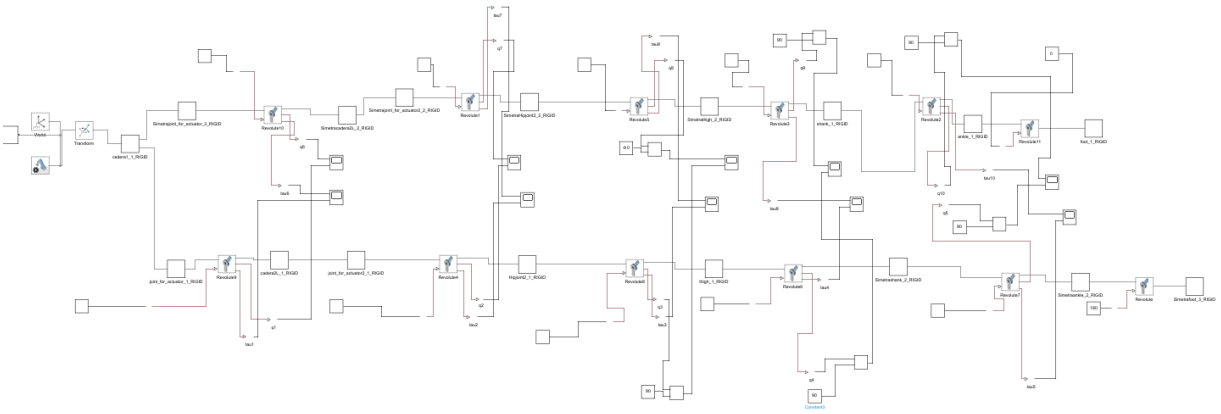

```
% Simscape(TM) Multibody(TM) version: 7.7

% This is a model data file derived from a Simscape Multibody Import XML file using
the smimport function.
% The data in this file sets the block parameter values in an imported Simscape
Multibody model.
% For more information on this file, see the smimport function help page in the
Simscape Multibody documentation.
% You can modify numerical values, but avoid any other changes to this file.
% Do not add code to this file. Do not edit the physical units shown in comments.

%%%VariableName:smiData


%============== RigidTransform ==============%

%Initialize the RigidTransform structure array by filling in null values.
smiData.RigidTransform(33).translation = [0.0 0.0 0.0];
smiData.RigidTransform(33).angle = 0.0;
smiData.RigidTransform(33).axis = [0.0 0.0 0.0];
smiData.RigidTransform(33).ID = "";

%Translation Method - Cartesian
%Rotation Method - Arbitrary Axis
smiData.RigidTransform(1).translation = [-1.9428902930940239e-13 -
1.1102230246251565e-13 39.00500000000001];  % mm
smiData.RigidTransform(1).angle = 3.1415926535897931;  % rad
smiData.RigidTransform(1).axis = [1 0 1.7763568394002505e-15];
smiData.RigidTransform(1).ID = "B[Simetríafoot-3:-:Simetríaankle-2]";

%Translation Method - Cartesian
%Rotation Method - Arbitrary Axis
```

```
smiData.RigidTransform(2).translation = [65.795294629773821 39.009999999999707
5.0000000000005969];  % mm
smiData.RigidTransform(2).angle = 2.094395102393197;  % rad
smiData.RigidTransform(2).axis = [0.57735026918962629 -0.57735026918962418
0.57735026918962673];
smiData.RigidTransform(2).ID = "F[Simetríafoot-3:-:Simetríaankle-2]";

%Translation Method - Cartesian
%Rotation Method - Arbitrary Axis
smiData.RigidTransform(3).translation = [-27.499999999999915 0 -42.000000000000121];
% mm
smiData.RigidTransform(3).angle = 2.0943951023931935;  % rad
smiData.RigidTransform(3).axis = [0.57735026918962506 0.57735026918962506
0.57735026918962717];
smiData.RigidTransform(3).ID = "B[Simetríajoint for actuator2-2:-:SimetríaHipjoint2-
2]";

%Translation Method - Cartesian
%Rotation Method - Arbitrary Axis
smiData.RigidTransform(4).translation = [-1.0658141036401503e-13 -
2.6645352591003757e-13 44.999999999996078];  % mm
smiData.RigidTransform(4).angle = 3.1415926535897927;  % rad
smiData.RigidTransform(4).axis = [1 9.4490370198572172e-31 3.6644809749076092e-15];
smiData.RigidTransform(4).ID = "F[Simetríajoint for actuator2-2:-:SimetríaHipjoint2-
2]";

%Translation Method - Cartesian
%Rotation Method - Arbitrary Axis
smiData.RigidTransform(5).translation = [-157.95293944990181 38.282032302754452
96.799999999999784];  % mm
smiData.RigidTransform(5).angle = 2.094395102393197;  % rad
smiData.RigidTransform(5).axis = [-0.5773502691896264 -0.57735026918962651 -
0.57735026918962451];
smiData.RigidTransform(5).ID = "B[Simetríacadera2L-2:-:Simetríajoint for actuator2-
2]";

%Translation Method - Cartesian
%Rotation Method - Arbitrary Axis
smiData.RigidTransform(6).translation = [2.9000000000000523 -12.050000000000022 -
7.4999999999999289];  % mm
smiData.RigidTransform(6).angle = 3.1415926535897927;  % rad
smiData.RigidTransform(6).axis = [-0.70710678118654879 -3.3306690738754691e-16
0.70710678118654635];
smiData.RigidTransform(6).ID = "F[Simetríacadera2L-2:-:Simetríajoint for actuator2-
2]";

%Translation Method - Cartesian
%Rotation Method - Arbitrary Axis
smiData.RigidTransform(7).translation = [0 0 94.999999999999915];  % mm
smiData.RigidTransform(7).angle = 3.1415926535897931;  % rad
smiData.RigidTransform(7).axis = [1 0 0];
smiData.RigidTransform(7).ID = "B[ankle-1:-:shank-1]";

%Translation Method - Cartesian
%Rotation Method - Arbitrary Axis
```

```
smiData.RigidTransform(8).translation = [-22.328669583904599 -379.8726408161682 -
81.499999999999133];  % mm
smiData.RigidTransform(8).angle = 1.0952027982818391e-15;  % rad
smiData.RigidTransform(8).axis = [-0.65242577802703428 0.75785262694393218 -
2.7075745394947645e-16];
smiData.RigidTransform(8).ID = "F[ankle-1:-:shank-1]";

%Translation Method - Cartesian
%Rotation Method - Arbitrary Axis
smiData.RigidTransform(9).translation = [-22.57667365095417 43.320949332552928
13.000000000000011];  % mm
smiData.RigidTransform(9).angle = 3.1415926535897931;  % rad
smiData.RigidTransform(9).axis = [1 0 8.3266726846886728e-17];
smiData.RigidTransform(9).ID = "B[shank-1:-:Simetríathigh-2]";

%Translation Method - Cartesian
%Rotation Method - Arbitrary Axis
smiData.RigidTransform(10).translation = [529.89905710259711 -0.80410192031700944
15.000000000000054];  % mm
smiData.RigidTransform(10).angle = 3.1415926535897927;  % rad
smiData.RigidTransform(10).axis = [1 -4.2059842642664121e-32 -2.38651807510468e-16];
smiData.RigidTransform(10).ID = "F[shank-1:-:Simetríathigh-2]";

%Translation Method - Cartesian
%Rotation Method - Arbitrary Axis
smiData.RigidTransform(11).translation = [1.1102230246251565e-13 0
15.000000000000014];  % mm
smiData.RigidTransform(11).angle = 3.1415926535897931;  % rad
smiData.RigidTransform(11).axis = [1 0 -3.6012859361278515e-15];
smiData.RigidTransform(11).ID = "B[Hipjoint2-1:-:joint for actuator2-1]";

%Translation Method - Cartesian
%Rotation Method - Arbitrary Axis
smiData.RigidTransform(12).translation = [32.500000000000171 -2.9842794901924208e-13
42.00000000000027];  % mm
smiData.RigidTransform(12).angle = 2.0943951023931944;  % rad
smiData.RigidTransform(12).axis = [-0.57735026918962529 -0.57735026918962529
0.57735026918962673];
smiData.RigidTransform(12).ID = "F[Hipjoint2-1:-:joint for actuator2-1]";

%Translation Method - Cartesian
%Rotation Method - Arbitrary Axis
smiData.RigidTransform(13).translation = [-169.99999999999997 53.282032302754359 -
77.899999999999821];  % mm
smiData.RigidTransform(13).angle = 2.0943951023931935;  % rad
smiData.RigidTransform(13).axis = [-0.57735026918962506 -0.57735026918962506 -
0.57735026918962717];
smiData.RigidTransform(13).ID = "B[cadera2L-1:-:joint for actuator2-1]";

%Translation Method - Cartesian
%Rotation Method - Arbitrary Axis
smiData.RigidTransform(14).translation = [-12.100000000000126 -0.0029394499018415843
-11.399999999999881];  % mm
smiData.RigidTransform(14).angle = 3.1415926535897927;  % rad
```

```
smiData.RigidTransform(14).axis = [0.70710678118654635 -9.7144514654701173e-17 -
0.70710678118654879];
smiData.RigidTransform(14).ID = "F[cadera2L-1:-:joint for actuator2-1]";

%Translation Method - Cartesian
%Rotation Method - Arbitrary Axis
smiData.RigidTransform(15).translation = [2.5000000000003353 -0.16440634884945515 -
47.153322989099159];  % mm
smiData.RigidTransform(15).angle = 2.0943951023931997;  % rad
smiData.RigidTransform(15).axis = [-0.57735026918962706 -0.57735026918962706
0.57735026918962318];
smiData.RigidTransform(15).ID = "B[SimetríaHipjoint2-2:-:Simetríathigh-2]";

%Translation Method - Cartesian
%Rotation Method - Arbitrary Axis
smiData.RigidTransform(16).translation = [3.7347902548390266e-13 -
5.5777604757167865e-13 -4.9999999999965006];  % mm
smiData.RigidTransform(16).angle = 6.4736570491389395e-16;  % rad
smiData.RigidTransform(16).axis = [-0.96504779683798136 0.26207393960132341 -
8.1863885463755626e-17];
smiData.RigidTransform(16).ID = "F[SimetríaHipjoint2-2:-:Simetríathigh-2]";

%Translation Method - Cartesian
%Rotation Method - Arbitrary Axis
smiData.RigidTransform(17).translation = [46.00000000000005 0 -15.800000000000022];
% mm
smiData.RigidTransform(17).angle = 0;  % rad
smiData.RigidTransform(17).axis = [0 0 0];
smiData.RigidTransform(17).ID = "B[cadera1-1:-:joint for actuator-1]";

%Translation Method - Cartesian
%Rotation Method - Arbitrary Axis
smiData.RigidTransform(18).translation = [-16.893967962294905 -6.5195848719667993e-11
27.899999999999615];  % mm
smiData.RigidTransform(18).angle = 3.1415926535897931;  % rad
smiData.RigidTransform(18).axis = [5.5511151231257827e-17 1 1.0728015698013849e-12];
smiData.RigidTransform(18).ID = "F[cadera1-1:-:joint for actuator-1]";

%Translation Method - Cartesian
%Rotation Method - Arbitrary Axis
smiData.RigidTransform(19).translation = [-46.000000000000057 0 -15.799999999999995];
% mm
smiData.RigidTransform(19).angle = 0;  % rad
smiData.RigidTransform(19).axis = [0 0 0];
smiData.RigidTransform(19).ID = "B[cadera1-1:-:Simetríajoint for actuator-3]";

%Translation Method - Cartesian
%Rotation Method - Arbitrary Axis
smiData.RigidTransform(20).translation = [-16.893967962294717 -6.5185190578631591e-11
-27.899999999999665];  % mm
smiData.RigidTransform(20).angle = 2.1453396368707959e-12;  % rad
smiData.RigidTransform(20).axis = [-0.99999991831765389 -0.00025875227529113619 -
0.00031050273034936339];
smiData.RigidTransform(20).ID = "F[cadera1-1:-:Simetríajoint for actuator-3]";
```

```
%Translation Method - Cartesian
%Rotation Method - Arbitrary Axis
smiData.RigidTransform(21).translation = [529.89905710259598 -0.80410192031837857 -
19.000000000000018];  % mm
smiData.RigidTransform(21).angle = 1.1102230246251568e-16;  % rad
smiData.RigidTransform(21).axis = [1 0 0];
smiData.RigidTransform(21).ID = "B[thigh-1:-:Simetríashank-2]";

%Translation Method - Cartesian
%Rotation Method - Arbitrary Axis
smiData.RigidTransform(22).translation = [-22.576673650955726 43.320949332553667 -
16.999999999997247];  % mm
smiData.RigidTransform(22).angle = 1.5582722720639768e-15;  % rad
smiData.RigidTransform(22).axis = [0.62503823432842365 -0.78059413630106556 -
3.8014144068103593e-16];
smiData.RigidTransform(22).ID = "F[thigh-1:-:Simetríashank-2]";

%Translation Method - Cartesian
%Rotation Method - Arbitrary Axis
smiData.RigidTransform(23).translation = [0 0 -94.999999999999972];  % mm
smiData.RigidTransform(23).angle = 0;  % rad
smiData.RigidTransform(23).axis = [0 0 0];
smiData.RigidTransform(23).ID = "B[Simetríaankle-2:-:Simetríashank-2]";

%Translation Method - Cartesian
%Rotation Method - Arbitrary Axis
smiData.RigidTransform(24).translation = [-22.328669583904457 -379.87264081616718
81.500000000001521];  % mm
smiData.RigidTransform(24).angle = 3.1415926535897927;  % rad
smiData.RigidTransform(24).axis = [-1 1.1617378097500632e-31 -4.9342813101478895e-
16];
smiData.RigidTransform(24).ID = "F[Simetríaankle-2:-:Simetríashank-2]";

%Translation Method - Cartesian
%Rotation Method - Arbitrary Axis
smiData.RigidTransform(25).translation = [2.5000000000003633 -0.16440634884945515
47.153322989099244];  % mm
smiData.RigidTransform(25).angle = 2.0943951023931913;  % rad
smiData.RigidTransform(25).axis = [-0.57735026918962451 -0.57735026918962462
0.57735026918962828];
smiData.RigidTransform(25).ID = "B[Hipjoint2-1:-:thigh-1]";

%Translation Method - Cartesian
%Rotation Method - Arbitrary Axis
smiData.RigidTransform(26).translation = [8.3355544688856753e-13 -
5.8930638147103309e-13 4.9999999999977973];  % mm
smiData.RigidTransform(26).angle = 3.1415926535897931;  % rad
smiData.RigidTransform(26).axis = [1 -1.2175218722312272e-32 -2.634865145636445e-16];
smiData.RigidTransform(26).ID = "F[Hipjoint2-1:-:thigh-1]";

%Translation Method - Cartesian
%Rotation Method - Arbitrary Axis
smiData.RigidTransform(27).translation = [65.795294629775853 34.000000000000256 -
5.0000000000000604];  % mm
smiData.RigidTransform(27).angle = 2.094395102393197;  % rad
```

```
smiData.RigidTransform(27).axis = [0.5773502691896264 -0.57735026918962462
0.5773502691896264];
smiData.RigidTransform(27).ID = "B[ankle-1:-:foot-1]";

%Translation Method - Cartesian
%Rotation Method - Arbitrary Axis
smiData.RigidTransform(28).translation = [-3.2507330161024584e-13
7.2830630415410269e-14 -33.994999999999919];  % mm
smiData.RigidTransform(28).angle = 4.0360510480693485e-15;  % rad
smiData.RigidTransform(28).axis = [-0.020630741746122741 0.99371406077157876
0.11003062264598797];
smiData.RigidTransform(28).ID = "F[ankle-1:-:foot-1]";

%Translation Method - Cartesian
%Rotation Method - Arbitrary Axis
smiData.RigidTransform(29).translation = [0 0 28.338737110994952];  % mm
smiData.RigidTransform(29).angle = 3.4694469519536146e-15;  % rad
smiData.RigidTransform(29).axis = [1 0 0];
smiData.RigidTransform(29).ID = "B[cadera2L-1:-:joint for actuator-1]";

%Translation Method - Cartesian
%Rotation Method - Arbitrary Axis
smiData.RigidTransform(30).translation = [-42.000000000002487 3.0148328278301051e-11
-16.238737110995281];  % mm
smiData.RigidTransform(30).angle = 3.1415926535876495;  % rad
smiData.RigidTransform(30).axis = [-1 9.4890959551396434e-28 -8.8524729039919402e-
16];
smiData.RigidTransform(30).ID = "F[cadera2L-1:-:joint for actuator-1]";

%Translation Method - Cartesian
%Rotation Method - Arbitrary Axis
smiData.RigidTransform(31).translation = [0 -1.3877787807814457e-13 -
28.338737110994952];  % mm
smiData.RigidTransform(31).angle = 3.1415926535897896;  % rad
smiData.RigidTransform(31).axis = [1 -1.0322984501915584e-31 -5.5511151231257827e-
17];
smiData.RigidTransform(31).ID = "B[Simetríacadera2L-2:-:Simetríajoint for actuator-
3]";

%Translation Method - Cartesian
%Rotation Method - Arbitrary Axis
smiData.RigidTransform(32).translation = [-42.000000000000512 3.2493119306309381e-11
16.238737110995515];  % mm
smiData.RigidTransform(32).angle = 2.1438540136580887e-12;  % rad
smiData.RigidTransform(32).axis = [-0.99999950649494063 0.00099348370646449918 -
1.0649414902496428e-15];
smiData.RigidTransform(32).ID = "F[Simetríacadera2L-2:-:Simetríajoint for actuator-
3]";

%Translation Method - Cartesian
%Rotation Method - Arbitrary Axis
smiData.RigidTransform(33).translation = [-230.79223803860359 134.96250946552496
28.055144663884196];  % mm
smiData.RigidTransform(33).angle = 3.1161324121562801;  % rad
```

```
smiData.RigidTransform(33).axis = [0.86741815878419903 0.3775523794425808
0.3240986556415742];
smiData.RigidTransform(33).ID = "RootGround[cadera1-1]";


%============= Solid =============%
%Center of Mass (CoM) %Moments of Inertia (MoI) %Product of Inertia (PoI)

%Initialize the Solid structure array by filling in null values.
smiData.Solid(17).mass = 0.0;
smiData.Solid(17).CoM = [0.0 0.0 0.0];
smiData.Solid(17).MoI = [0.0 0.0 0.0];
smiData.Solid(17).PoI = [0.0 0.0 0.0];
smiData.Solid(17).color = [0.0 0.0 0.0];
smiData.Solid(17).opacity = 0.0;
smiData.Solid(17).ID = "";

%Inertia Type - Custom
%Visual Properties - Simple
smiData.Solid(1).mass = 0.039472073858398911;  % kg
smiData.Solid(1).CoM = [1.1057517414284692 0 -26.124424491540211];  % mm
smiData.Solid(1).MoI = [20.423508728617538 20.705239073608247 13.725196927282697];  %
kg*mm^2
smiData.Solid(1).PoI = [0 -0.8914667709987828 0];  % kg*mm^2
smiData.Solid(1).color = [0.792156862745098 0.81960784313725488 0.93333333333333335];
smiData.Solid(1).opacity = 1;
smiData.Solid(1).ID = "Simetríajoint for actuator2*:*Predeterminado";

%Inertia Type - Custom
%Visual Properties - Simple
smiData.Solid(2).mass = 0.036238248963255663;  % kg
smiData.Solid(2).CoM = [-0.00018527492351479448 2.9295370280422861 -
16.303426688888145];  % mm
smiData.Solid(2).MoI = [15.132559871017667 12.865383386081527 9.0550297599929603];  %
kg*mm^2
smiData.Solid(2).PoI = [-0.97658730949638939 5.9106548483985626e-05 -
9.1352509076571373e-05];  % kg*mm^2
smiData.Solid(2).color = [0.792156862745098 0.81960784313725488 0.93333333333333335];
smiData.Solid(2).opacity = 1;
smiData.Solid(2).ID = "SimetríaHipjoint2*:*Predeterminado";

%Inertia Type - Custom
%Visual Properties - Simple
smiData.Solid(3).mass = 0.28826169379074351;  % kg
smiData.Solid(3).CoM = [-108.99754644917911 32.255681339409286 7.844917610537653];  %
mm
smiData.Solid(3).MoI = [464.79778802502375 1429.6540395454074 1277.4544773998532];  %
kg*mm^2
smiData.Solid(3).PoI = [-92.145321716756641 350.64403137651465 346.59707364588934];
% kg*mm^2
smiData.Solid(3).color = [0.792156862745098 0.81960784313725488 0.93333333333333335];
smiData.Solid(3).opacity = 1;
smiData.Solid(3).ID = "Simetríacadera2L*:*Predeterminado";

%Inertia Type - Custom
```

```
%Visual Properties - Simple
smiData.Solid(4).mass = 0.24190785341249949;  % kg
smiData.Solid(4).CoM = [-43.296019528131701 -19.62165332645953 67.036411919254448];
% mm
smiData.Solid(4).MoI = [1160.0557549856535 1352.3902355512805 198.38201552019643];  %
kg*mm^2
smiData.Solid(4).PoI = [6.1347957664120987 34.901009134572519 -3.962443993027235];  %
kg*mm^2
smiData.Solid(4).color = [0.792156862745098 0.81960784313725488 0.93333333333333335];
smiData.Solid(4).opacity = 1;
smiData.Solid(4).ID = "Simetríafoot*:*Predeterminado";

%Inertia Type - Custom
%Visual Properties - Simple
smiData.Solid(5).mass = 0.038058429117842942;  % kg
smiData.Solid(5).CoM = [35.620223114208081 0 4.3651299590299004];  % mm
smiData.Solid(5).MoI = [12.57222767612507 21.136782725497817 33.09842886193529];  %
kg*mm^2
smiData.Solid(5).PoI = [0 -0.81023558981520982 0];  % kg*mm^2
smiData.Solid(5).color = [0.792156862745098 0.81960784313725488 0.93333333333333335];
smiData.Solid(5).opacity = 1;
smiData.Solid(5).ID = "Simetríaankle*:*Predeterminado";

%Inertia Type - Custom
%Visual Properties - Simple
smiData.Solid(6).mass = 1.1441617523847181;  % kg
smiData.Solid(6).CoM = [257.33312332252655 2.2079691120410581 4.19750211072963];  %
mm
smiData.Solid(6).MoI = [278.81299956519598 25171.946526432308 25375.618010038459];  %
kg*mm^2
smiData.Solid(6).PoI = [-1.2876476323473383 -60.662171757469103 -920.99618885214386];
% kg*mm^2
smiData.Solid(6).color = [0.89803921568627454 0.91764705882352937
0.92941176470588238];
smiData.Solid(6).opacity = 1;
smiData.Solid(6).ID = "Simetríathigh*:*Predeterminado";

%Inertia Type - Custom
%Visual Properties - Simple
smiData.Solid(7).mass = 0.24160274666437279;  % kg
smiData.Solid(7).CoM = [-23.20913302169766 -167.5835183096255 -3.7564682605011539];
% mm
smiData.Solid(7).MoI = [3243.819023458118 31.399129102239772 3259.717052355074];  %
kg*mm^2
smiData.Solid(7).PoI = [-12.880231161699532 0.055498828676277721 32.699371042717978];
% kg*mm^2
smiData.Solid(7).color = [0.792156862745098 0.81960784313725488 0.93333333333333335];
smiData.Solid(7).opacity = 1;
smiData.Solid(7).ID = "Simetríashank*:*Predeterminado";

%Inertia Type - Custom
%Visual Properties - Simple
smiData.Solid(8).mass = 0.42376361199434004;  % kg
smiData.Solid(8).CoM = [257.33312332252655 2.2079691120410549 -4.19750211072963];  %
mm
```

```
smiData.Solid(8).MoI = [103.2640739130355 9322.9431579378906 9398.3770407549837];  %
kg*mm^2
smiData.Solid(8).PoI = [0.47690653049901538 22.467471021284879 -341.10969957486776];
% kg*mm^2
smiData.Solid(8).color = [0.792156862745098 0.81960784313725488 0.93333333333333335];
smiData.Solid(8).opacity = 1;
smiData.Solid(8).ID = "thigh*:*Predeterminado";

%Inertia Type - Custom
%Visual Properties - Simple
smiData.Solid(9).mass = 0.039472073858398911;  % kg
smiData.Solid(9).CoM = [1.1057517414284705 0 26.124424491540211];  % mm
smiData.Solid(9).MoI = [20.423508728617531 20.70523907360824 13.725196927282694];  %
kg*mm^2
smiData.Solid(9).PoI = [0 0.89146677099878135 0];  % kg*mm^2
smiData.Solid(9).color = [0.792156862745098 0.81960784313725488 0.93333333333333335];
smiData.Solid(9).opacity = 1;
smiData.Solid(9).ID = "joint for actuator2*:*Predeterminado";

%Inertia Type - Custom
%Visual Properties - Simple
smiData.Solid(10).mass = 0.038058429117842948;  % kg
smiData.Solid(10).CoM = [35.620223114208088 0 -4.3651299590299004];  % mm
smiData.Solid(10).MoI = [12.572227676125074 21.136782725497817 33.098428861935297];
% kg*mm^2
smiData.Solid(10).PoI = [0 0.81023558981521004 0];  % kg*mm^2
smiData.Solid(10).color = [0.792156862745098 0.81960784313725488
0.93333333333333335];
smiData.Solid(10).opacity = 1;
smiData.Solid(10).ID = "ankle*:*Predeterminado";

%Inertia Type - Custom
%Visual Properties - Simple
smiData.Solid(11).mass = 0.043448158312540397;  % kg
smiData.Solid(11).CoM = [-28.461343763051349 0.2990388040218705 -6.9624344425673081];
% mm
smiData.Solid(11).MoI = [19.624505417823581 26.49162189843004 23.113608472322902];  %
kg*mm^2
smiData.Solid(11).PoI = [0.20187469959696494 2.2658435820642775 0.17251202015738765];
% kg*mm^2
smiData.Solid(11).color = [0.792156862745098 0.81960784313725488
0.93333333333333335];
smiData.Solid(11).opacity = 1;
smiData.Solid(11).ID = "joint for actuator*:*Predeterminado";

%Inertia Type - Custom
%Visual Properties - Simple
smiData.Solid(12).mass = 0.03623824896325567;  % kg
smiData.Solid(12).CoM = [-0.00018527492351558519 2.929537028042287
16.303426688888148];  % mm
smiData.Solid(12).MoI = [15.132559871017667 12.865383386081527 9.0550297599929603];
% kg*mm^2
smiData.Solid(12).PoI = [0.9765873094963885 -5.9106548483458351e-05 -
9.1352509076837816e-05];  % kg*mm^2
```

```
smiData.Solid(12).color = [0.792156862745098 0.81960784313725488
0.93333333333333335];
smiData.Solid(12).opacity = 1;
smiData.Solid(12).ID = "Hipjoint2*:*Predeterminado";

%Inertia Type - Custom
%Visual Properties - Simple
smiData.Solid(13).mass = 0.10595648849165942;  % kg
smiData.Solid(13).CoM = [0 0 12.1];  % mm
smiData.Solid(13).MoI = [24.627472474577058 89.367412445596386 103.67464183675074];
% kg*mm^2
smiData.Solid(13).PoI = [0 0 0];  % kg*mm^2
smiData.Solid(13).color = [0.792156862745098 0.81960784313725488
0.93333333333333335];
smiData.Solid(13).opacity = 1;
smiData.Solid(13).ID = "cadera1*:*Predeterminado";

%Inertia Type - Custom
%Visual Properties - Simple
smiData.Solid(14).mass = 0.24160274666437279;  % kg
smiData.Solid(14).CoM = [-23.20913302169766 -167.5835183096255 3.756468260501153];  %
mm
smiData.Solid(14).MoI = [3243.8190234581175 31.399129102239758 3259.7170523550735];
% kg*mm^2
smiData.Solid(14).PoI = [12.880231161699543 -0.055498828676279366
32.699371042717992];  % kg*mm^2
smiData.Solid(14).color = [0.792156862745098 0.81960784313725488
0.93333333333333335];
smiData.Solid(14).opacity = 1;
smiData.Solid(14).ID = "shank*:*Predeterminado";

%Inertia Type - Custom
%Visual Properties - Simple
smiData.Solid(15).mass = 0.24190796237313297;  % kg
smiData.Solid(15).CoM = [-43.296030398305717 -19.621652659770682 -
67.036412095397566];  % mm
smiData.Solid(15).MoI = [1160.0508877916163 1352.3857805960238 198.3824309389245];  %
kg*mm^2
smiData.Solid(15).PoI = [-6.1347793689337937 -34.90255933310975 -3.9624386513814556];
% kg*mm^2
smiData.Solid(15).color = [0.792156862745098 0.81960784313725488
0.93333333333333335];
smiData.Solid(15).opacity = 1;
smiData.Solid(15).ID = "foot*:*Predeterminado";

%Inertia Type - Custom
%Visual Properties - Simple
smiData.Solid(16).mass = 0.28825908287428348;  % kg
smiData.Solid(16).CoM = [-108.99710925297258 32.255411415262969 -7.844333112578199];
% mm
smiData.Solid(16).MoI = [464.7846968665537 1429.63625872229 1277.4447517370786];  %
kg*mm^2
smiData.Solid(16).PoI = [92.139945433863588 -350.63533498638333 346.59318083541928];
% kg*mm^2
```

```
smiData.Solid(16).color = [0.792156862745098 0.81960784313725488
0.93333333333333335];
smiData.Solid(16).opacity = 1;
smiData.Solid(16).ID = "cadera2L*:*Predeterminado";

%Inertia Type - Custom
%Visual Properties - Simple
smiData.Solid(17).mass = 0.043448158312540383;  % kg
smiData.Solid(17).CoM = [-28.461343763051349 0.29903880402187105 6.9624344425673037];
% mm
smiData.Solid(17).MoI = [19.62450541782357 26.491621898430026 23.113608472322895];  %
kg*mm^2
smiData.Solid(17).PoI = [-0.20187469959696694 -2.2658435820642739
0.17251202015738629];  % kg*mm^2
smiData.Solid(17).color = [0.792156862745098 0.81960784313725488
0.93333333333333335];
smiData.Solid(17).opacity = 1;
smiData.Solid(17).ID = "Simetríajoint for actuator*:*Predeterminado";


%============= Joint =============%
%X Revolute Primitive (Rx) %Y Revolute Primitive (Ry) %Z Revolute Primitive (Rz)
%X Prismatic Primitive (Px) %Y Prismatic Primitive (Py) %Z Prismatic Primitive (Pz)
%Spherical Primitive (S)
%Constant Velocity Primitive (CV) %Lead Screw Primitive (LS)
%Position Target (Pos)

%Initialize the RevoluteJoint structure array by filling in null values.
smiData.RevoluteJoint(11).Rz.Pos = 0.0;
smiData.RevoluteJoint(11).ID = "";

smiData.RevoluteJoint(1).Rz.Pos = 179.99999999999991;  % deg
smiData.RevoluteJoint(1).ID = "[Simetríafoot-3:-:Simetríaankle-2]";

smiData.RevoluteJoint(2).Rz.Pos = 5.8912118679786118;  % deg
smiData.RevoluteJoint(2).ID = "[Simetríajoint for actuator2-2:-:SimetríaHipjoint2-
2]";

smiData.RevoluteJoint(3).Rz.Pos = 81.058183863276668;  % deg
smiData.RevoluteJoint(3).ID = "[ankle-1:-:shank-1]";

smiData.RevoluteJoint(4).Rz.Pos = 94.458778827075406;  % deg
smiData.RevoluteJoint(4).ID = "[shank-1:-:Simetríathigh-2]";

smiData.RevoluteJoint(5).Rz.Pos = -5.8912118679786136;  % deg
smiData.RevoluteJoint(5).ID = "[Hipjoint2-1:-:joint for actuator2-1]";

smiData.RevoluteJoint(6).Rz.Pos = 92.31382914569366;  % deg
smiData.RevoluteJoint(6).ID = "[SimetríaHipjoint2-2:-:Simetríathigh-2]";

smiData.RevoluteJoint(7).Rz.Pos = 94.458778827075392;  % deg
smiData.RevoluteJoint(7).ID = "[thigh-1:-:Simetríashank-2]";

smiData.RevoluteJoint(8).Rz.Pos = -81.058183863276668;  % deg
smiData.RevoluteJoint(8).ID = "[Simetríaankle-2:-:Simetríashank-2]";
```

```
smiData.RevoluteJoint(9).Rz.Pos = -92.313829145693674;  % deg
smiData.RevoluteJoint(9).ID = "[Hipjoint2-1:-:thigh-1]";

smiData.RevoluteJoint(10).Rz.Pos = -1.3481978824235858;  % deg
smiData.RevoluteJoint(10).ID = "[cadera2L-1:-:joint for actuator-1]";

smiData.RevoluteJoint(11).Rz.Pos = 1.3481978824235707;  % deg
smiData.RevoluteJoint(11).ID = "[Simetríacadera2L-2:-:Simetríajoint for actuator-3]";
```

```
% Define the values array to put them in the model
hipAdl = [
    2.68000000
    1.94000000
    0.99000000
   -0.19000000
   -1.48000000
   -2.69000000
   -3.62000000
   -4.10000000
   -4.16000000
   -3.88000000
   -3.38000000
   -2.79000000
   -2.18000000
   -1.61000000
   -1.10000000
   -0.66000000
   -0.28000000
    0.03000000
    0.27000000
    0.44000000
    0.53000000
    0.57000000
    0.59000000
    0.67000000
    0.86000000
    1.18000000
    1.09000000
    1.59000000
    2.22000000
    3.01000000
    3.92000000
    4.78000000
    5.45000000
    5.85000000
    6.01000000
    5.96000000
    5.80000000
    5.57000000
    5.31000000
    5.06000000
    4.83000000
    4.64000000
    4.49000000
    4.38000000
    4.31000000
    4.26000000
    4.20000000
    4.11000000
    3.95000000
    3.68000000
    3.26000000
];
```

```
% Create a time vector spanning 10 seconds
duration = 10; % seconds
num_samples = numel(values);
time = linspace(0, duration, num_samples);

% Create a table with time and values
data = table(time', hipAdl, 'VariableNames', {'Time', 'Values'});

% Display the table
disp(data);
% Define the new values array
hipadr = [
    1.09000000
    1.59000000
    2.22000000
    3.01000000
    3.92000000
    4.78000000
    5.45000000
    5.85000000
    6.01000000
    5.96000000
    5.80000000
    5.57000000
    5.31000000
    5.06000000
    4.83000000
    4.64000000
    4.49000000
    4.38000000
    4.31000000
    4.26000000
    4.20000000
    4.11000000
    3.95000000
    3.68000000
    3.26000000
    2.68000000
    1.94000000
    0.99000000
   -0.19000000
   -1.48000000
   -2.69000000
   -3.62000000
   -4.10000000
   -4.16000000
   -3.88000000
   -3.38000000
   -2.79000000
   -2.18000000
   -1.61000000
   -1.10000000
   -0.66000000
   -0.28000000
    0.03000000
```

```
    0.27000000
    0.44000000
    0.53000000
    0.57000000
    0.59000000
    0.67000000
    0.86000000
    1.18000000
];

% Create a time vector spanning 10 seconds
duration = 10; % seconds
num_samples = numel(values);
time = linspace(0, duration, num_samples);

% Create a table with time and values
data = table(time', hipadr, 'VariableNames', {'Time', 'Values'});

% Display the table
disp(data);

% Define the new values array
hiprotl = [
    1.28
    1.41
    1.16
    0.41
    0.48
    0.99
    0.66
    0.31
    1.09
    1.09
    0.33
    0.74
    1.71
    2.48
    3.11
    3.7
    4.35
    4.98
    5.28
    4.96
    4.03
    2.81
    1.85
    1.38
    1.27
    1.21
    1.35
    0.37
    1.36
    3.02
    3.99
    4.23
```

```
    4.18
    3.83
    3.23
    2.72
    2.4
    2.14
    1.83
    1.5
    1.21
    0.96
    0.71
    0.45
    0.2
    0.01
    0.09
    0.02
    0.21
    0.56
    0.95
];

% Create a time vector spanning 10 seconds
duration = 10; % seconds
num_samples = numel(values);
time = linspace(0, duration, num_samples);

% Create a table with time and values
data = table(time', hiprot, 'VariableNames', {'Time', 'Values'});

% Display the table
disp(data);

% Define the new values array
hiprotr = [
    1.35
    0.37
    1.36
    3.02
    3.99
    4.23
    4.18
    3.83
    3.23
    2.72
    2.4
    2.14
    1.83
    1.5
    1.21
    0.96
    0.71
    0.45
    0.2
    0.01
    0.09
```

```
    0.02
    0.21
    0.56
    0.95
    1.28
    1.41
    1.16
    0.41
    0.48
    0.99
    0.66
    0.31
    1.09
    1.09
    0.33
    0.74
    1.71
    2.48
    3.11
    3.7
    4.35
    4.98
    5.28
    4.96
    4.03
    2.81
    1.85
    1.38
    1.27
    1.21
];

% Create a time vector spanning 10 seconds
duration = 10; % seconds
num_samples = numel(values);
time = linspace(0, duration, num_samples);

% Create a table with time and values
data = table(time', hiprot, 'VariableNames', {'Time', 'Values'});

% Display the table
disp(data);
% Define the new values array
hipflexl = [
    16.56
    16.82
    16.53
    15.4
    13.44
    10.65
    7.15
    3.16
    0.95
    4.93
    8.63
```

```
    11.96
    14.96
    17.62
    19.89
    21.76
    23.24
    24.33
    24.98
    25.26
    25.25
    25.04
    24.8
    24.66
    24.66
    24.7
    24.61
    24.45
    24.13
    23.68
    22.96
    21.78
    20.24
    18.41
    16.38
    14.19
    11.91
    9.58
    7.22
    4.87
    2.57
    0.33
    1.85
    3.98
    6.06
    8.1
    10.06
    11.88
    13.5
    14.85
    15.88
];

% Create a time vector spanning 10 seconds
duration = 10; % seconds
num_samples = numel(values);
time = linspace(0, duration, num_samples);

% Create a table with time and values
data = table(time', hipflexl, 'VariableNames', {'Time', 'Values'});

% Display the table
disp(data);

% Define the new values array for hip_flexion_r
hip_flexion_r = [
```

```
    24.61
    24.45
    24.13
    23.68
    22.96
    21.78
    20.24
    18.41
    16.38
    14.19
    11.91
    9.58
    7.22
    4.87
    2.57
    0.33
   -1.85
   -3.98
   -6.06
   -8.1
   -10.06
   -11.88
   -13.5
   -14.85
   -15.88
   -16.56
   -16.82
   -16.53
   -15.4
   -13.44
   -10.65
   -7.15
   -3.16
    0.95
    4.93
    8.63
    11.96
    14.96
    17.62
    19.89
    21.76
    23.24
    24.33
    24.98
    25.26
    25.25
    25.04
    24.8
    24.66
    24.66
    24.7
];

% Create a time vector spanning 10 seconds
duration = 10; % seconds
```

```
num_samples = numel(hip_flexion_r);
time = linspace(0, duration, num_samples);

% Create a table with time and hip_flexion_r values
hip_flexion_r_data = table(time', hip_flexion_r, 'VariableNames', {'Time',
'hip_flexion_r'});

% Display the table
disp(hip_flexion_r_data);
% Define the new values array for knee_angle_l
knee_angle_l = [
    8.2
    11.29
    15.19
    20.17
    26.06
    32.67
    39.6
    46.16
    51.68
    55.66
    57.83
    58.25
    57.28
    55.06
    51.58
    46.99
    41.48
    35.19
    28.31
    21.23
    14.44
    8.48
    4.3
    2.27
    2.35
    4.14
    3.94
    6.66
    9.45
    12.26
    14.76
    16.37
    17.04
    16.93
    16.24
    15.15
    13.87
    12.46
    10.95
    9.42
    7.96
    6.59
    5.37
    4.29
```

```
    3.4
    2.72
    2.37
    2.44
    3
    4.08
    5.83
];

% Create a time vector spanning 10 seconds
duration = 10; % seconds
num_samples = numel(knee_angle_l);
time = linspace(0, duration, num_samples);

% Create a table with time and knee_angle_l values
knee_angle_l_data = table(time', knee_angle_l, 'VariableNames', {'Time',
'knee_angle_l'});

% Display the table
disp(knee_angle_l_data);
% Define the new values array for knee_angle_r
knee_angle_r = [
    -3.94
    -6.66
    -9.45
    -12.26
    -14.76
    -16.37
    -17.04
    -16.93
    -16.24
    -15.15
    -13.87
    -12.46
    -10.95
    -9.42
    -7.96
    -6.59
    -5.37
    -4.29
    -3.4
    -2.72
    -2.37
    -2.44
    -3
    -4.08
    -5.83
    -8.2
    -11.29
    -15.19
    -20.17
    -26.06
    -32.67
    -39.6
    -46.16
```

```
    -51.68
    -55.66
    -57.83
    -58.25
    -57.28
    -55.06
    -51.58
    -46.99
    -41.48
    -35.19
    -28.31
    -21.23
    -14.44
    -8.48
    -4.3
    -2.27
    -2.35
    -4.14
];

% Create a time vector spanning 10 seconds
duration = 10; % seconds
num_samples = numel(knee_angle_r);
time = linspace(0, duration, num_samples);

% Create a table with time and knee_angle_r values
knee_angle_r_data = table(time', knee_angle_r, 'VariableNames', {'Time',
'knee_angle_r'});

% Display the table
disp(knee_angle_r_data);
% Define the new values array for ankle_angle_l
ankle_angle_l = [
    9.81
    8.26
    5.52
    1.11
    4.36
    9.73
    13.37
    14.07
    12.62
    10.16
    7.6
    5.28
    3.2
    1.34
    0.23
    1.44
    2.24
    2.58
    2.39
    1.83
    1.16
    0.54
```

```
    0.18
    0.07
    0.01
    0.5
    1.7
    3.25
    4.68
    5.08
    4.17
    2.5
    0.83
    0.65
    1.92
    2.98
    3.88
    4.64
    5.25
    5.78
    6.28
    6.78
    7.3
    7.86
    8.44
    9.05
    9.63
    10.16
    10.56
    10.75
    10.54
];

% Create a time vector spanning 10 seconds
duration = 10; % seconds
num_samples = numel(ankle_angle_l);
time = linspace(0, duration, num_samples);

% Create a table with time and ankle_angle_l values
ankle_angle_l_data = table(time', ankle_angle_l, 'VariableNames', {'Time',
'ankle_angle_l'});

% Display the table
disp(ankle_angle_l_data);
% Define the new values array for ankle_angle_r
ankle_angle_r = [
    1.7
    3.25
    4.68
    5.08
    4.17
    2.5
    0.83
    0.65
    1.92
    2.98
    3.88
```

```
    4.64
    5.25
    5.78
    6.28
    6.78
    7.3
    7.86
    8.44
    9.05
    9.63
    10.16
    10.56
    10.75
    10.54
    9.81
    8.26
    5.52
    1.11
    4.36
    9.73
    13.37
    14.07
    12.62
    10.16
    7.6
    5.28
    3.2
    1.34
    0.23
    1.44
    2.24
    2.58
    2.39
    1.83
    1.16
    0.54
    0.18
    0.07
    0.01
    0.5
];

% Create a time vector spanning 10 seconds
duration = 10; % seconds
num_samples = numel(ankle_angle_r);
time = linspace(0, duration, num_samples);

% Create a table with time and ankle_angle_r values
ankle_angle_r_data = table(time', ankle_angle_r, 'VariableNames', {'Time',
'ankle_angle_r'});

% Display the table
disp(ankle_angle_r_data);
```